

**Final Report to the Health Effects Task Force (HETF),
Breathe California of Sacramento-Emigrant Trails**

**Mass, Organic, and Elemental Aerosols by size, time, and
composition at the Union Pacific Rail Road's
Roseville Railyard**

November 27, 2007

Prof. Thomas A. Cahill, P.I.^{1,2}, and Prof. Thomas M. Cahill^{3,4}, co-P.I.s, Dr. David E. Barnes¹ and
Nicholas J. Spada¹, Project Managers, Dr. Steven S. Cliff¹, and Prof. Kevin D. Perry^{1,5}, Staff
Scientists, and Erin Fujii¹, Student Research Assistant

¹DELTA* Group, Depts. of Physics, Chemical Engineering/Materials Science, and Applied
Science, University of California, Davis, CA

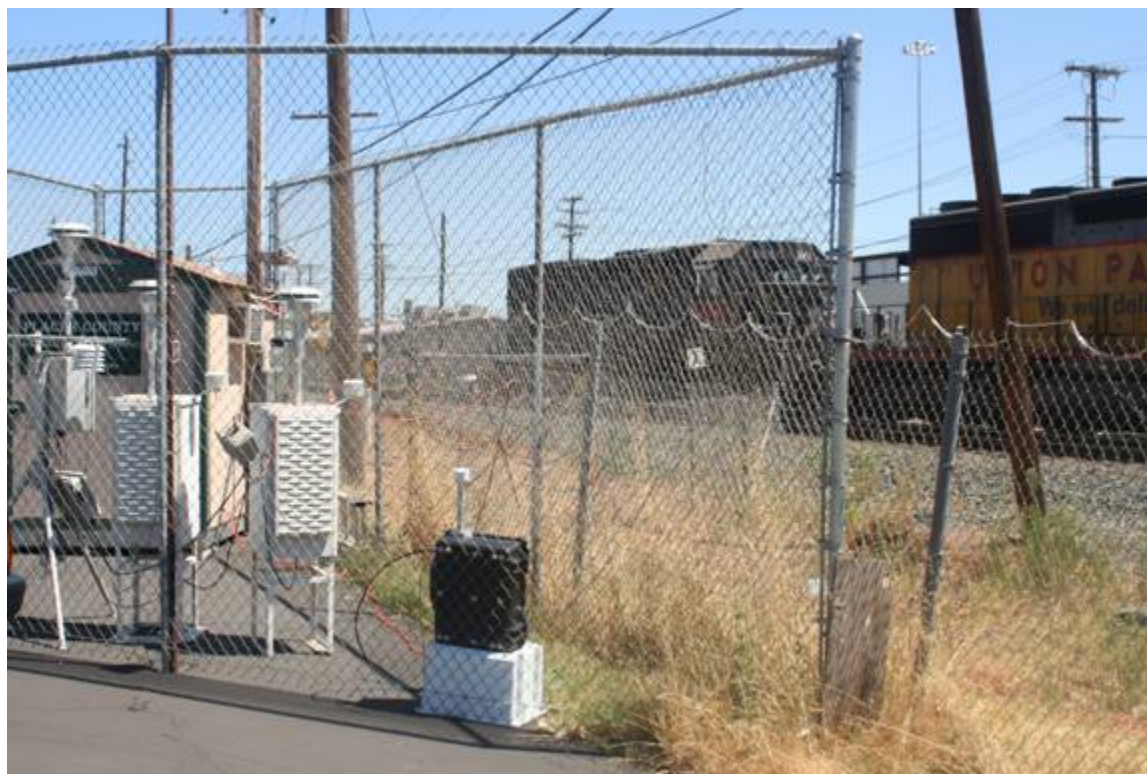
²Breathe California of Sacramento/Emigrant Trails (BC/SET), Sacramento, CA,

³Department of Integrated Physical Sciences, Arizona State University, Glendale, AZ,

⁴Department of Eco-toxicology, University of California, Davis, CA,

⁵Department of Meteorology, University of Utah, Salt Lake City, UT

- DELTA – Detection and Evaluation in Long-range Transport of Aerosols



Executive Summary

This report has seven components, all bearing on aerosol emissions from Union Pacific Roseville Railyard (UPRR). Component A represents data from the Roseville Railyard Aerosol Monitoring Project (RRAMP), Components C and D (**in bold**) were funded on a grant to Placer County from EPA Region IX extending RRAMP aerosol data, using samples collected by the Breathe California Health Effects Task Force (HETF). Component E was a winter study, an HETF study. The final report for these components (A, C, D, and E) was submitted October 1, 2007, and is posted on the Placer County Air Pollution Control District web site. The remaining components of this report are additional programs of the HETF and the DELTA Group, University of California, Davis. However, all seven are included for completeness and ease of interpretation. Note that while Components A, C, D, and E were reviewed in detail by the RRAMP Technical Advisory Committee, the conclusions presented herein are those of the investigators and are not an official RRAMP project.

Component A RRAMP monitoring data, NO, NO₂, EC, and PM_{2.5}, Pool site (upwind of the rail yard at night) and Denio site (downwind of the rail yard at night), with the difference representing the rail yard contributions to atmospheric aerosols and gasses.

Component B UC Davis DELTA /Breathe California of Sacramento-Emigrant Trails (BC/SET) collaborative contributions, with
1. Mass every 3 hrs, 8 size modes, Denio site, mass in the very fine size mode ($0.26 > D_p > 0.09 \mu\text{m}$), Pool site, and
2. Very fine S-XRF elemental S-XRF composition, 32 elements, every 3 hr, (Pool and Denio).

Component C UC Davis DELTA Group S-XRF elemental analysis of all 7 size fractions, 10.0 to 0.26 μm , every 3 hr, at the Denio site, and

Component D Organic analysis at the Denio site for PAHs, n-alkanes, sugars, and fatty acids, 5 to 8 size modes, 3 integrated periods.

This component includes an explicit comparison to diesel truck data from the literature.

Component E UC Davis DELTA Group analysis of mass and elements, Denio site, February, 2006, as part of the Breathe California (BC/SET) studies of Sacramento aerosols.

This work included a comparison to Watt Ave at Arden Way, which is included for completeness.

Component F Collection of aerosols at the Pool and Denio sites, summer, 2006, and at the Pool, Denio, and Church Street sites, summer, 2007.

Component G Mitigation options proposed by the HETF for the Roseville Railyard and surrounding area.

Component QA The DELTA Group's DRUM Quality Assurance Protocols (DQAP, ver. 1/05) are included by reference, and a copy is provided. A short summary is included as Appendix QA.

The UC Davis DELTA Group and Breathe California of Sacramento-Emigrant Trails (BC/SET) collaborated with the RRAMP project to assist BC/SET ongoing studies of aerosol sources and transport in general and diesel exhaust in particular. The RRAMP program was ideal for this purpose, with an upwind-downwind measurement protocol across the Roseville Railyard and numerous pollutant measurements. The DELTA Group contributions for summer, 2005, included mass by soft beta rays every 3 hours for 5 weeks (8 size modes Denio site, the very fine mode, $0.26 > D_p > 0.09 \mu\text{m}$, Pool Site) and very fine elemental concentrations by synchrotron-induced X-ray fluorescence (S-XRF) every 3 hours (Denio and Pool site) for the period July 12 through August 17, 2005. Samples were also taken suitable for later organic analysis at the Denio site from August 5 through October 17, and archived in a freezer.

The results of this early effort lead to a proposal via Placer County to the US EPA Region IX for funding to analyze the remainder of the DRUM stages for the coarser elements, 10.0 to $0.26 \mu\text{m}$. July 12 through August 17, and analyze the organic samples for PAHs, n-alkanes, sugars, and fatty acids by GC/MS (Gas Chromatography/Mass Spectrometry). These efforts are presented in the Final Report, "Mass, elemental, and organic aerosols by size, time, and composition for the Roseville Railyard Aerosol Monitoring Project (RRAMP)", Prof. Thomas M. Cahill, P.I.^{1,2}, and Prof. Thomas A. Cahill^{3,4}, co-P.I.s, Nicholas J. Spada³, Project Manager, Drs. David E. Barnes³, Steven S. Cliff³, and Prof. Kevin D. Perry^{3,5}, Staff Scientists, and Erin Fujii³, Oct.1, 2007.

Additional studies were proposed to the Placer County APCD with Cahill/HETF input in winter, 2006, summer, 2006, and summer, 2007, in order to extend the summer, 2005 data deeper into ongoing UPRR mitigation efforts and prepare for potential future work summer, 2008, if the Denio and Pool sites were to be removed.

Finally, mitigation options have been developed for aerosol emissions from the Roseville Railyard by the investigators, with input from the HETF, based partially on current HETF studies and mitigation on Watt Avenue.

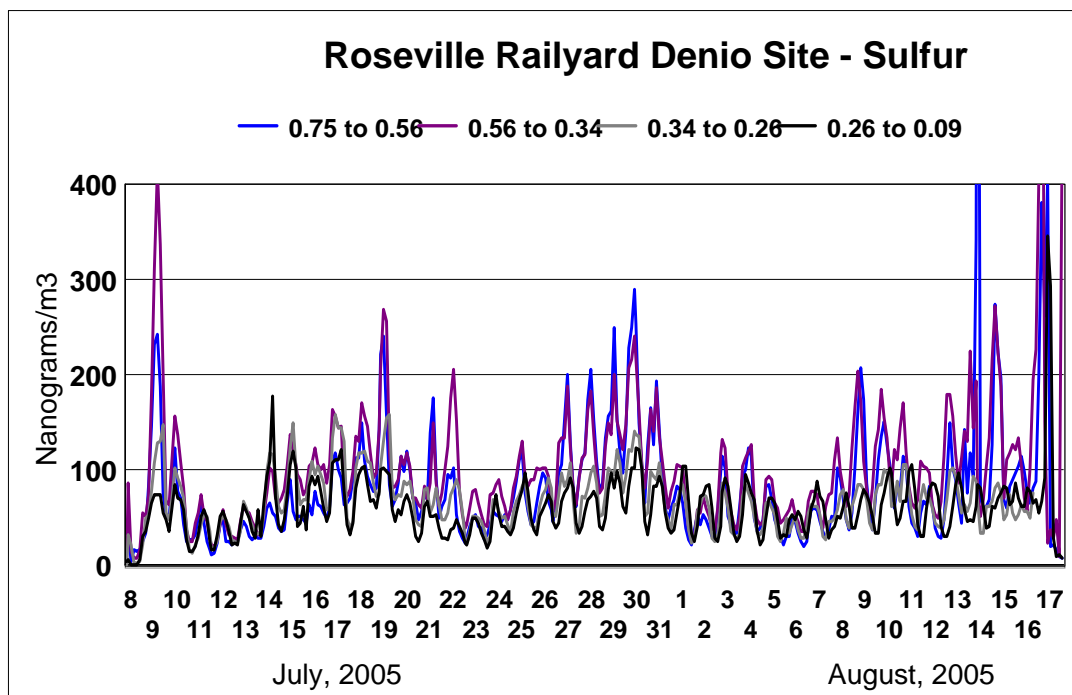
The key findings are:

1. The key assumptions behind the RRAMP project are sound, with several characteristic diesel species having large railyard versus background ratios; NO, x 22.1; NO₂, x 7.2; very fine mass and very fine sulfur; x 4.0, black carbon, x 2.3; and a number of anthropogenic metals, x 1.6 to 2.8.

2. Exhaust from diesel engines as seen downwind of the Roseville Railyard differs in important ways from prior published studies of truck diesel engines

- a. The size of the diesel exhaust peaks in mass (and sulfur) is about $0.3 \mu\text{m}$, roughly 3 times that of a diesel truck under load but similar to size distributions of idling diesel engines.

- b. However, the PAH's (pyrene, coronene) peak well below $0.1 \mu\text{m}$, finer than those seen in truck studies (Zielinska et al 2004).



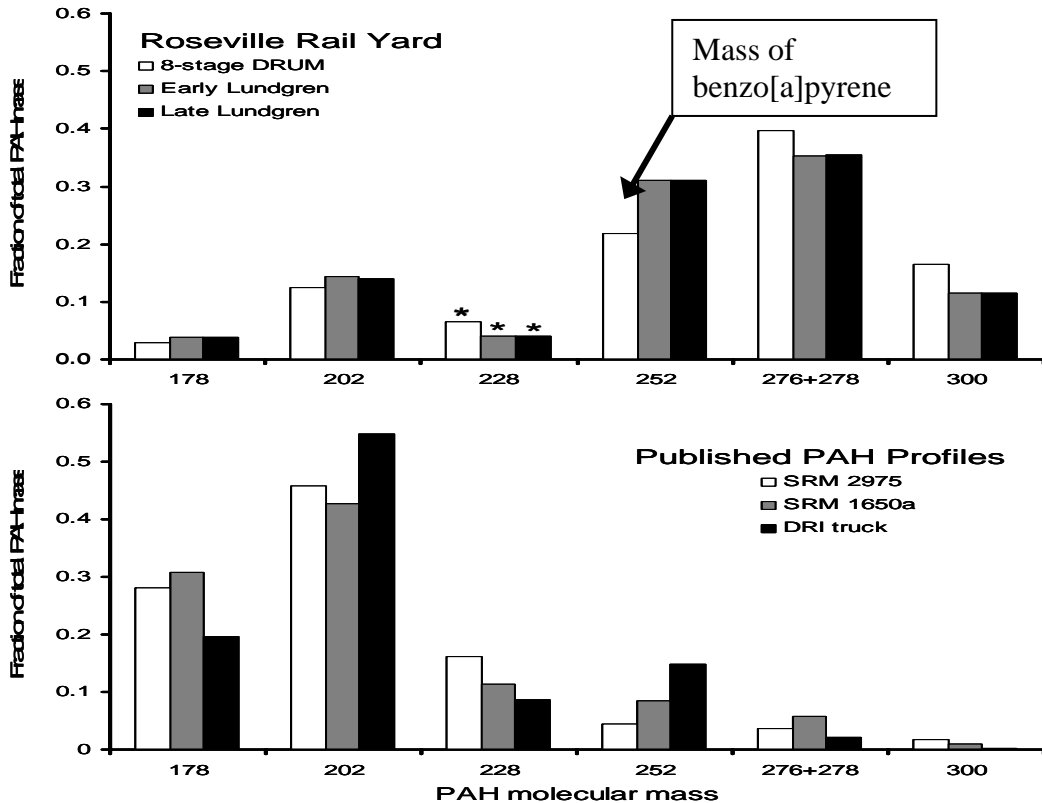
3. The coarse ($10.0 > D_p > 2.5 \mu\text{m}$) soils of the Roseville Railyard and its vicinity contain anthropogenic metals at levels many times that of standard soil, with Enrichment Factor (EF) values such as times 33 (zinc) and times 43 (copper). Some of these materials are also present in fine mode aerosols smaller than $2.5 \mu\text{m}$.

4. The data for n-alkanes suggest that the soil is also contaminated by heavy petroleum-based hydrocarbons, supporting the elemental data.

5. The diesel exhaust from the Roseville Railyard is about 5.5 times richer in the most carcinogenic components of diesel exhaust (benzo[a]pyrene, among others) than is the exhaust from diesel trucks.

Below we show profiles of relative PAHs as a function of molecular mass from the Roseville Railyard and the literature. RRAMP aerosols have a relative enhancement of benzo[a]pyrene and similar heavy PAHs of about a factor of 3. Combining the absolute emission rates, and using ratios of both very fine/ultra fine mass and elemental carbon (EC), we generate 11 different ratios based on the method used. A weighted average of the 11 values, very fine mass and EC, gives a ratio of the RRAMP BaP to diesel trucks of 5.5 ± 0.7 . This means that there was about 5.5 times more benzo[a]pyrene from the RRAMP aerosols than from diesel truck aerosols, per unit very fine/ultra fine mass and per unit elemental carbon (EC).

With Key Finding 2 a and 2 b (above), this implies that the PAHs are derived from the used lubricating oil, not the diesel fuel.



6. About ½ of the PM_{2.5} organic mass was in largely biogenic sugars and fatty acids, ½ was in petroleum based n-alkanes, and only a few percent was in PAHs.

7. The winter very fine particle mass at the Denio site, 6.6 µg/m³, in the size range 0.34 - 0.09 µm, was about three times the summer mass at the Denio site, 2.25 µg/m³.

8. A qualitative comparison of downtown Sacramento (ARB's 13th and T Street site) and the Roseville Pool site, summer 2007, appear similar in time behavior and color, confirming that the Pool site represents regional aerosols. The downwind Denio and Church Street sites are much darker in the finer modes, probably from soot. This is consistent with the design of the RRAMP upwind-downwind protocols to isolate railyard emissions.

9. Many options exist for mitigation of aerosols from the Roseville Railyard, with the HETF suggestions in Component G, including:

- a) Mitigation of railyard emissions sources (work in progress as part of an MOU between UPRR, Placer County, and others; plus additional suggestions discussed in Component G),
- b) Mitigation on railyard properties to lower the generation of coarse, contaminated soils on site, and to lower the transport of all railyard aerosols off-site,
- c) Mitigation from the railyard boundary into nearby receptor areas, including use of distance to receptors and vegetative barriers, and
- d) Mitigation of railyard aerosols within homes and other nearby receptors.

Table of Contents		
Executive Summary		2
Component A		
RRAMP monitoring data		9
Component B		
Mass at the Denio and Pool site		
Elemental analysis of very fine particles at the Denio and Pool sites		15
Component C		
Elemental analysis of 8 size ranges PM ₁₀ to very fine at the Denio Site		32
Component D		43
Organic analysis of aerosols at the Denio site: PAHs		47
PAHs	n-alkanes	51
Alkanes	organic acids	55
Organic acids	sugars and polyols	57
Comparison to truck diesel data		63
Component E		67
Aerosol sampling, winter, 2006, and comparison to heavily traveled secondary streets		
Component F		76
Collection of aerosols at the Pool and Denio sites, summer, 2006, and at the Pool, Denio, and Church Street sites, summer, 2007.		
Component G		
Mitigation options proposed by the HETF for the Roseville rail yard		79
References		83
Acknowledgements		84
Appendix QA		85
List of Tables		
Table 1	Regional meteorology during the study	10
Table 2	Placer County pollutant emissions for the 8 largest contributors to NO _x	14
Table 3	Organics sampling and RRAMP data	15
Table 4a, 4b	Denio site versus Pool site comparisons in parallel with DELTA Group sampling periods.	16
Table 5	S-XRF comparison, all blind tests since 1999	18
Table 6	Samples collected for organic analysis	47
Table 7.	Concentrations (pg/m ³) of particulate PAHs observed at the Roseville Railyard in the Summer of 2005	48
Table 8.	Concentrations (ng/m ³) of particulate n-alkanes observed at the Roseville Railyard in the Summer of 2005	51
Table 9.	Concentrations (ng/m ³) of particulate organic acids observed at the Roseville Railyard in the Summer of 2005	56
Table 10.	Concentrations (ng/m ³) of particulate sugars observed at the Roseville Railyard in the Summer of 2005	58
Table 11	Comparison of RRAMP Benzo{a}pyrene results to literature values for diesel trucks	65

List of Figures

Figure 1	The Davis Union Pacific Rail Road Roseville Railyard.	9
Figure 2 a, b, and c	Data on nitric oxide (NO), July – October, 2005	11
Figure 3 a, b, and c	Data on “black carbon”, EC for July - October, 2005	12
Figure 4 a, b, and c	Data on PM _{2.5} mass, July – October, 2005	13
Figure 5	Nick Spade (left) and David Barnes at the Denio site	17
Figure 6	Precision test for mass	18
Figure 7	Mass from 10.0 to 0.75 μm	19
Figure 8	Mass from 0.75 to 0.09 μm	19
Figure 9	Three components of fine mass versus time	20
Figure 10	Comparison of the Pool and Denio sites for very fine mass	20
Figure 11	Nighttime (9 PM – 6 AM) mass size profiles for early August at the Denio site.	21
Figure 12	Size mode of aerosol mass, July 15, versus other diesel studies	22
Figure 13	Typical elemental signatures of diesel, Denio site very fine mode	23
Figure 14	Zielenska et al 2004 diesel characterization results	23
Figure 15	Transition mode elements nickel, copper, and zinc in the Denio site very fine mode.	24
Figure 16	Crustal elements in the very fine mode, Denio site	24
Figure 17	Mass versus typically diesel signature elements, Denio site	25
Figure 18	Comparison of very fine sulfur, Denio Site vs Pool Site	26
Figure 19	Comparison of very fine phosphorus, Denio Site vs Pool Site	27
Figure 20	Comparison of very fine zinc, Denio Site vs Pool Site	27
Figure 21	Comparison of very fine calcium, Denio Site vs Pool Site	28
Figure 22	Comparison of very fine copper, Denio Site vs Pool Site	28
Figure 23	Comparison of very fine nickel, Denio Site vs Pool Site	29
Figure 24	Comparison of very fine potassium, Denio Site vs Pool Site	29
Figure 25	Comparison of very fine vanadium, Denio Site vs Pool Site	30
Figure 26	Comparison of very fine chromium, Denio Site vs Pool Site	31
Figure 27	Sea salt signature in coarse particle fluorine.	32
Figure 28	HYSPLIT trajectory showing Bay Area transport, July 22, 2005	33
Figure 29	Sub-micron Fine sulfur at the Denio site	34
Figure 30	Components of fine sulfur at the Denio site	34
Figure 31	Sub-micron sulfur versus fine iron at the Denio site	35
Figure 32	Size distribution of sulfur and soils, daytime, July 18, 2006	35
Figure 33	Time plots of coarse and fine silicon, Denio site	36
Figure 34	Size distribution of sulfur and soils, nighttime, July 18, 2006	37
Figure 35	Time plots of coarse and fine potassium, Denio site	37
Figure 36	2.5 to 1.15 μm vanadium and chromium, summer, 2005	38
Figure 37	Time plots of sub-microns zinc, summer, 2005	38
Figure 38	HYSPLIT Wind trajectories at the beginning of the zinc episode, on the morning of July 27.	39
Figure 39	Comparison of very fine copper and zinc at the Pool and Denio sites. Most of the largest metal spikes occur at the Denio site.	40
Figure 40	Size Distribution of elements on July 18, 2006, during night time cross rail yard winds	41

Figure 41	Size Distribution of elements on July 18, 2006, during day time winds from the southwest roughly parallel to the rail yard.	42
Figure 42.	Coronene and pyrene concentrations (pg/m^3) in the different size fractions of the 8-stage DRUM sampler and the afterfilter.	48
Figure 43.	Profiles of PAHs as a function of molecular mass from the Roseville Railyard and the literature.	50, 63
Figure 44.	A selected ion chromatogram of m/z 57 showing the undifferentiated hydrocarbon “envelope”. The n -alkanes are labeled by their carbon number.	53
Figure 45	Concentrations of undifferentiated hydrocarbons in different size fractions of the 8-stage DRUM sampler.	54
Figure 46.	The fraction of n -alkanes collected on the after filter of the 8-stage DRUM. The C_{33} to C_{36} alkanes were not detected on the filter.	55
Figure 47.	Concentration of octadecanoic, hexadecanoic and 9-octadenoic (oleic) acid as a function of particle size.	57
Figure 48.	Sucrose and glucose concentrations (ng/m^3) as a function of aerosol size.	59
Figure 49	Fraction of the identified organic mass belonging to the four different classes of chemicals identified.	60
Figure 50.	Mass of aerosols as determined by beta gauge and by the sum of The elements and oxides as determined by S-XRF.	61
Figure 51.	Composition of aerosol mass as determined by beta-gauge.	62
Figure 52	Meteorology during the winter sampling, 2006	67
Figure 53	Photograph of winter drum strips, Watt Ave at Arden versus Denio site	68
Figure 54	Coarse and fine mass at Watt and Arden versus the Denio site, winter, 2006	69
Figure 55	Photographs of winter DRUM strips, Watt/Arden, 2004, vs Watt/Arden and Denio, 2006	70
Figure 56	Chlorine aerosols (sea salt) at Watt/Arden and Denio, winter, 2006	70
Figure 57	Iron aerosols (soil) at Watt/Arden vs Denio, winter, 2006	71
Figure 58	Sulfur aerosols (soil) at Watt/Arden vs Denio, winter, 2006	72
Figure 59	Vanadium aerosols (heavy fuel oil) at Watt/Arden vs Denio, winter	72
Figure 60	Coarse potassium aerosols (soil) at Watt/Arden vs Denio, winter	73
Figure 61 a,b	Accumulation mode potassium aerosols (wood smoke) and very fine potassium aerosols (vehicular) at Watt vs Denio, winter	74
Figure 62	Very fine mode phosphorus and zinc aerosols (vehicular, Lubricating oil) at Watt/Arden vs Denio, winter 2006	75
Figure 63	Very fine mode Ni, Cu, and Zn zinc aerosols at Watt/Arden vs Denio 2006	75
Figure 64	Comparison of downtown and the Roseville Pool site	77
Figure 65	Comparison of the Denio and Church Street sites	78
Figure 66	Preliminary data on removal rate of very fine ($0.26 > D_p > 0.09 \mu\text{m}$) on redwood branches in the UC Davis wind tunnel	81

Component A
Introduction and RRAMP monitoring data

The Davis Railyard of Union Pacific Railroad (UPRR) in Roseville, California, hosts typically 31,000 trains/years for maintenance, repair, and testing, and re-routing, while an additional 16,000 trains/year pass through the yard without stopping. The pollutants emitted by the rail yard are significant components of the gas and aerosol inventory for the region. Through a joint agreement between UPRR and the California Air Resources Board (ARB), Placer and Sacramento Counties APCDs, and the US EPA, Region IX, a multi-year plan is in place for reduction of pollutants and measuring the improvement through the Roseville Railyard Aerosol Monitoring Project (RRAMP)

The RRAMP program is based upon a robust air monitoring program upwind and downwind of the rail yard during summer periods when the winds are especially regular and predictable. This program also includes collaborative programs of Breathe California of Sacramento-Emigrant Trails and specific purpose grants, including the present one from EPA Region IX that funded additional aerosol elemental and organic measurements.



Figure 1 The Davis Union Pacific Rail Road Roseville Railyard

The sites used for the present program are marked, the “Pool Site”, upwind in summer nights, and the “Denio Site”, downwind in summer nights. Two other sites also are being used in the program. The stability of the metrology during the period was typical of summer conditions near Sacramento.

July	2005	Mather AFB weather														Direction			
		Temp						Press						Visibility			Precip	160 night	270 day
		Max	F	Min	RH	%	Avg	Min	Avg	Max	In	Avg	Max	mph	Gust				
8	Friday	87	72	57	83	59	35	29.92	10	10	10	14	8	-	0.00	SSW			
9	Saturday	84	73	62	88	65	35	29.91	10	10	10	15	10	18	0.00	SSW			
10	Sunday	80	68	57	94	76	37	29.93	10	10	10	9	7	-	0.00	SSE			
11		96	78	60	94	60	23	29.91	10	10	10	12	1	-	0.00	WSW			
12		102	82	62	83	48	18	29.89	10	10	10	9	4	-	0.00	WSW			
13		104	86	68	78	40	20	29.85	10	10	10	12	5	-	0.00	SW			
14		105	87	69	64	42	20	29.82	10	10	10	10	7	-	0.00	SSW			
15	Friday	105	87	69	69	40	18	29.77	10	10	10	10	6	-	0.00	SW			
16	Saturday	107	88	68	60	38	12	29.77	10	10	10	12	6	-	0.00	S			
17	Sunday	105	86	66	68	40	20	29.77	10	10	10	10	3	-	0.00	SSW			
18		98	82	66	68	46	27	29.76	10	10	10	12	5	-	0.00	SSW			
19		98	80	62	82	53	25	29.76	10	10	10	9	8	-	0.00	SSW			
20		102	81	60	77	42	15	29.8	10	10	10	9	7	-	0.00	SW			
21		87	78	64	73	44	21	29.84	10	10	10	17	9	21	0.00	SSW			
22	Friday	95	77	59	82	50	14	29.9	10	10	10	13	8	16	0.00	SSW			
23	Saturday	104	80	57	94	43	7	29.89	10	10	10	10	4	-	0.00	SSW			
24	Sunday	102	83	64	64	38	15	29.86	10	10	10	15	1	-	0.00	S			
25		100	80	59	82	43	11	29.85	10	10	10	12	6	-	0.00	SSW			
26		102	83	64	73	43	17	29.83	10	10	10	12	3	-	0.00	S			
27		100	81	62	72	43	14	29.86	10	10	10	12	7	-	0.00	SSW			
28		98	78	59	77	47	13	29.84	10	10	10	12	6	-	0.00	SSW			
29	Friday	96	79	62	68	43	22	29.87	10	10	10	12	7	-	0.00	SSW			
30	Saturday	100	81	62	72	47	21	29.94	10	10	10	13	6	-	0.00	SSW			
31	Sunday	100	81	62	68	42	11	29.92	10	10	10	9	4	-	0.00	SSW			
1		102	80	59	82	40	9	29.89	10	10	10	14	6	-	0.00	SSW			
2		96	78	59	67	40	12	29.87	10	10	10	9	6	-	0.00	SSW			
3		98	78	59	82	46	16	29.87	10	10	10	12	6	-	0.00	WSW			
4		100	80	60	77	45	18	29.93	10	10	10	9	7	-	0.00	SW			
5	Friday	102	83	64	68	40	15	29.93	10	10	10	12	5	-	0.00	SW			
6	Saturday	105	84	64	68	36	9	29.89	10	10	10	10	5	-	0.00	SSW			
7	Sunday	102	83	64	68	41	13	29.83	10	10	10	10	6	-	0.00	S			
8		96	79	62	72	44	22	29.83	10	10	10	9	5	-	0.00	SSW			
9		100	81	62	77	49	17	29.87	10	10	10	9	6	-	0.00	SSW			
10		96	78	60	77	50	22	29.9	10	10	10	9	3	-	0.00	SSW			
11		98	78	59	77	43	13	29.89	10	10	10	12	6	-	0.00	SSW			
12	Friday	100	81	62	68	43	18	29.79	10	10	10	15	5	-	0.00	SSW			
13	Saturday	86	70	53	94	63	33	29.8	10	10	10	12	5	-	0.00	S			
14	Sunday	87	71	55	94	66	35	29.81	20	11	10	12	6	-	0.00	S			
15		84	70	55	94	60	37	29.89	10	10	10	14	6	18	0.00	SSW			
16		95	80	66	73	48	23	29.94	10	10	10	10	3	-	0.00	W			
17		95	77	59	82	44	19	29.83	20	11	10	14	6	-	0.00	SSW			
18		84	68	53	100	67	27	29.83	10	10	8	14	8	20	0.00	SSW			
19	Friday	87	72	57	94	62	16	29.89	10	10	10	9	8	-	0.00	SSW			
	Saturday																		
	Sunday																		

Table 1 Regional meteorology during the study

Generally, the regional weather (Mather AFB) showed wind direction roughly 160 ° at night, and roughly 270 ° during the day, with small variations. This pattern,

confirmed by on-site meteorology, makes the Denio site downwind each night for about 8 hr every night from the Pool site direction.

Below we show the major data from the monitoring program for 2005. The pollutants were chosen to reflect a primarily diesel based emissions.

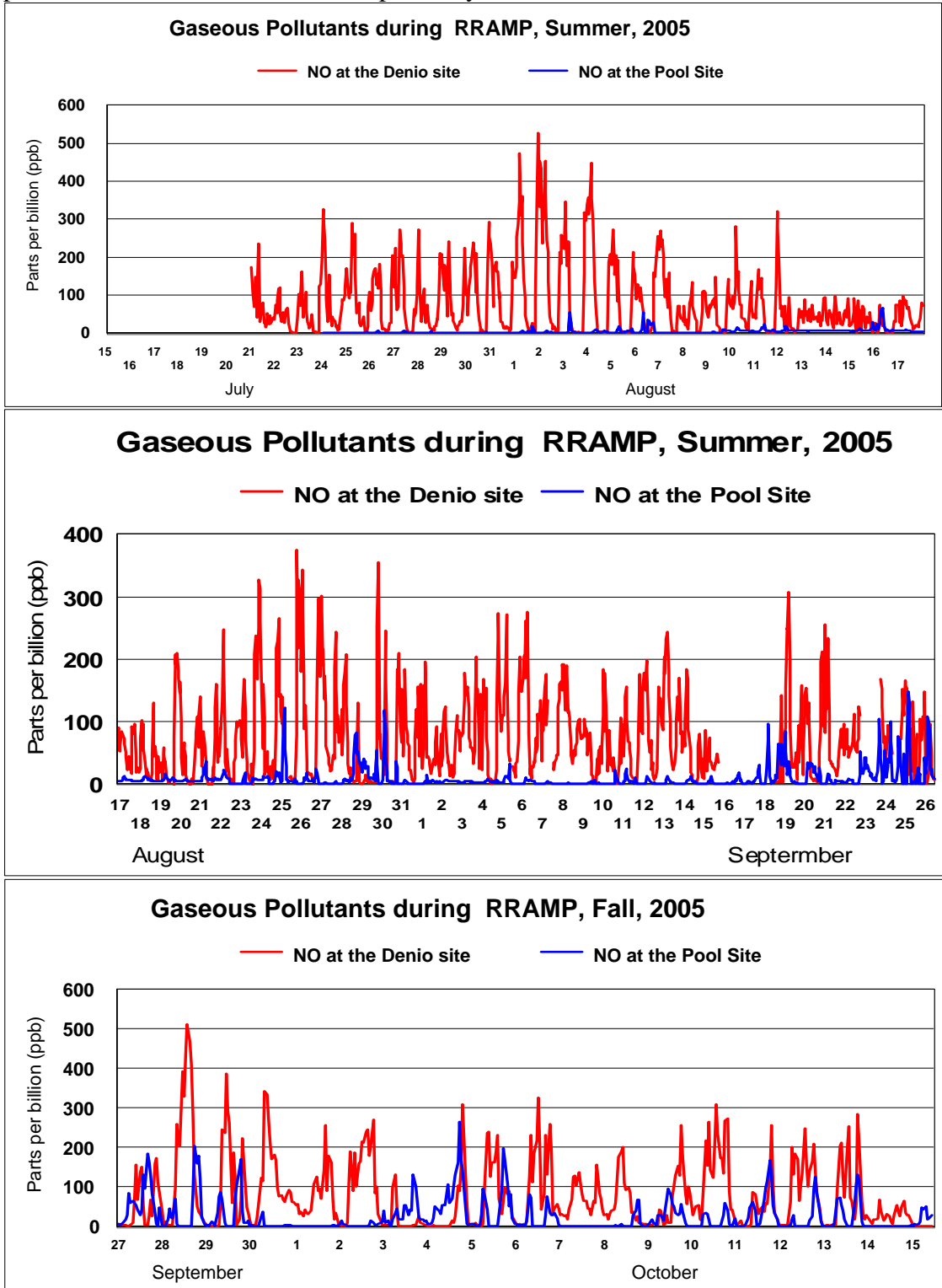


Figure 2 a, b, and c Data on nitric oxide (NO), July – October, 2005

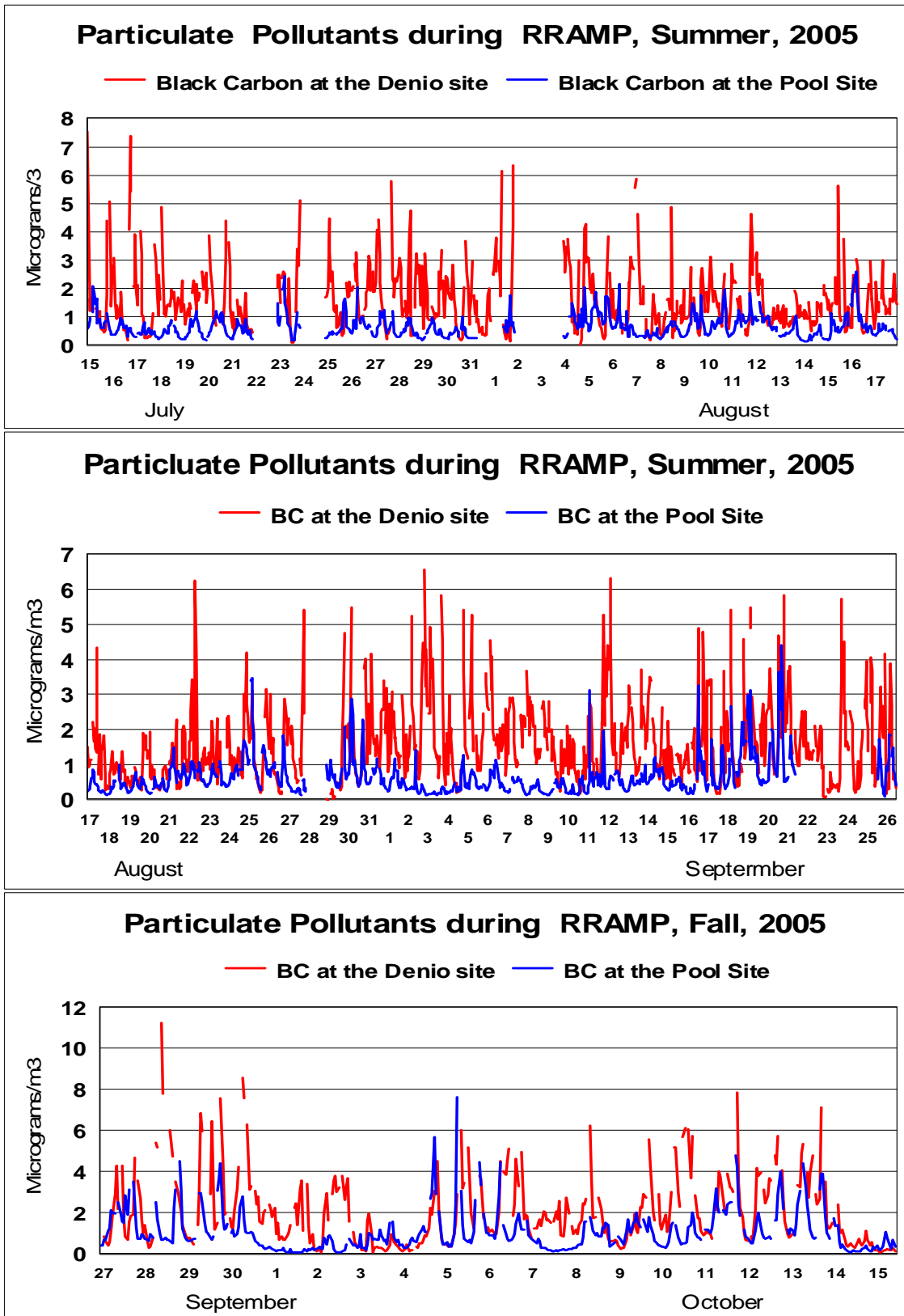


Figure 3 a, b, and c Data on “black carbon”, EC for July - October, 2005

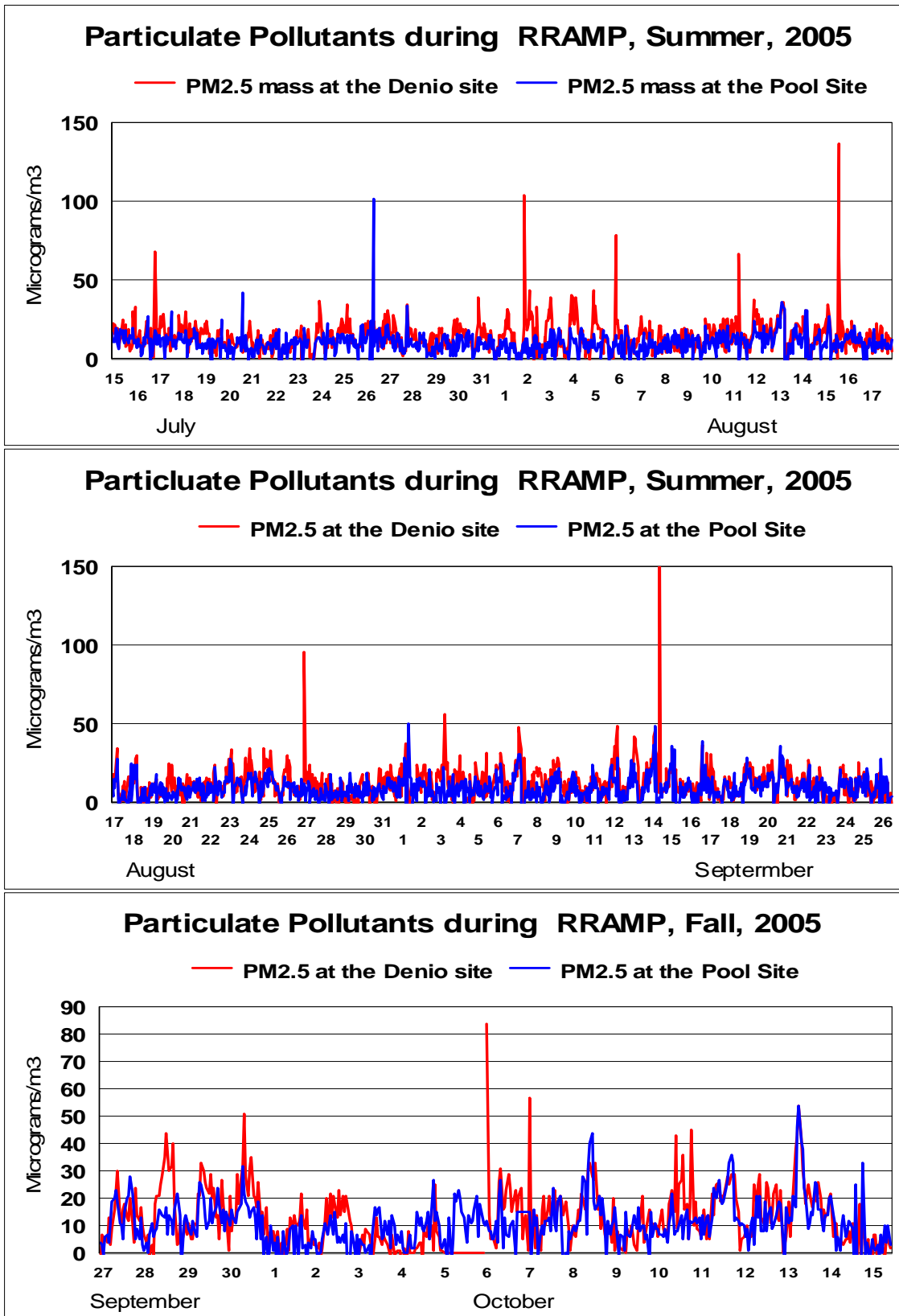


Figure 4 a, b, and c Data on PM_{2.5} mass, July – October, 2005

The role of trains, roughly 3/4 road haul, 1/4 switching, in generating NO_x for Placer County is shown in the 2005 Almanac summary, expressed as fraction of the total pollutant in each category. The table lists the top 8 contributors to NO_x, which amount to 96.9% of the total from all sources. Trains dominate NO_x, 24.2 % of the total, and SO_x, 63.3% of the total emissions.

Pollutant	TOG	ROG	CO	NO _x	SO _x	TSP	PM ₁₀	PM _{2.5}
Total (ordered by NO _x)	100.0	100.0	100.0	100.0	100.0	100.0	100.0	100.0
Trains	0.7	1.5	0.8	24.2	63.3	0.5	0.8	1.8
Off road vehicles (no trains)	8.4	19.6	25.1	21.1	4.1	1.5	2.4	5.1
Heavy duty trucks on road – diesels	0.3	0.6	0.5	13.4	4.1	0.2	0.4	0.9
Light duty trucks	5.0	11.8	18.4	10.7	2.0	0.3	0.5	0.8
Fuel combustion - commercial/utilities	1.4	1.5	1.1	10.1	4.1	0.5	0.9	2.0
Passenger cars	4.5	10.8	14.8	7.5	2.0	0.3	0.6	0.8
Medium and heavy Trucks - Gas	2.5	5.7	8.7	6.6	1.0	0.1	0.2	0.2
Residential fuel combustion	7.1	7.9	14.8	3.2	14.3	9.3	14.9	34.9
Fraction of total – 8 largest categories	29.9	59.4	84.2	96.9	94.9	12.9	20.7	46.5

Table 2 Placer County pollutant emissions for the 8 largest contributors to NO_x

2. Component B

UC Davis DELTA Group and Breathe California of Sacramento-Emigrant Trails (BC/SET) collaboration

The UC Davis DELTA Group and Breathe California of Sacramento-Emigrant Trails (BC/SET) collaborated with the RRAMP project to assist its ongoing studies of aerosol sources and transport in general and diesel exhaust in particular. The RRAMP program was ideal for this purpose, with an upwind-downwind measurement protocol across the Roseville Railyard and numerous measurements. The regional meteorology was stable (above), with typical summer conditions and a persistent across-yard air transport almost every night.

1. Sampling

a. Duration and Sites

Aerosol sampling was initiated on July 8 at the Denio site, 3 hr resolution, with 2 DELTA 8 DRUM inertial impactors operated on a side by side mode for quality assurance validation until July 12. One 8 DRUM was then moved to the Pool site. Both samplers delivered data until August 15, but only the very fine (vf) size mode ($0.26 D_p > 0.09 \mu\text{m}$) of the Pool site sampler met all QA checks because of an internal leak.

Sampling for organic analysis commenced with another DELTA 8 DRUM at the Denio site on August 5, running to September 27. Finally, two sets of samples were collected with high flow Lundgren impactors, Sept. 27 – Oct. 7, and Oct. 7 - Oct. 17, the latter only operating for 8 hrs each night, 10 PM – 6 AM. In all three cases, samples were integrated over the sampling time.

Denio Site	Sampler	Analysis	NO	NO _x	Black Carbon	PM _{2.5} mass
Sampling Periods	Substrate		ppb	ppb	$\mu\text{g}/\text{m}^3$	$\mu\text{g}/\text{m}^3$
7/21 – 8/17, 3 hr	8 DRUM, 16 L/min, Mylar	Mass, elements	81.0	120.2	1.2	14.4
8/5 – 9/27	8 DRUM, 16 L/min, aluminum	Organics	62.8	94.2	1.4	12.9
Average						
9/27 – 10/7 nights	Lundgren, 150 L/min, aluminum	Organics	87.6	120.8	1.8	11.1
10/7 – 10/17 nights	Lundgren, 150 L/min aluminum	Organics	69.2	101.3	1.8	14.2
Pool Site						
7/21 – 8/17, 3 hr	8 DRUM, 16 L/min, Mylar	Mass, vf elements	3.7	17.0	0.5	9.7
8/5 – 9/27,	None	None	8.3	26.2	0.6	9.3
9/27 – 10/7,	None	None	30.8	59.5	1.0	9.6
10/7 – 10/17,	None	None	17.7	45.9	1.0	12.2

Table 3 Sampling schedule and mean RRAMP monitoring data for the four time periods utilized.

Below we summarize the RRAMP air monitoring data averaged over the sampling periods of the DRUM samplers.

Site	Wind	Pool	Denio	Pool	Denio	Pool	Denio	Pool	Denio
Pollutant	Speed	NO	NO	NO ₂	NO ₂	EC	EC	PM _{2.5}	PM _{2.5}
Units	mph	Ppb	ppb	ppb	ppb	µg/m ³	µg/m ³	µg/m ³	µg/m ³
7/21 – 8/15	4.32	3.63	80.34	16.60	119.20	0.5	1.2	9.7	14.3
8/5 – 9/27	4.36	8.10	63.02	26.01	94.80	0.6	1.4	9.4	13.0
9/27 – 10/7	3.67	31.39	85.63	60.01	118.29	1.0	1.8	9.3	10.9
10/7 – 10/17	3.83	17.87	73.87	46.08	107.36	1.0	1.8	12.5	14.6
2/10 - 2/24									

Calculating differences and ratios, it become clear that nitric oxide (NO) has the best discrimination between rail yard and non-rail yard sources in summer, (x 22.1) with NO₂ close behind (x 7.2). Black carbon (EC) (x 2.3) is significantly worse, while PM_{2.5} is not very specific to the rail yard, as expected. (x 1.48)

Site	Denio - Pool	Denio/Pool	Denio - Pool	Denio/Pool	Denio - Pool	Denio/Pool	Denio - Pool	Denio/Pool
Pollutant	NO	NO	NO ₂	NO ₂	EC	EC	PM _{2.5}	PM _{2.5}
Units	ppb	Ratio	ppb	Ratio	µg/m ³	ratio	µg/m ³	ratio
7/21–8/15	76.7	22.1	102.6	7.2	0.7	2.3	1.5	1.48
8/5 – 9/27	54.9	7.8	68.8	3.6	0.8	2.5	1.4	1.38
9/27–10/7	54.2	2.7	58.3	2.0	0.8	1.8	1.2	1.17
10/7–10/17	56.0	4.1	61.3	2.3	0.8	1.8	1.2	1.17
2/10 - 2/24								

Table 4a, 4b Denio site versus Pool site comparisons in parallel with DELTA Group sampling periods.

Note the breakdown of the clean summer Denio versus Pool downwind-upwind relationship as the program pushed into fall months.

The excess black carbon, assigned to the rail yard, is remarkably constant at 0.7 µg/m³, or about ½ of the PM_{2.5} mass increment. It is also clear that the relationship, rail yard to non rail yard sources, is significantly poorer by the fall months, but the rail yard contribution is still about the same value. This may, however, be misleading as the Pool Site upwind values are rising sharply by fall, as much as a factor of 2 to 5 for the tracer species, so the difference and ratio are degraded while the concentrations are relatively stable.

Thus, the monitoring data show that the Denio Site is the optimum site for measuring organic species at the Roseville Railyard even in the early fall periods

b. Sampling Equipment

The samplers used were DELTA Group 8 DRUM inertial impactors (Cahill et al, 1985). These slotted impactors are based on the Lundgren impactor (Cahill and Wakabayashi, 1993) with theoretical and experimental validation of sizing (Raabe et al, 1989). The DRUM collects aerosols continuously onto 8 slowly rotating drums in 8 size modes: 10 to 5.0, 2.5, 1.15, 0.75, 0.56, 0.34, 0.26, and 0.09 μm aerodynamic diameters. One sampler, the Pool site, was an older model that had to be modified to meet equivalent upwind – downwind comparison.

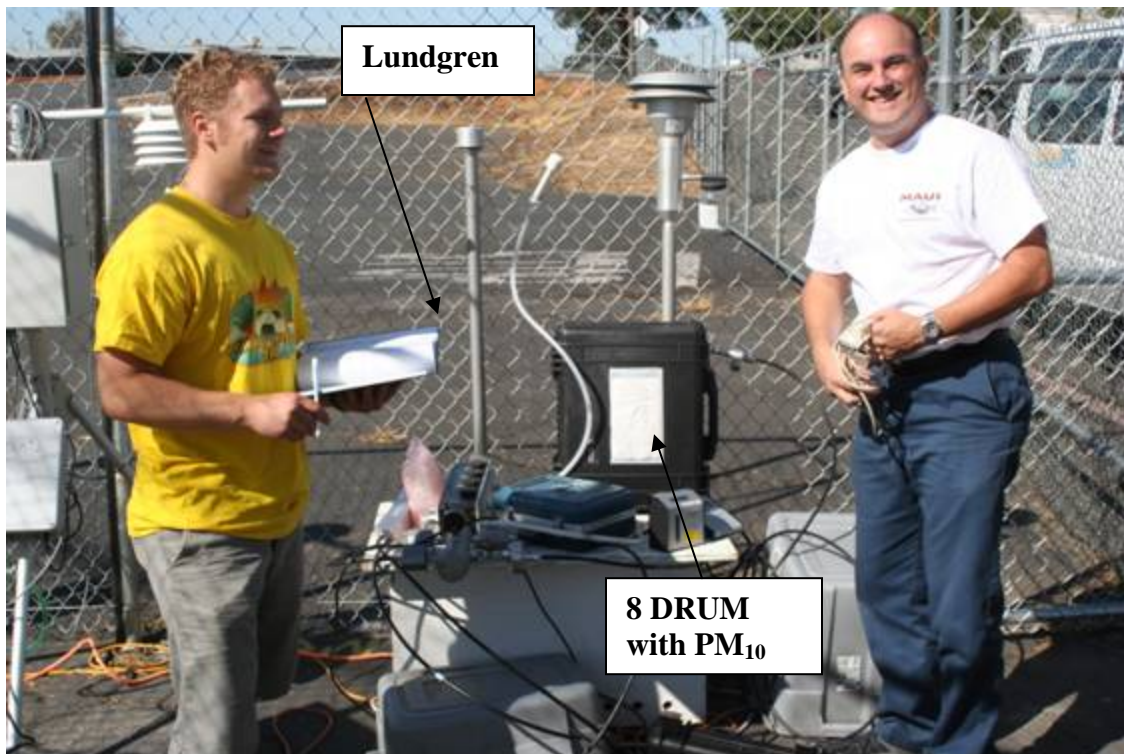


Figure 5 Nick Spade (left) and David Barnes at the Denio site, Sept. 27, 2005. The cattle auction buildings of the Denio's Farmer's Market are seen behind them, across a large parking lot.

c. Quality assurance

Full quality assurance documentation for DRUM samplers, and references on their use, are contained in the DRUM Quality Assurance Protocols version 1/05 (DQAP v 1/05) available on the DELTA web site: <http://delta.ucdavis.edu>. A printed copy will be supplied with this Final Report, and a summary is included in Appendix QA.

As an example, we include below a precision test of soft beta ray mass analysis on a RRAMP DRUM strip. Analysis was completed for mass values every 1 ½ hours in 8 size modes for the entire period. Each strip was analyzed at least 2 times, and the standard deviation of the data is included in the data file.

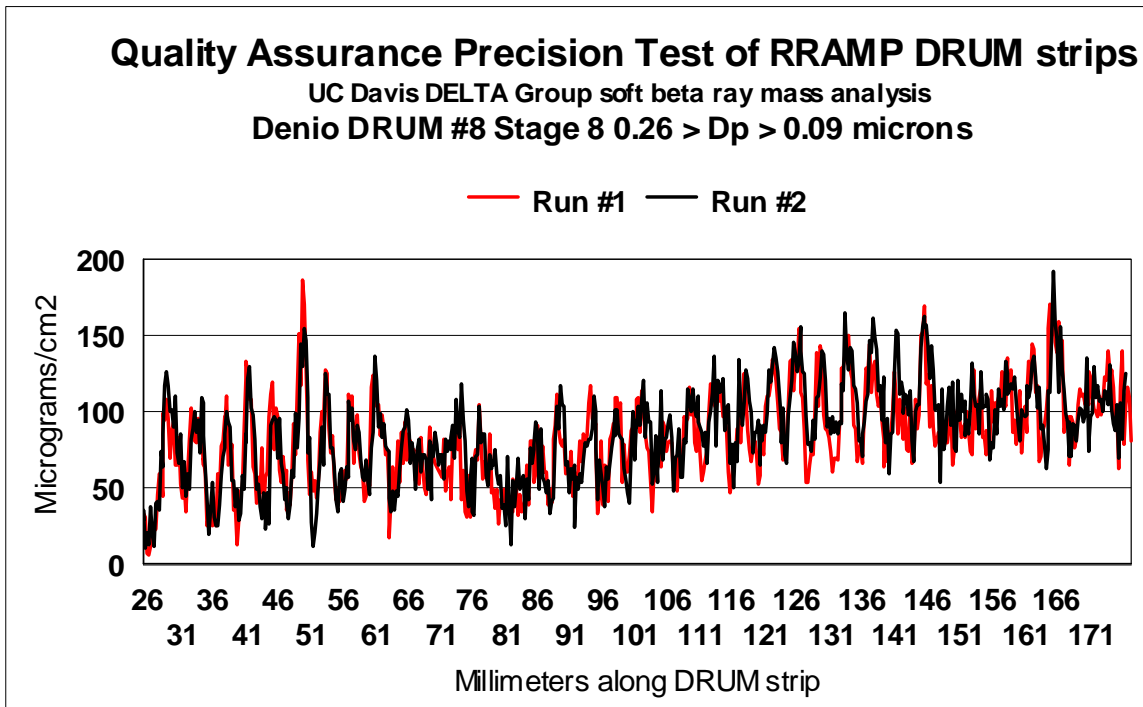


Figure 6 Precision test for mass

Note that since the strip was remounted, the test also validates relative time precision. Any measurements where the analysis differs by more than $\pm 10\%$ are independently re-run until agreement is achieved.

The samples collected by the DRUM sampler are designed to allow highly sensitive elemental analysis by the new DELTA Group designed aerosol analysis system of the x-ray micro beam of the Advanced Light Source, Lawrence Berkeley NL (Bench et al, 2002). The method, synchrotron-induced x-ray fluorescence (S-XRF) has been used by the DELTA Group since 1992, (Cahill et al, 1992) but in its present form since 1999.

Study and date	Methods	Average ratio, Al to Fe	Std. dev.	Average ratio, Cu to Pb	Std. dev.
BRAVO, 1999	PIXE vs S-XRF	0.99	0.04		
BRAVO, 1999	CNL XRF vs S-XRF			1.24	0.14
FACES, 2001	ARB XRF vs S-XRF	0.93	0.21	1.02	0.08
FACES, 2001	ARB RAAS vs S-XRF	(0.98)	0.27	(0.74)	0.23
ARB LTAD 2005	DRI XRF vs S-XRF	1.037	0.085	0.907	0.009
All prior studies	Average	0.984	0.15	0.977	0.115

Table 5 S-XRF comparison, all blind tests since 1999

The S-XRF system has been tested in blind inter-comparisons since 1999, and all of these are shown above. Typically 32 elements are recorded for each analysis, all of which can be traced back to NIST primary (SRM # 1832, SRM # 1833) or secondary (Micromatter thin film) standards. MDLs are included in Appendix QA.

2. Results
a. Mass

All results are provided on a CD in the form of Excel spread sheets. The DRUM Quality Assurance Protocols (DQAP ver 1/05) are included by reference, but a hard copy (135 pages) can be downloaded if required.

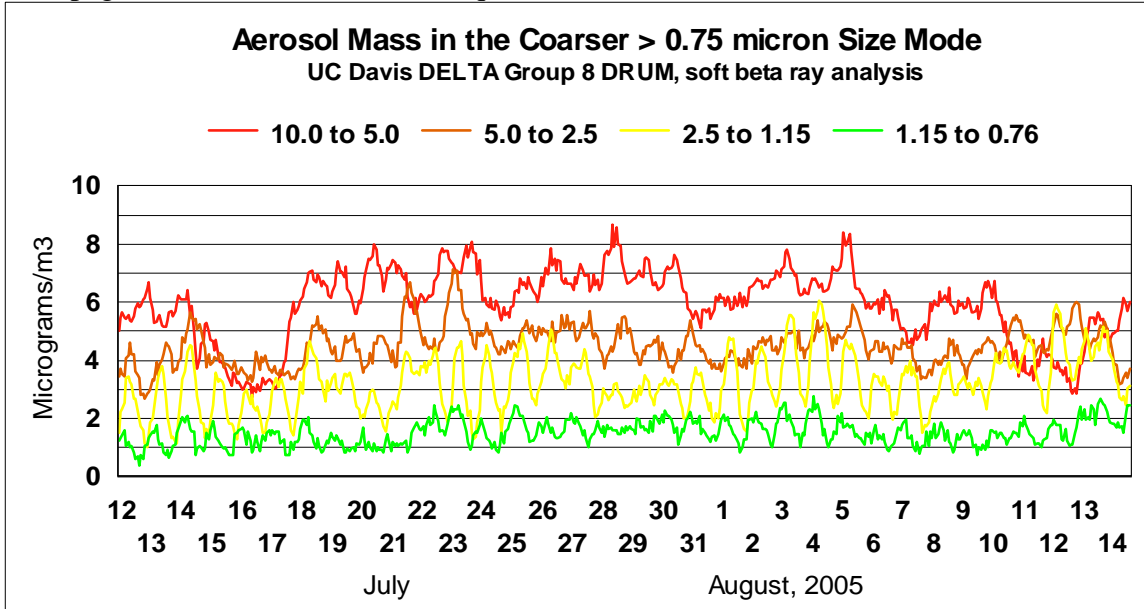


Figure 7 Mass from 10.0 to 0.75 μm

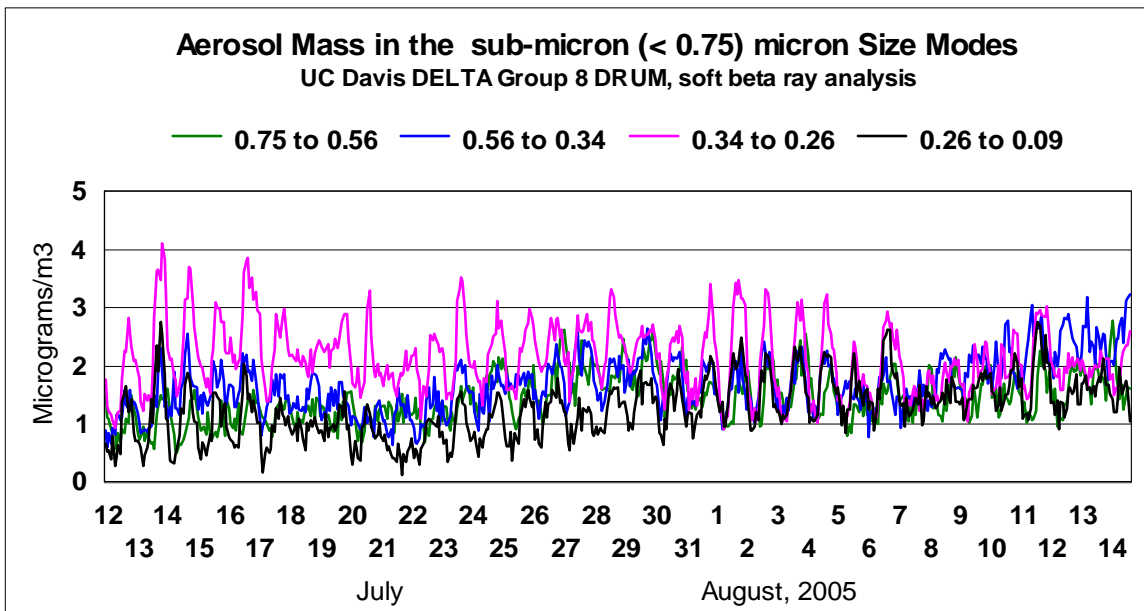


Figure 8 Mass from 0.75 to 0.09 μm

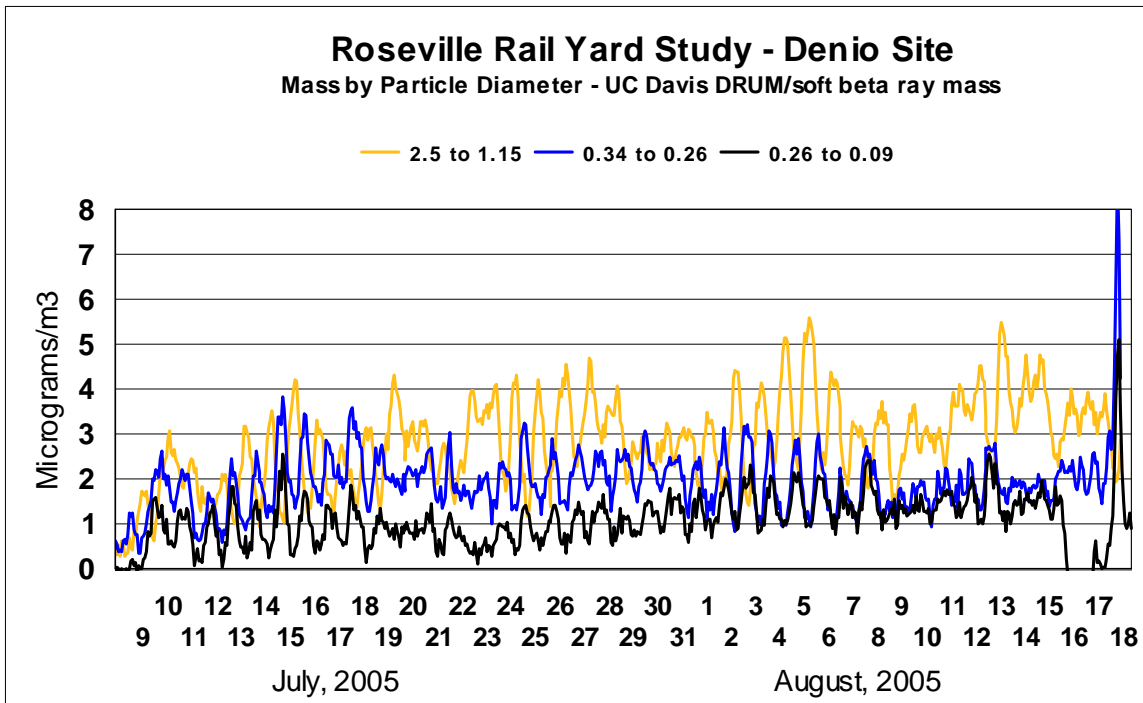


Figure 9 Three components of fine mass versus time

Above we present the sub-2.5 μm soils (to 1.15) and the very fines soot like particles. The most striking results were the very highly correlated very fine particles (0.34 μm) at night anti-correlated with fine mass in the 2.5 to 1.15 μm mode, typically fine soil in the summer Central Valley conditions. The night mass peaks can confidently be assigned to rail yard aerosols. Below we compare the very fine micron mass (0.26 > D_p > 0.09 μm) from the Pool site and the Denio site.

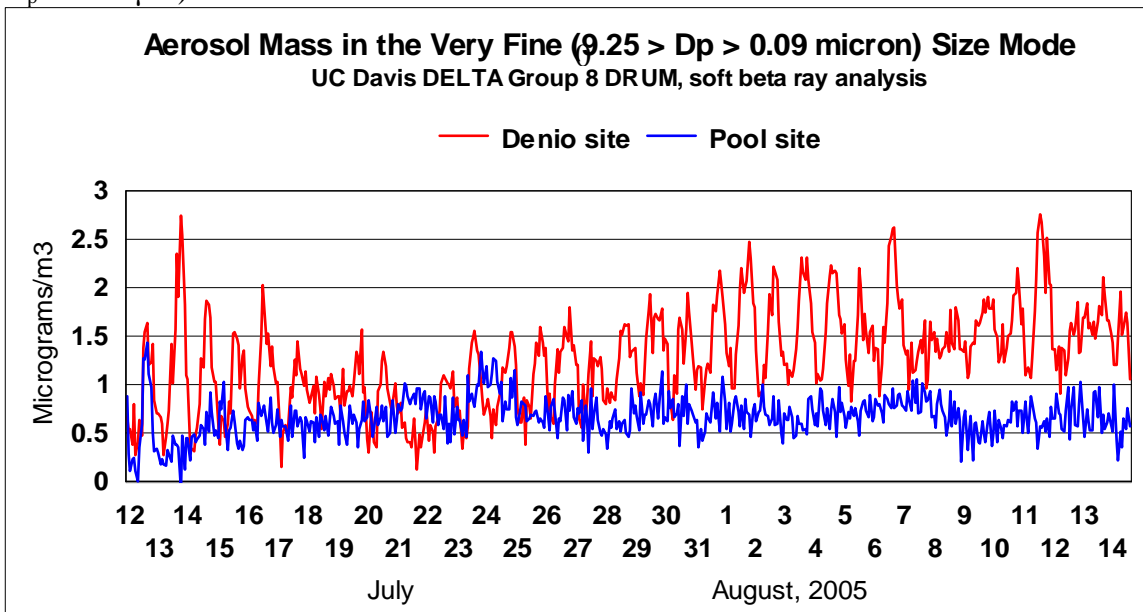


Figure 10 Comparison of the Pool and Denio sites for very fine mass

Detailed meteorological analysis is needed to interpret these data, augmented by high resolution data such as NO to properly assign DRUM time signatures. However, there are periods (July 14 – 16, July 29 – August 7) when daytime values at the Denio and Pool sites are similar and 6 hr average nighttime values at the Denio site are enhanced, with an approximate mean value of $1.35 \pm 0.27 \mu\text{g}/\text{m}^3$.

Average Denio/Pool difference for 9 hrs, 10:30 PM to 7:30 AM, for the July-August DRUM sampling period, was $0.83 \mu\text{g}/\text{m}^3$. The median (a better estimate) was $0.87 \mu\text{g}/\text{m}^3$, and maximum was $1.53 \mu\text{g}/\text{m}^3$. We can compare these data with the data for mass of black carbon (EC), since EC is known to be primarily in the very fine mode. The EC difference, Denio – Pool, was $0.7 \mu\text{g}/\text{m}^3$, while the average DRUM very fine mass difference was $0.83 \mu\text{g}/\text{m}^3$ (for $\text{PM}_{2.5}$, the value was $1.5 \mu\text{g}/\text{m}^3$). However, recall that this DRUM did not have an after filter for the $< 0.09 \mu\text{m}$ particles and thus would lose some mass.

There is an enormous amount of information on particle size, but interpretation of these data is hampered by lack of Pool site data and elemental analysis of the coarser modes. Nevertheless, below we plot 9 hr (9 PM- 6 AM) nighttime mass distributions at the Denio site for 5 days in early August when the very fine mode Pool site-Denio site comparisons indicate direct rail yard influence.

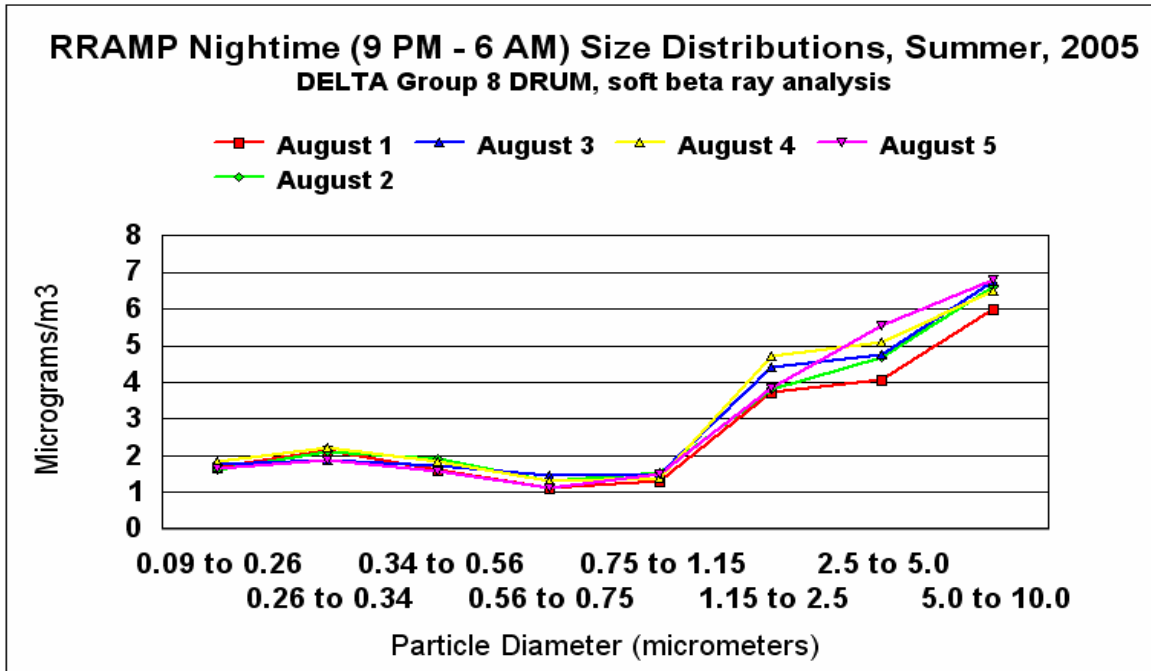


Figure 11 Nighttime (9 PM – 6 AM) mass size profiles for early August at the Denio site.

We can compare these data to other measurements of diesel exhaust in laboratory and field conditions. Below we plot these data for July 15 and compare them with a recent (2005) study we are doing with Johns Hopkins University on the Baltimore McHenry tunnels, one bore of which is all truck traffic and overwhelmingly diesel. These

data are then compared to a 2002 study with the U. of Minnesota diesels in the laboratory, an average of 6 different runs, mostly with California fuel (Zielinska et al, 2004).

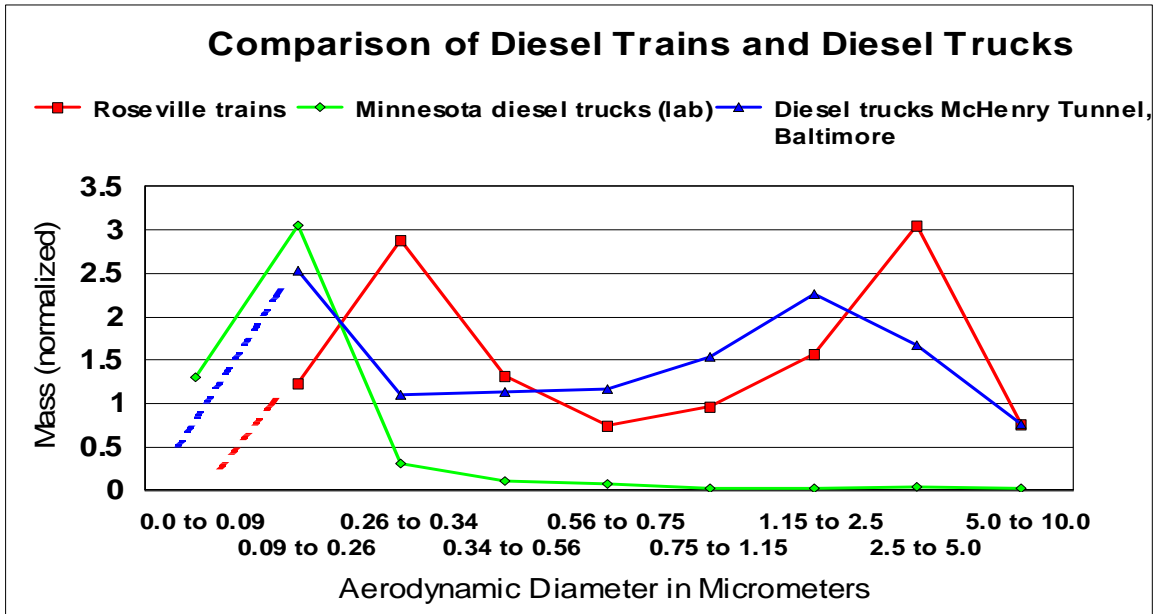


Figure 12 Size mode of aerosol mass, July 15, versus other recent diesel studies

From the plots, it is clear that the very fine and accumulation size modes of the diesel exhaust from the rail yard are considerably coarser in particle size than that in the laboratory or tunnel diesel trucks signature, while the coarse modes mimic the tunnel data.

b. Elemental data – very fine particles at the Denio and Pool sites
i. Denio Site

The Stage 8 sample from the Denio site was selected for elemental analysis by S-XRF as this stage is the size mode heavily represented in diesel exhaust (Zielinska et al, 2004). The strip was analyzed in 3 hr increments, resulting in 320 analyses with almost 9,000 data values and 9,000 individually calculated errors.

An example of the almost 9,000 elemental data, each with an associated error, is shown below for three elements previously identified with diesel exhaust from trucks (Zielinska et al, 2004), phosphorus and zinc from the zinc thio phosphate stabilizer in lubricating oils, sulfur from the fuel.

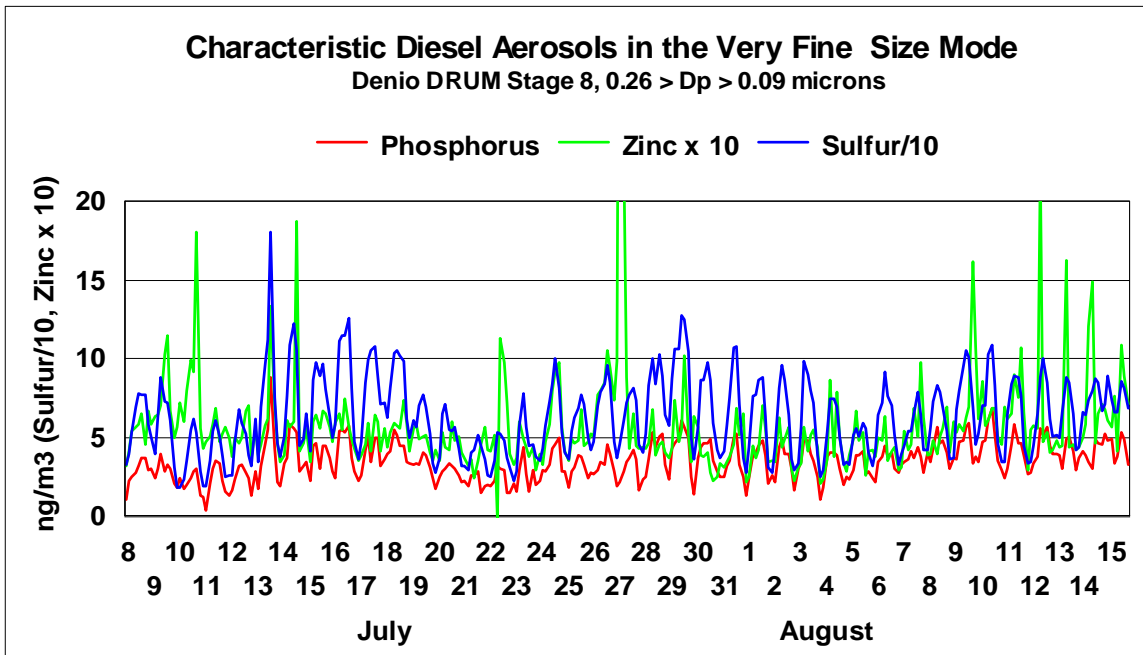


Figure 13 Typical elemental signatures of diesel, Denio site very fine mode

These elements had been seen earlier in this size mode in our work in Zielinska et al 2004, and tied to their sources in the fuel and lubricating oil.

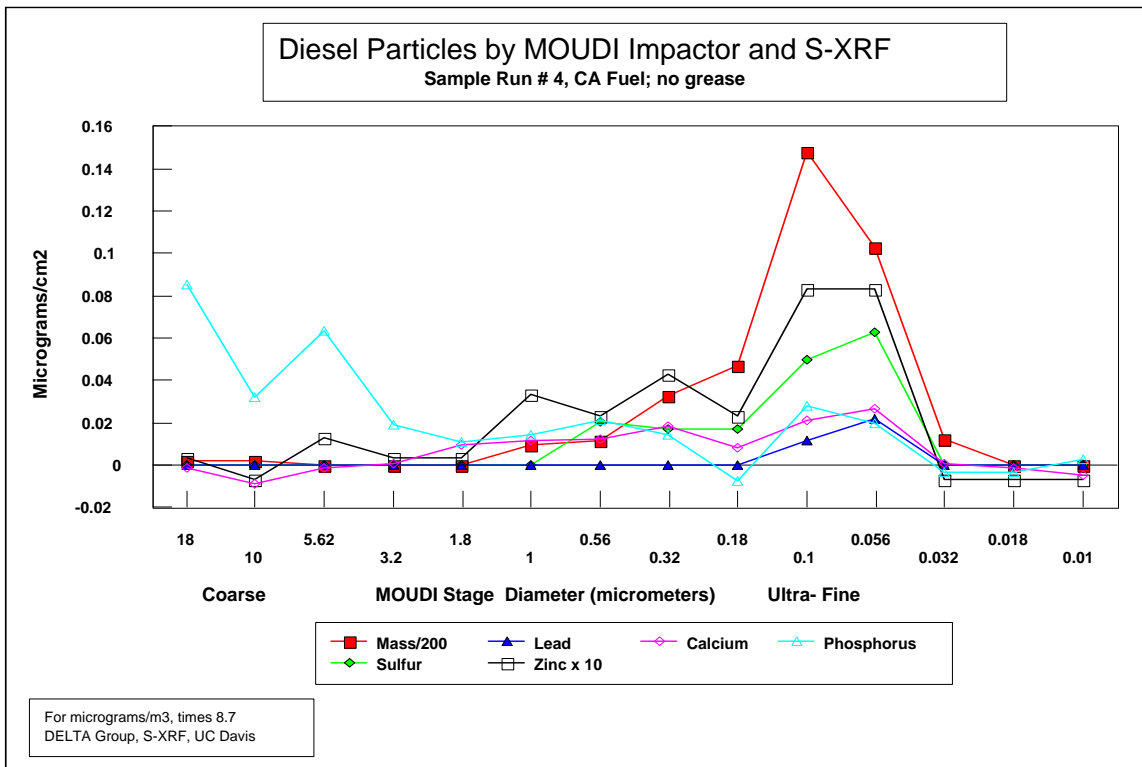


Figure 14. Zielinska et al diesel characterization results

There are additional very fine aerosols that have strong nighttime signatures.

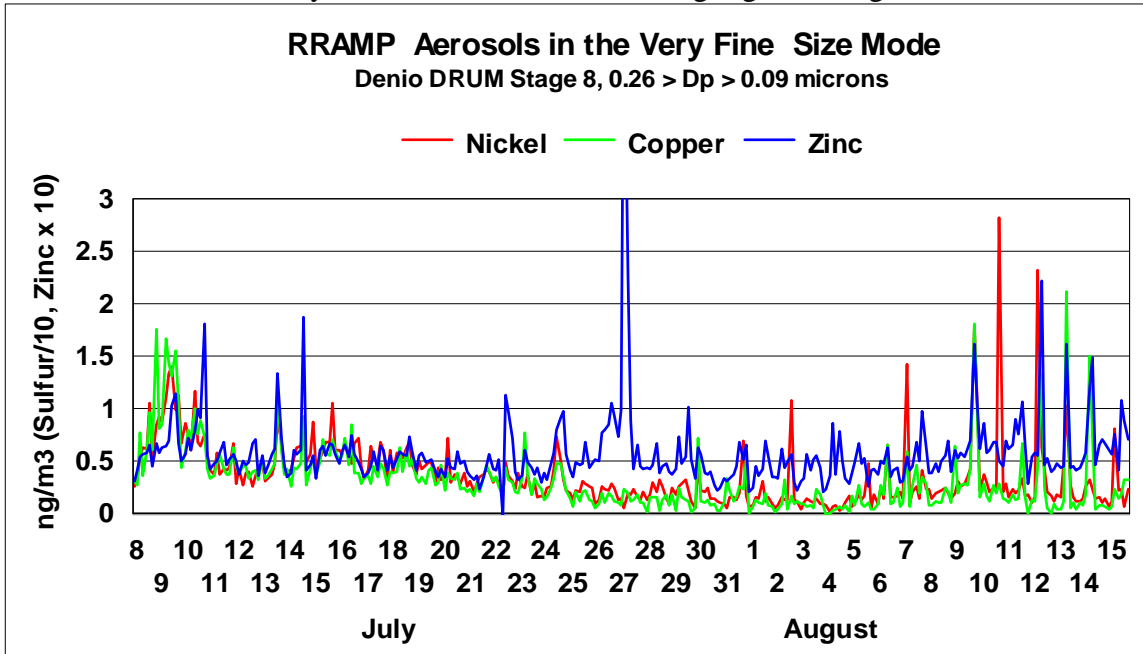


Figure 15 Transition mode elements nickel, copper, and zinc in the Denio site very fine mode.

Below we show some aerosols that would be, in coarser modes, derived from soil (Si, K, Ca, Fe) or in a finer mode, wood smoke (K).

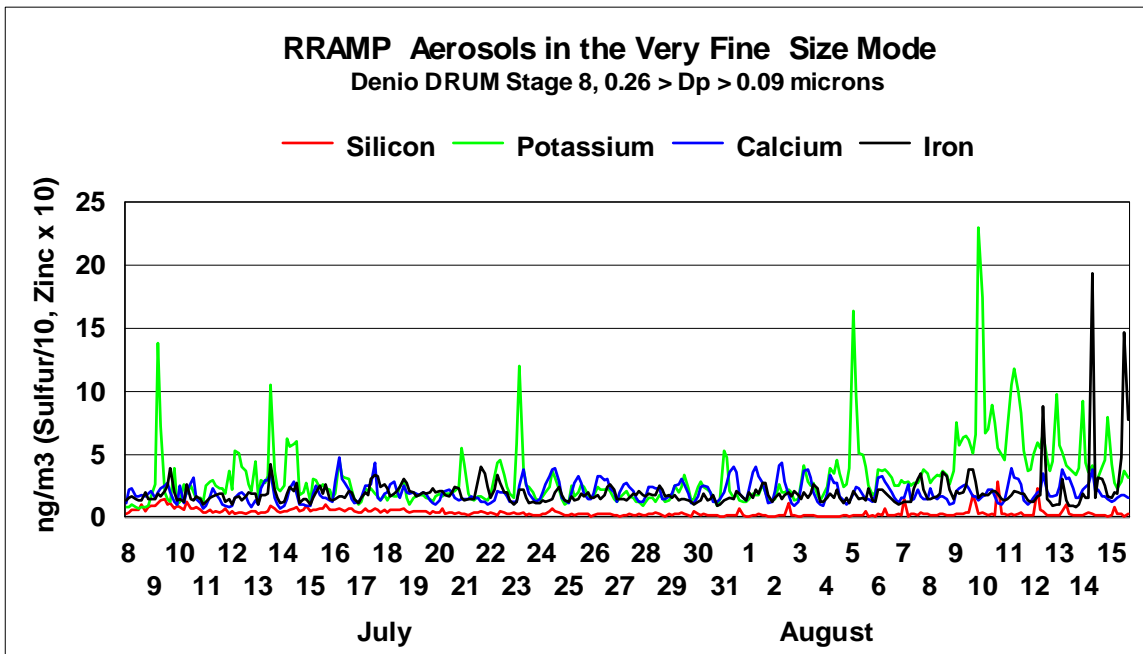


Figure 16 Crustal elements in the very fine mode, Denio site

Combining the mass and elemental data, we can identify sources for the observed mass. Below we show a few days in early August, associating the nighttime mass peaks with characteristic diesel effluents. Note the anti correlated mass near PM_{2.5}, associated with stronger daytime winds

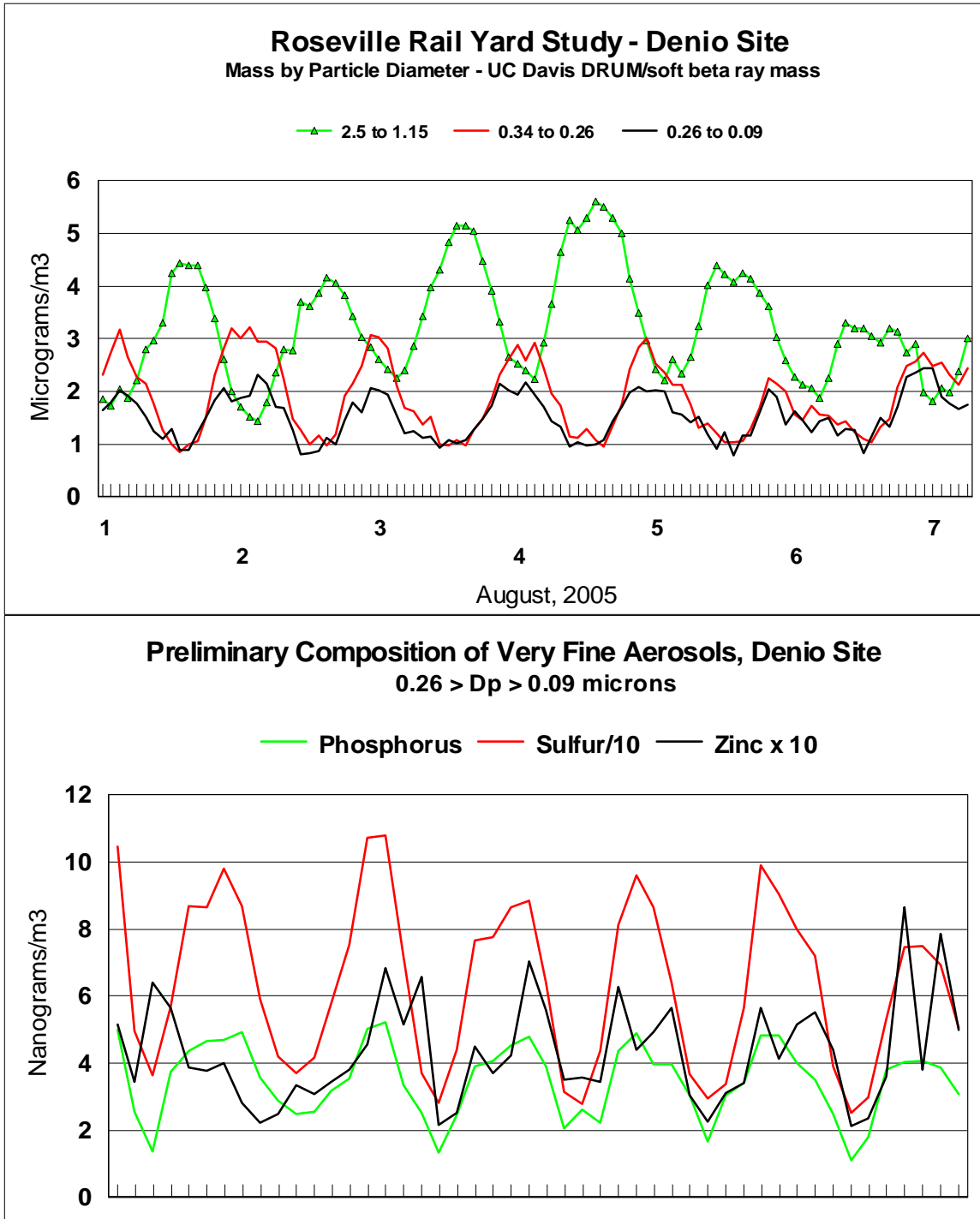


Figure 17 Mass versus typically diesel signature elements, Denio site

ii. Pool Site

The mass data show that in the very finest mode of the Pool site DRUM sampler, the critical orifice Stage 8 from $0.26 > D_p > 0.09 \mu\text{m}$, had run properly. The mass delivered was equivalent ($0.72 \mu\text{g}/\text{m}^3$ Denio, $0.68 \mu\text{g}/\text{m}^3$ Pool, each with an error of $\pm 0.2 \mu\text{g}/\text{m}^3$) when the Denio and Pool samplers were co-located at the Denio site from July 8 through July 12. Thus, the DELTA Group could safely compositionally analyze the samples by S-XRF. We report here the preliminary data pending the required S-XRF precision re-analysis protocol Level 1 of DQAP ver 1/06.

The results were again compared at the co-located site and were again equivalent. For the 5 major elements, which make up 87% of all S-XRF elemental mass, the ratio, Pool/Denio, was 0.97 ± 0.27 . On the other hand, two trace elements, Ni and Cu, did not agree, while there was also some excess soil seen in the first few hours of sampling, probably from contamination in handling. Since the amount of soil on this stage is \ll soil on coarser stages, we are hesitant to make conclusions on the small amount seen even though, because of the greased stages, the bounce-through is < 1 part in 5,000.

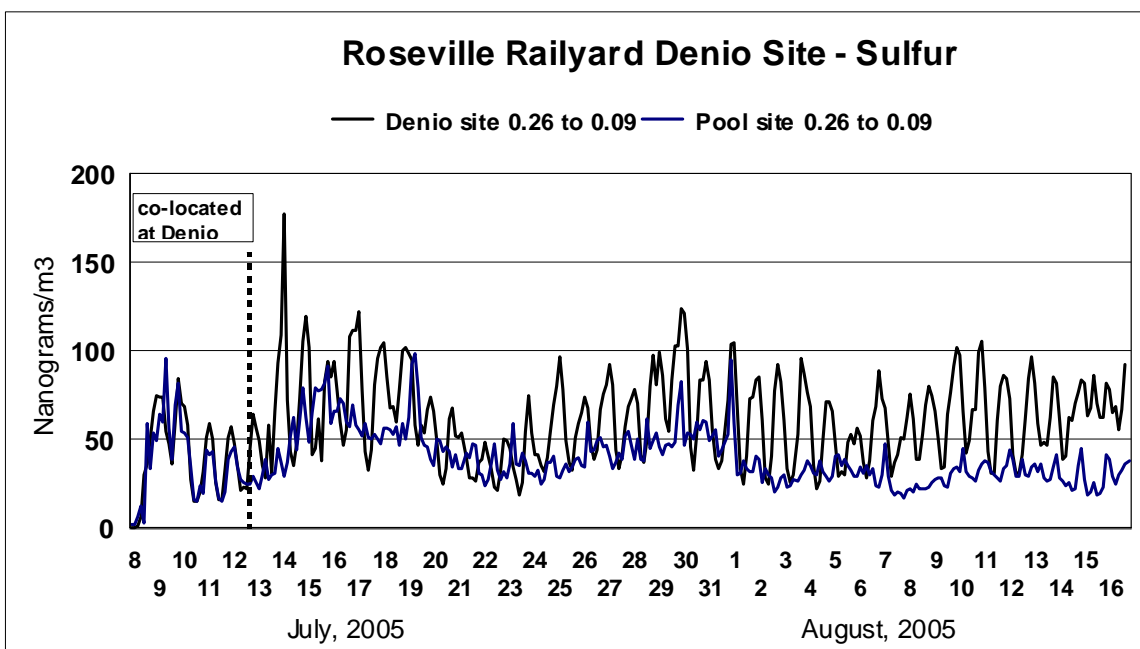


Figure 18 Comparison of very fine sulfur, Denio Site vs Pool Site

The largest element in the very fine particle mode was sulfur, which is most likely in the sulfate state. This will cause the values below to be increased by a factor of 3.0, making sulfate a major fraction of the observed very fine mass. The agreement during the co-located days is excellent. After moving the second DRUM sampler to the Pool site, the systematic nighttime enhancement disappears except for rare instances (August 1). Very fine sulfur is normally a signature of diesel fuel combustion.

Phosphorus is normally a signature of the combustion of lubricating oil from the zinc thio-phosphate stabilizer. It, too, shows a nighttime enhancement synchronous with sulfur, but there are also other sources present at the upwind site, perhaps reflecting the heavy nighttime truck traffic on I-80. However, the phosphorus spike on July 18 is clearly some special situation that requires much more analysis.

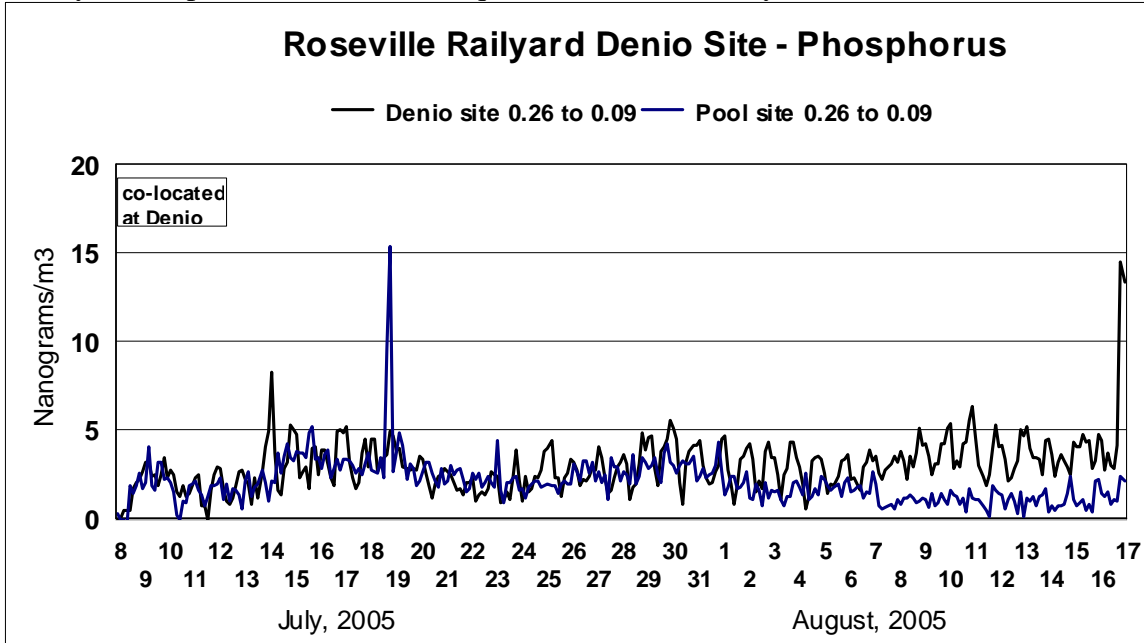


Figure 19 Comparison of very fine phosphorus, Denio Site vs Pool Site

Zinc, on the other hand, clearly has numerous sources in the area, although in August we do see a systematic nighttime enhancement.

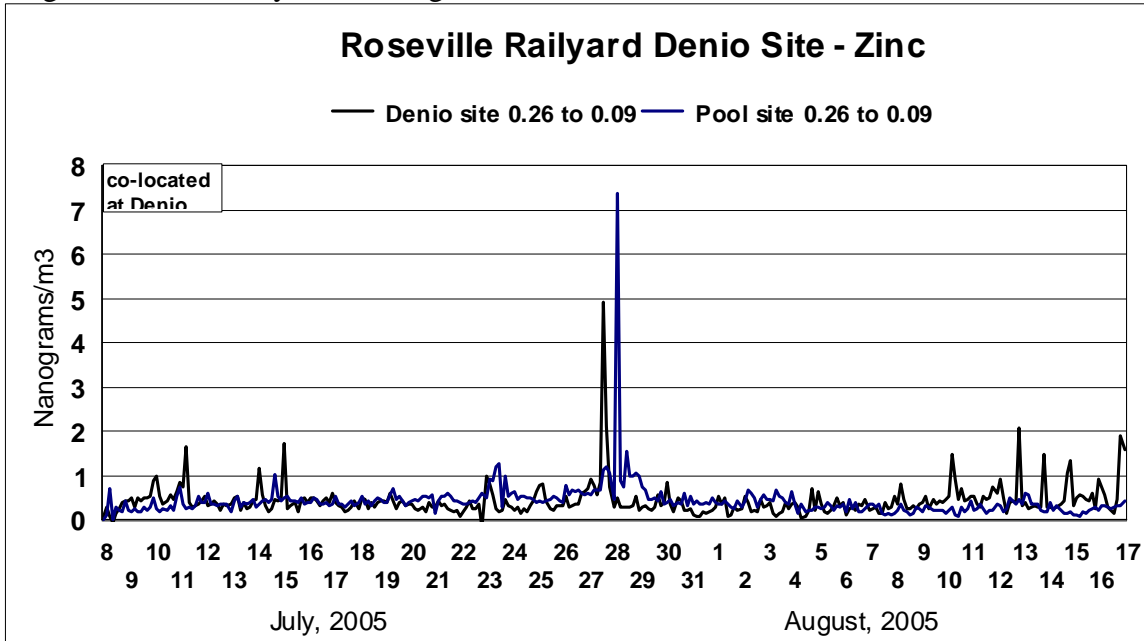


Figure 20 Comparison of very fine zinc, Denio Site vs Pool Site

The last element systematically associated with diesel combustion is calcium, which in this very fine size mode is a tracer of calcium carbonate, an antacid in the lubricating oil. Sodium carbonate is also used in some oils, which may be the source of the relatively high sodium numbers.

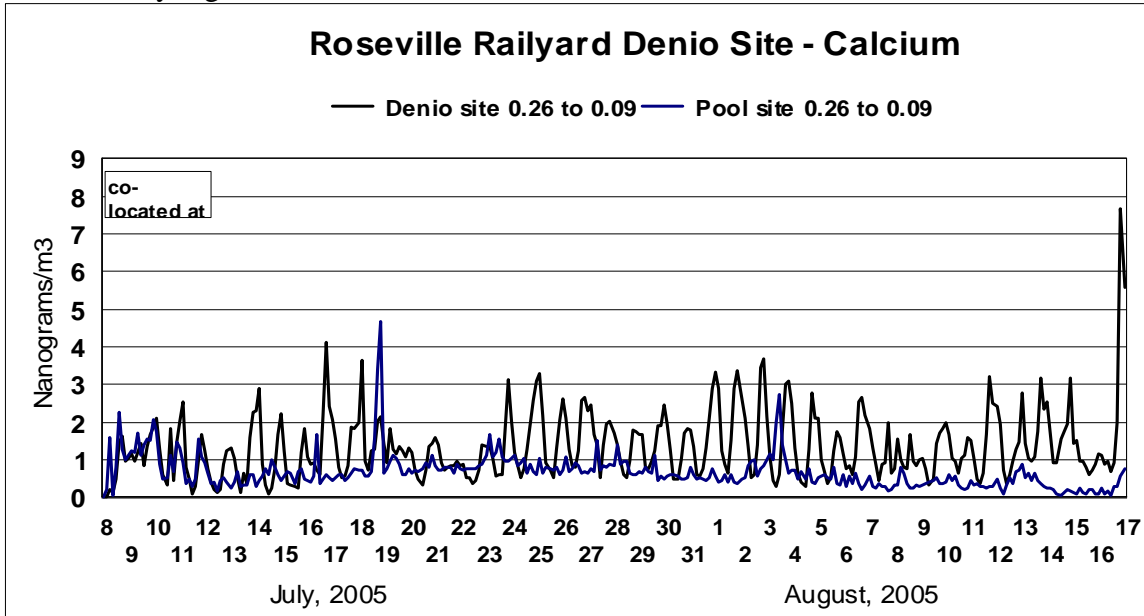


Figure 21 Comparison of very fine calcium, Denio Site vs Pool Site

In addition to the expected elements from the combustion of diesel fuel and lubricating oil, we observe other elements. Copper and nickel behave in a similar manner and have poor agreement at the co-located site for reasons that are not clear at this time, but based upon agreement in re-analysis, is probably accidental contamination of the first 8 cm (first 20 days of July).

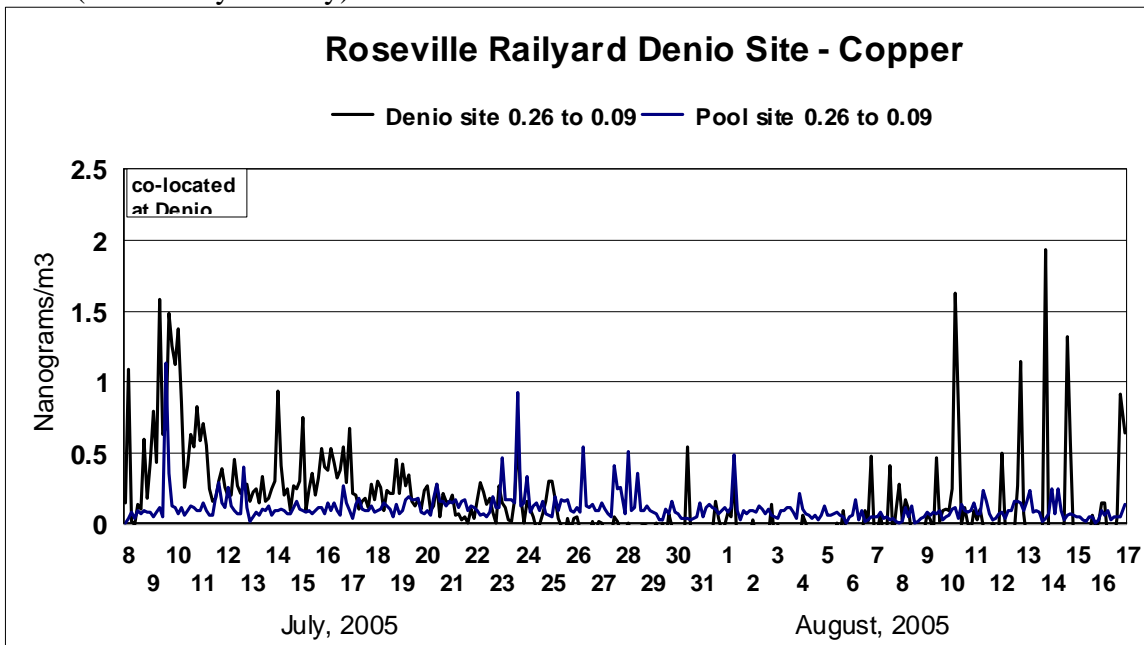


Figure 22 Comparison of very fine copper, Denio Site vs Pool Site

Until we can do further analyses, we must assign much of the Denio signal for these elements for the first 10 days to contamination, either on the drums or perhaps in the air, since it is well known that some motors give off a fine copper aerosol. Note that there was also an anomalous mass signature for the very coarsest particles for the first few days at Denio site, strengthening the argument for contamination.

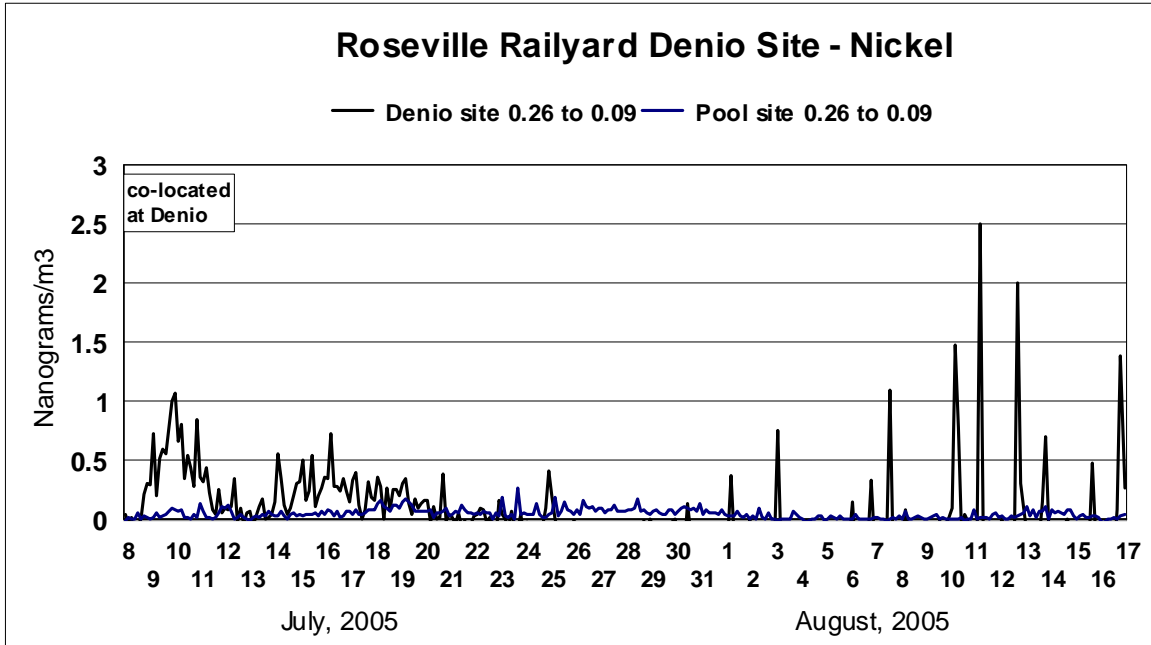


Figure 23 Comparison of very fine nickel, Denio Site vs Pool Site

Potassium, on the other hand, is usually dominated by internal combustion engines in this size mode. Potassium from wood smoke peaks in the 0,34 to 0.56 μm mode.

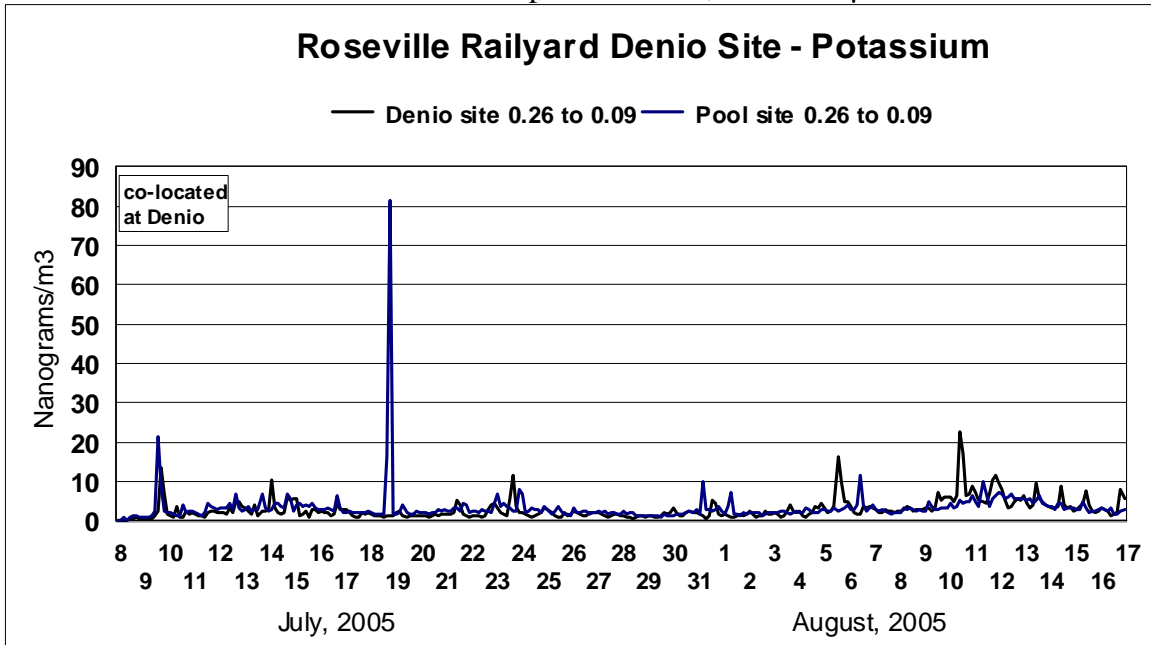


Figure 24 Comparison of very fine potassium, Denio Site vs Pool Site

Vanadium is used in metallurgy and has a very high boiling point. It also occurs naturally in soil at a trace level. However, in this size mode, it is almost certainly from some high temperature process. The nighttime enhancement was unexpected.

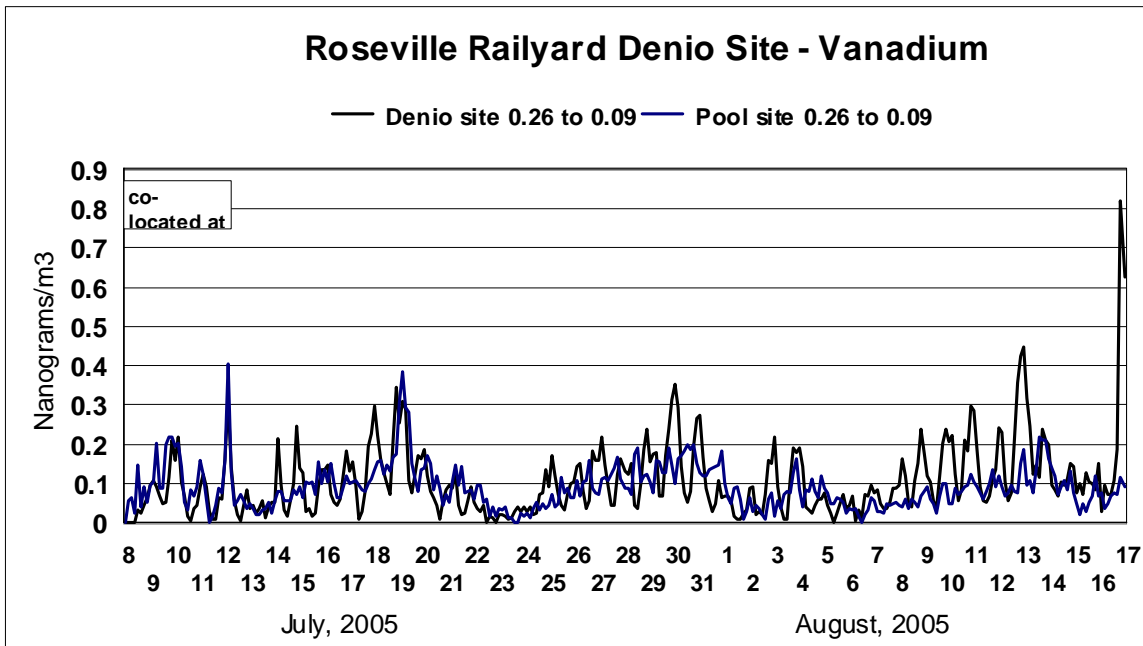


Figure 25 Comparison of very fine vanadium, Denio Site vs Pool Site

Chromium has similar behavior to vanadium metallurgically, but has a very different behavior in RRAMP.

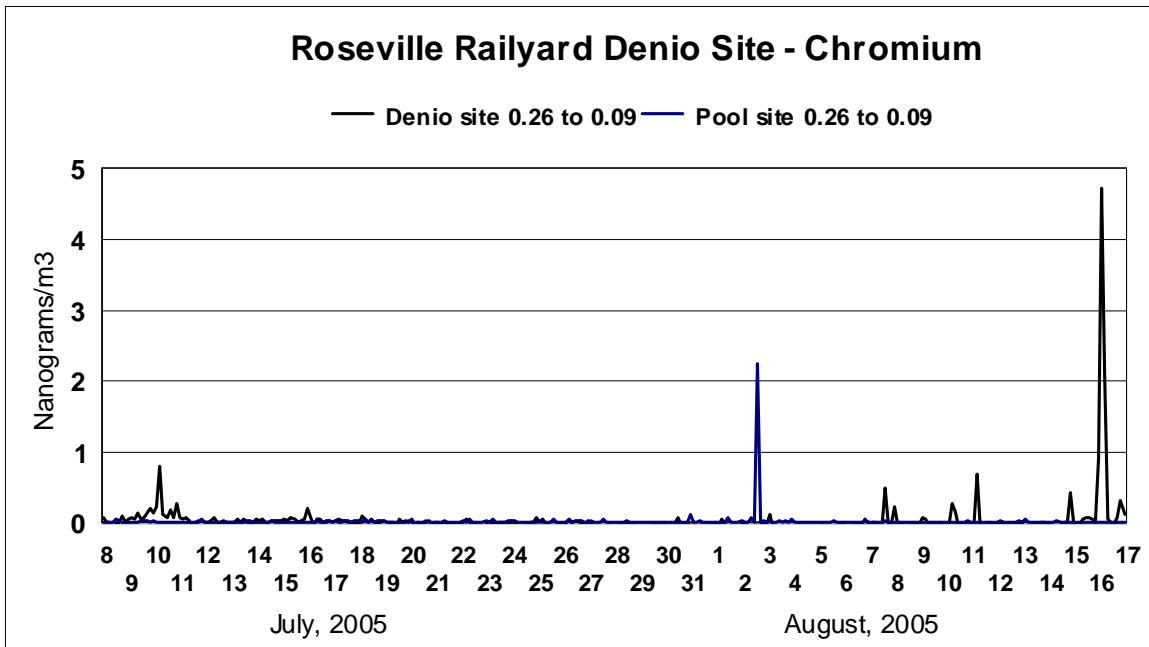


Figure 26 Comparison of very fine chromium, Denio Site vs Pool Site

In summary, the elemental data support and confirm the nighttime enhancement of aerosols expected from operations of the Roseville Railyard while identifying other components of unknown origin. With the completion of the EPA Region 9 grant, full elemental size distributions will be available at the Denio site, which will greatly assist us in interpreting the data. We will also have the repeat runs which are part of the Level 1 quality assurance protocols for S-XRF, similar to those shown earlier for mass.

3. Component C

Enhancement of aerosol data by S-XRF analysis at the Denio site; all size modes

The presence of a relatively large amount of mass (Figures 8 and 9) at sizes not typical of fresh diesel exhaust encourage DELTA to propose to measure these species to complete the picture of aerosols at the Denio site in summer. Thus, the un-analyzed DRUM Stages 1 through 7 (10.0 to 5.0, 5.0 to 2.5, 2.5 to 1.15, 1.15 to 0.75, 0.75 to 0.56, 0.56 to 0.34, 0.34 to 0.26 μm aerodynamic diameter) were analyzed by S-XRF in 3 hr increments.

The first result was the discovery of periodic oceanic influence in the form of sea salt.

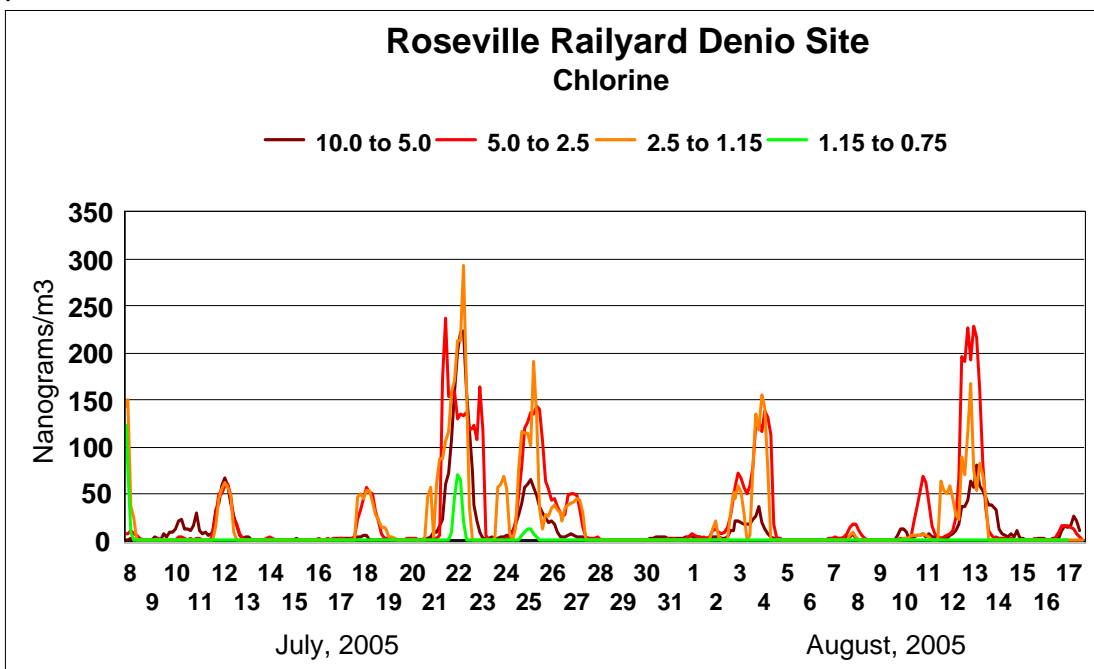


Figure 27 Sea salt signature in coarse particle fluorine.

This hypothesis was confirmed via trajectory analysis from the NOAA RERADY ARL HYSPLIT isentropic trajectory program, version 4. High speed transport trajectories for the chlorine peaks were associated with rapid transport of air from the ocean near Point Reyes to Roseville.

NOAA HYSPLIT MODEL
 Backward trajectories ending at 19 UTC 22 Jul 05
 FNL Meteorological Data

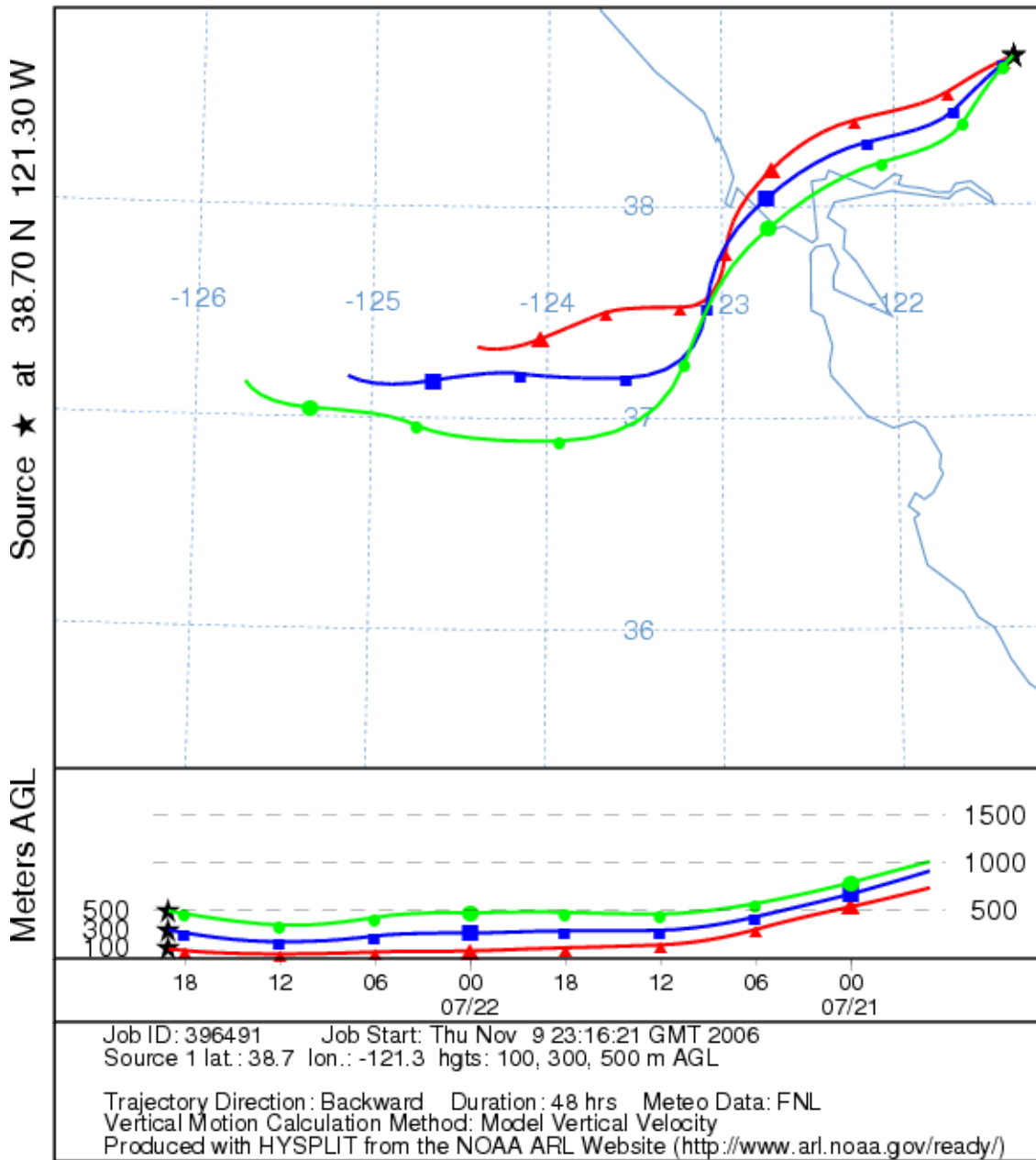


Figure 28 HYSPLIT trajectory showing Bay Area transport, July 22, 2005

The strongest correlation between nighttime transport across the rail yard was sulfur, a component of burned diesel fuel in the very fine particle mode (Figure 11). Examining the variation of sulfur with size and time, we can see that the pattern in the expected very fine ($0.26 > D_p > 0.09 \mu\text{m}$) mode extends into the accumulation mode.

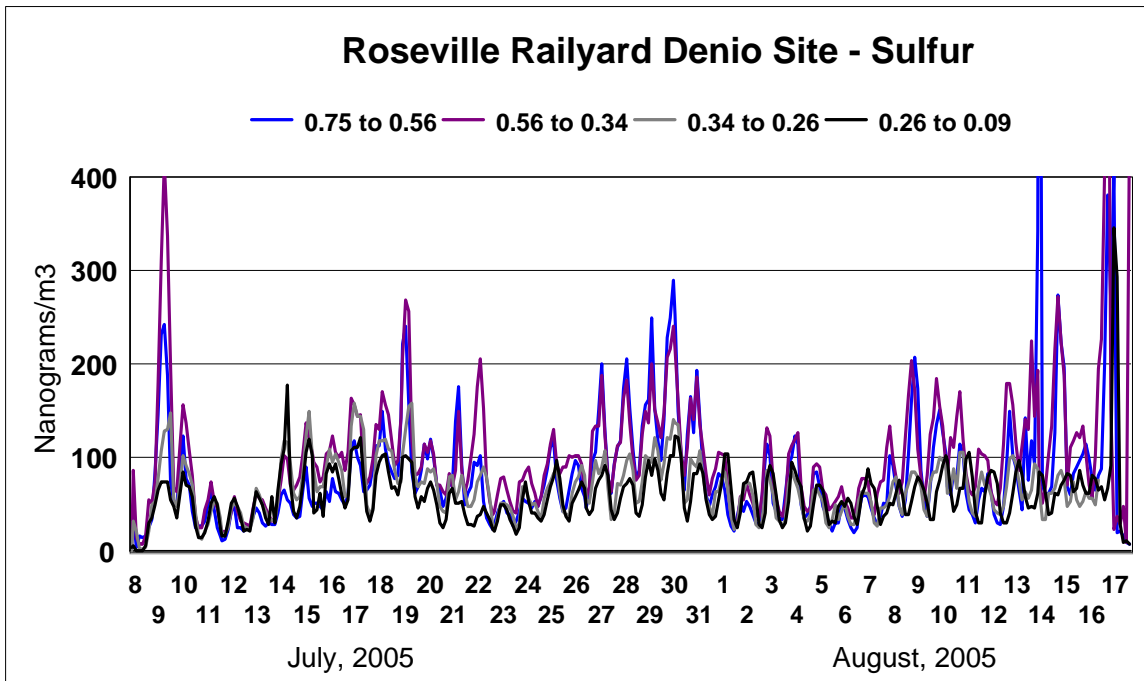


Figure 29 Sub-micron sulfur at the Denio site

While the strong day night pattern in very fine sulfur was expected, what was not expected was the continuation of this pattern into accumulation mode aerosols up to 0.75 μm diameter, and even larger, although mass measurements (Figures 8 and 9) had shown mass present in these sizes.

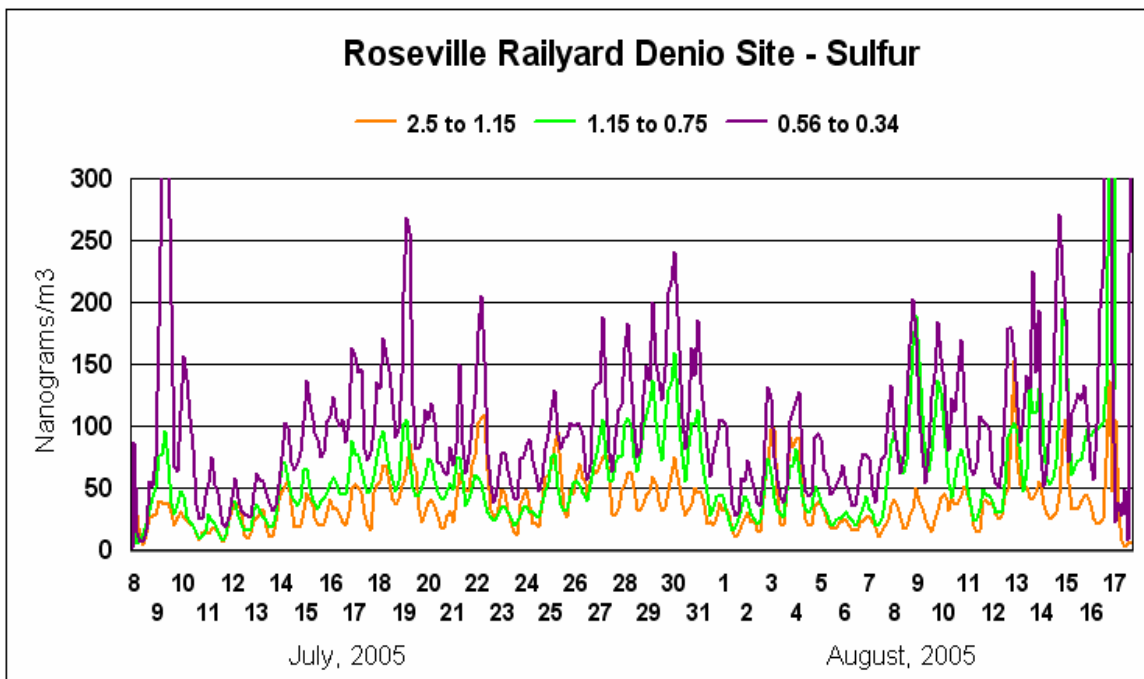


Figure 30 Components of fine sulfur at the Denio site

Then results from sulfur can be contrasted with that of soils, as shown by the iron tracer in the larger size modes.

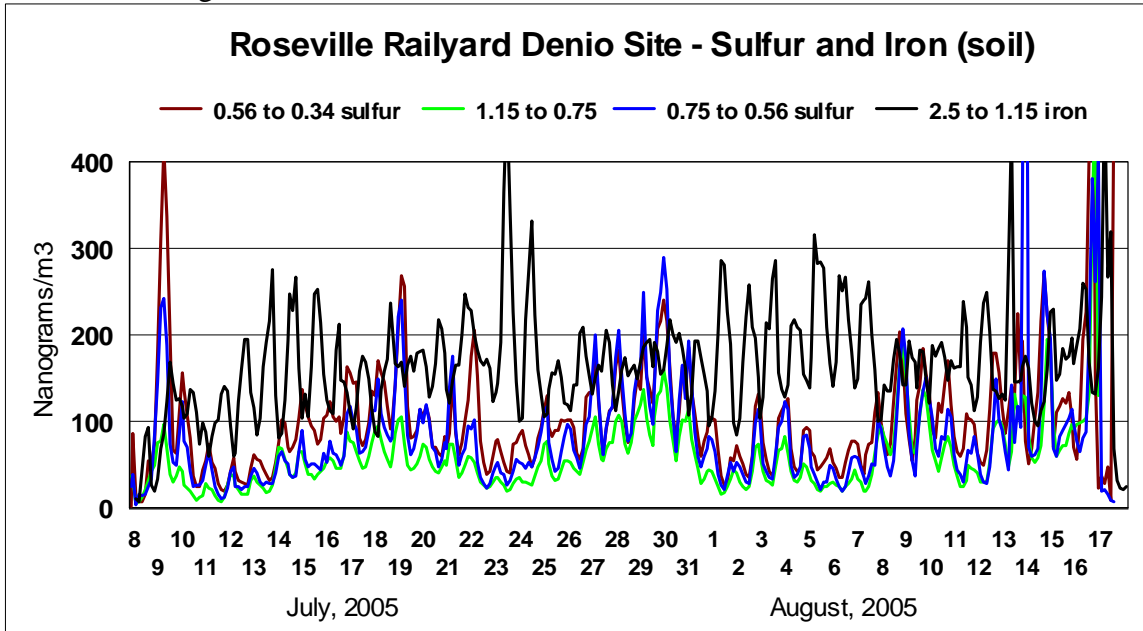


Figure 31 Sub-micron sulfur versus fine iron at the Denio site

The almost perfect anti-correlation of fine sulfur to coarse soil is fully consistent with the meteorology of the site and the stronger daytime winds from the southwest. However, the situation becomes more complex than simply soil in day and diesels at night. Below we show the graph for the major soil elements, silicon, for the summer period. The high levels on July 9 came on strong winds, gust to 18 mph, from the southwest, across the Denio’s Farmer’s Market, which was in operation that day. The size distribution is somewhat finer than typical wind blown dust.

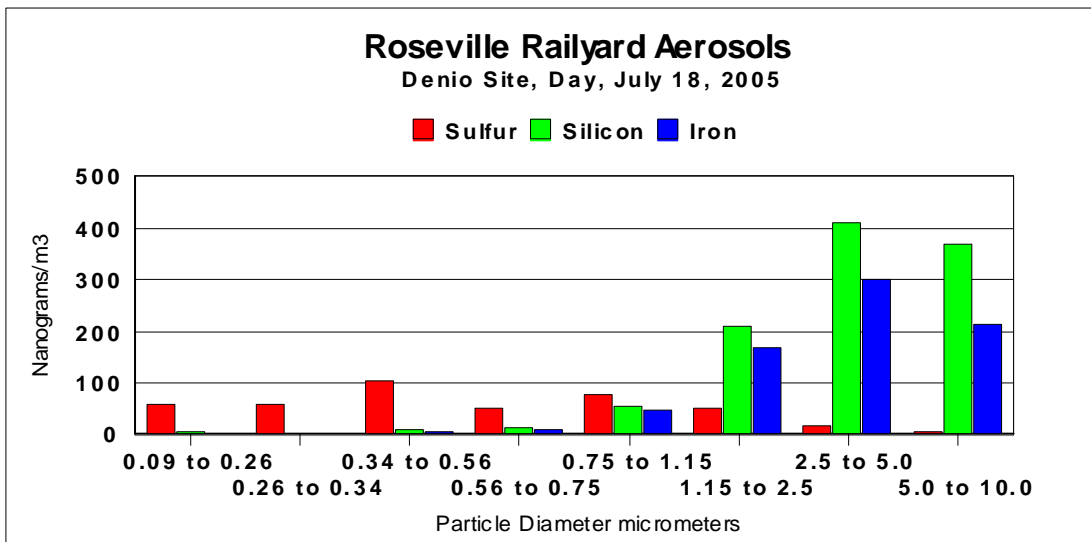


Figure 32 Size distribution of sulfur and soils, daytime, July 18, 2006

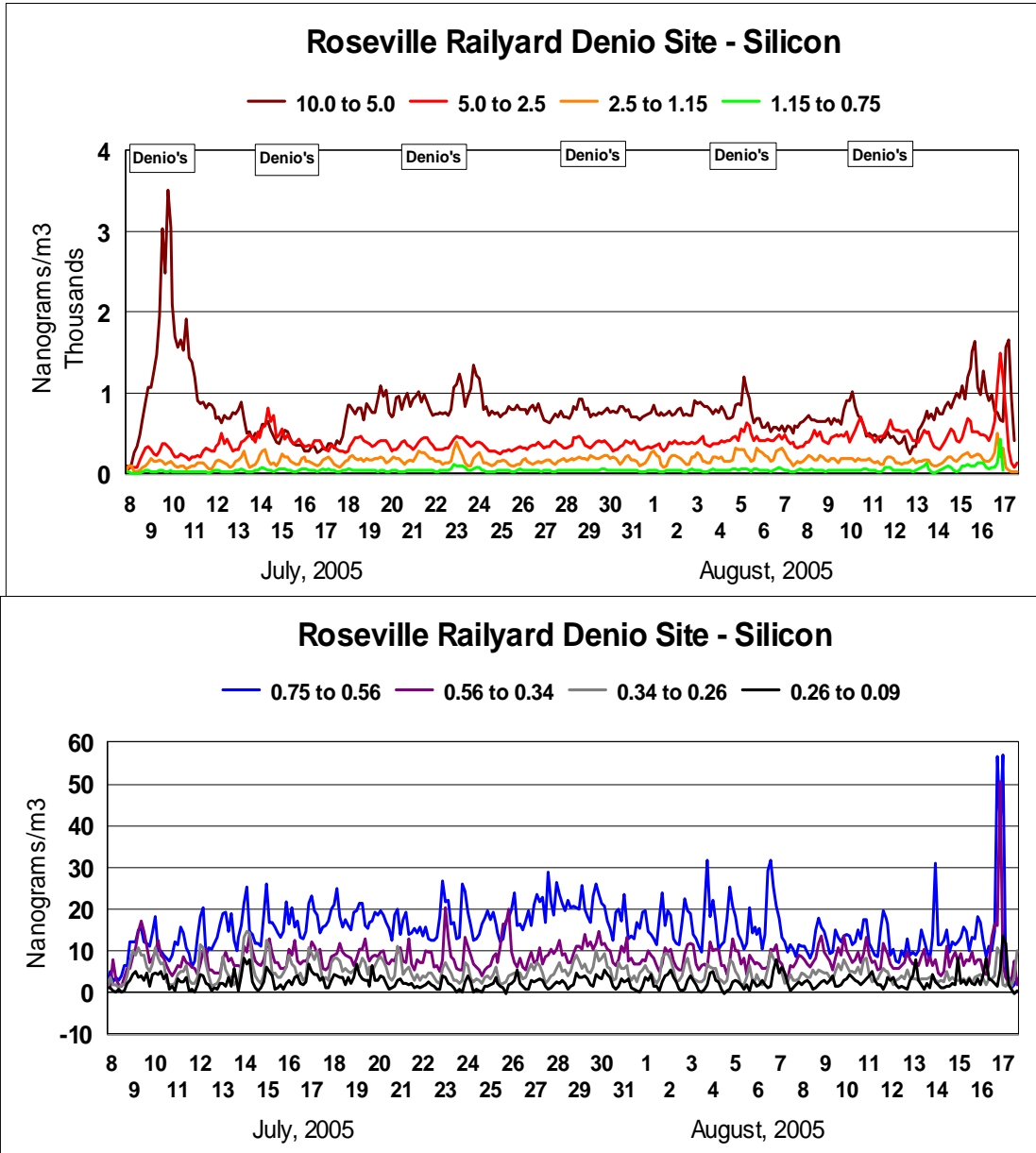


Figure 33 Time plots of coarse and fine silicon, Denio site

But there is also a small amount of silicon seen each night in very fine size modes, coming from the rail yard. The source of this material is unknown at this time

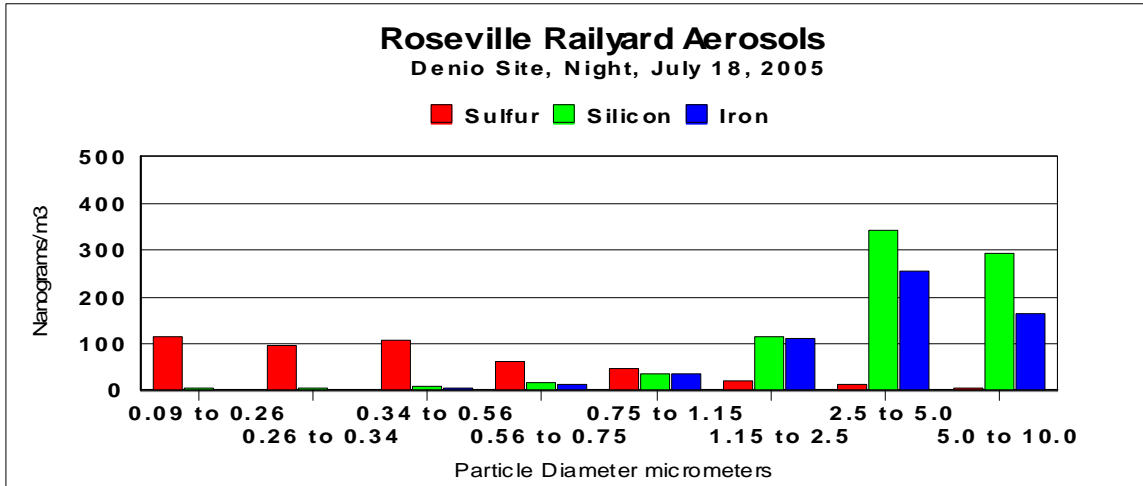


Figure 34 Size distribution of sulfur and soils, nighttime, July 18, 2006

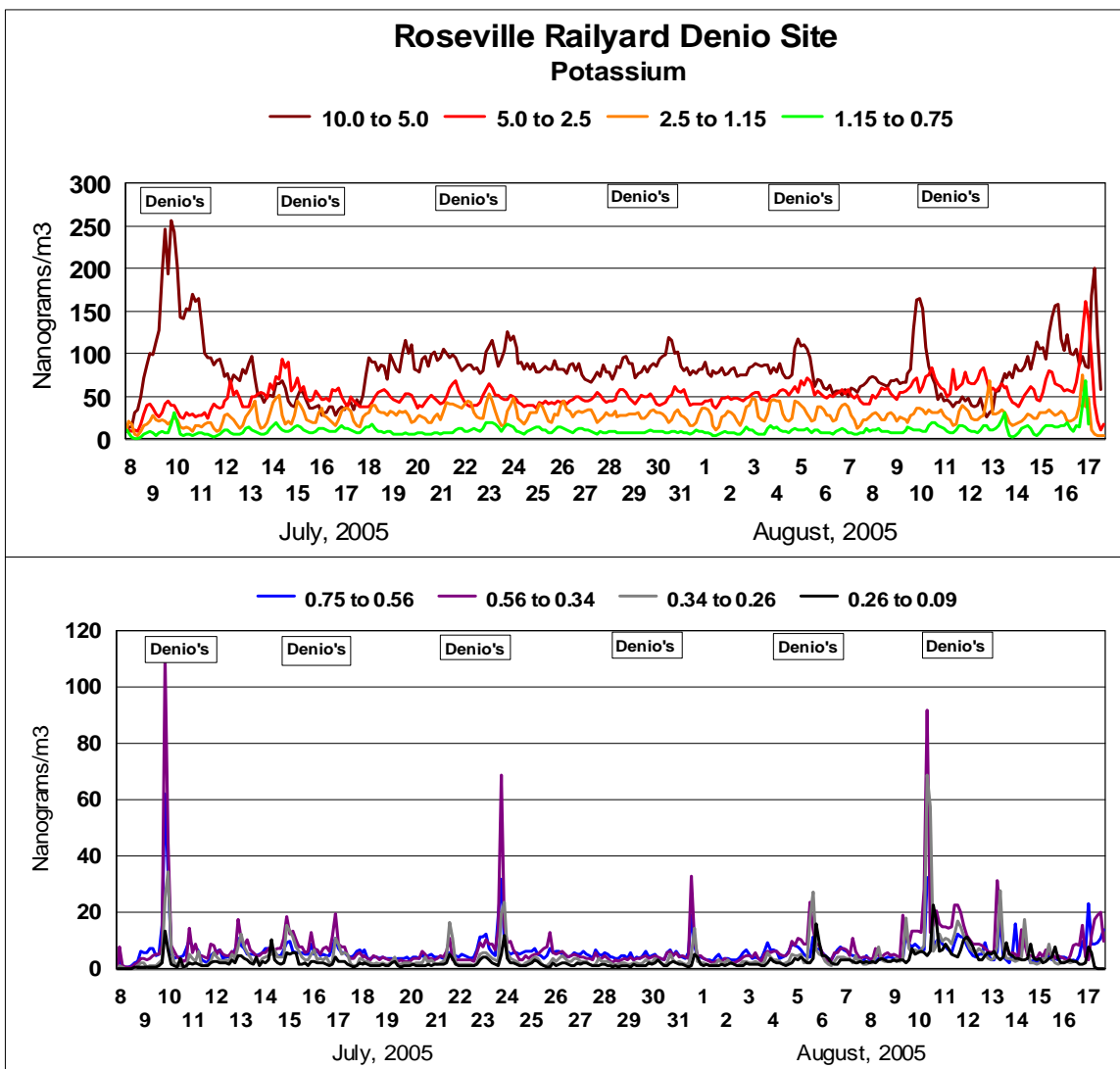


Figure 35 Time plots of coarse and fine potassium, Denio site

The large zinc episode around July 27 though July 28, for example, largely came into the site from the southwest, not from across the rail yard, and was also seen at the Pool Site. The nighttime wind on July 28 was weak and of short duration.

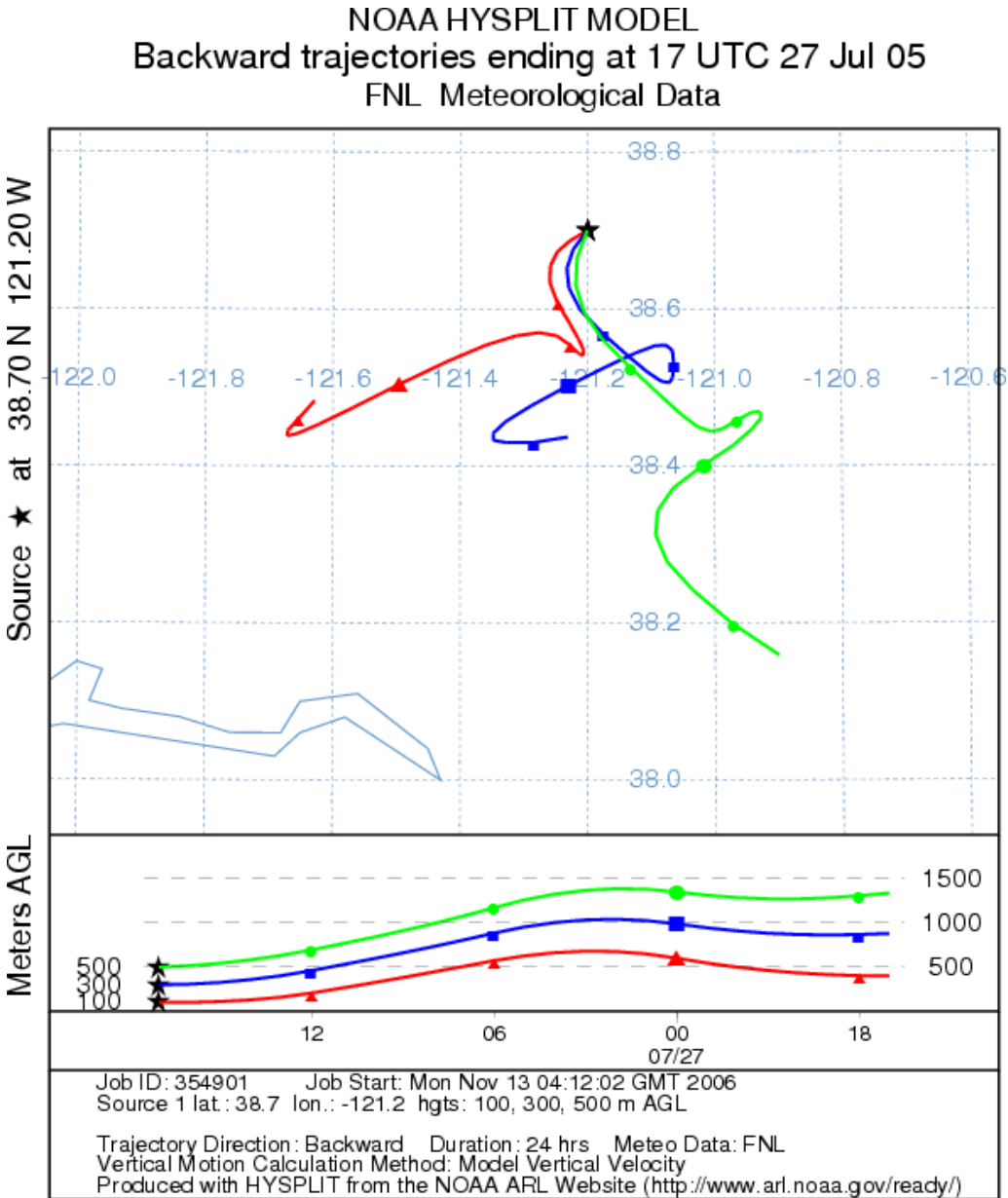


Figure 38 Wind trajectories at the beginning of the zinc episode, on the morning of July 27. The typical night time cross-rail yard winds were weak and of short duration. during this episode.

Other elements may or may not be involved in these episodic spikes of metals. For example, below we show the very fine data from both the Denio site and the pool site. Note that there is little copper in the zinc episode around July 27, and that the Pool site

was also involved. All the evidence points to a source or sources southwest of and outside of the Roseville Railyards.

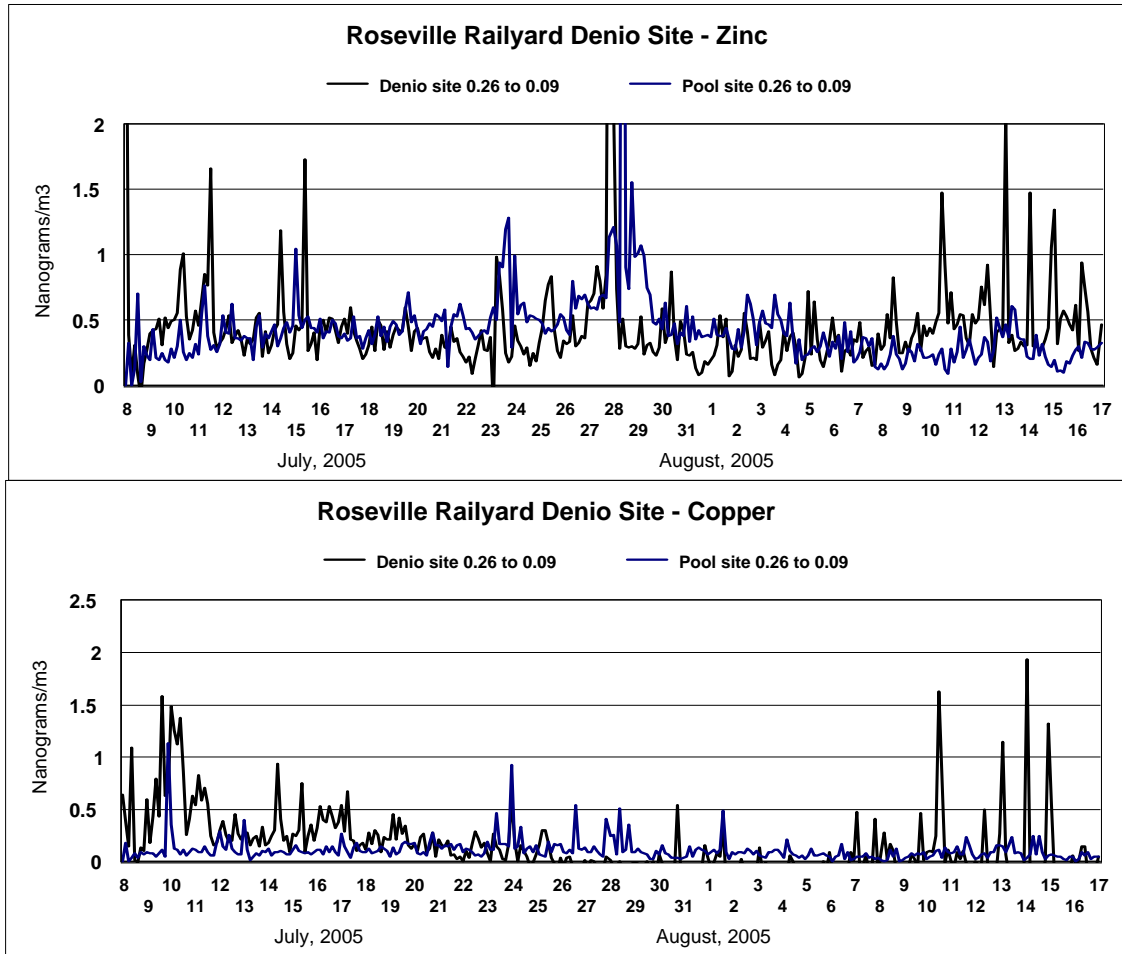


Figure 39 Comparison of very fine copper and zinc at the Pool and Denio sites. Most of the largest metal spikes occur at the Denio site.

As an example of the complexity of the coarse particle data, we have selected just one day-night period when the upwind-downwind vectors across the rail yard were well established. We then calculated the size of soil (silicon, iron, and coarse potassium), wood smoke and cars (fine potassium), sulfur (diesel fuel), phosphorus and zinc (lubricating oil), and other trace elements vanadium, nickel, copper, and lead. These are greatly enhanced over what one would expect in soil, with enrichment factors versus mean Earth crustal values (Handbook of Chemistry and Physics, F - 143 1989) such as times 33 (zinc) and times 43 (copper).

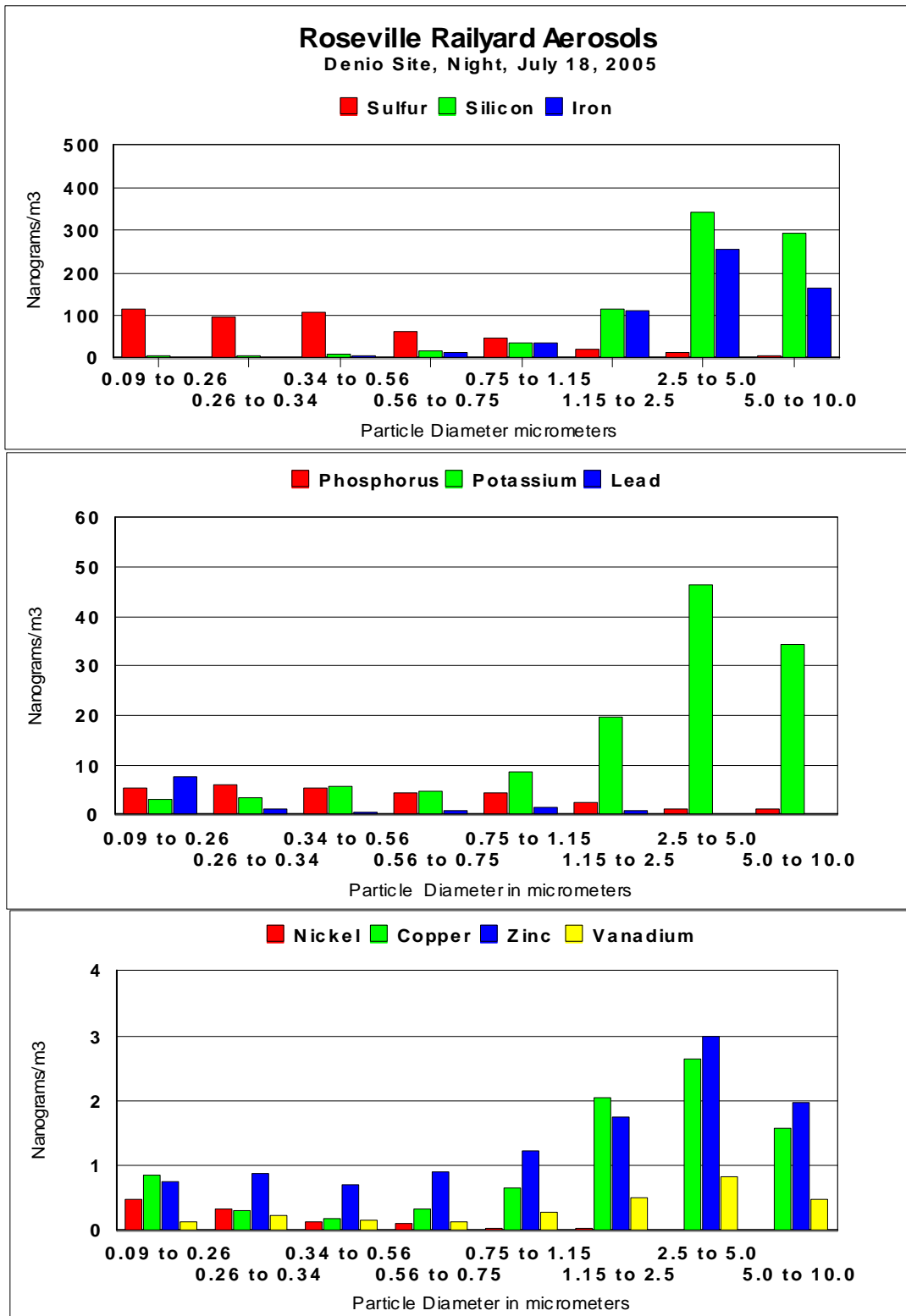


Figure 40 Size Distribution of elements on July 18, 2006, during night time cross rail yard winds.

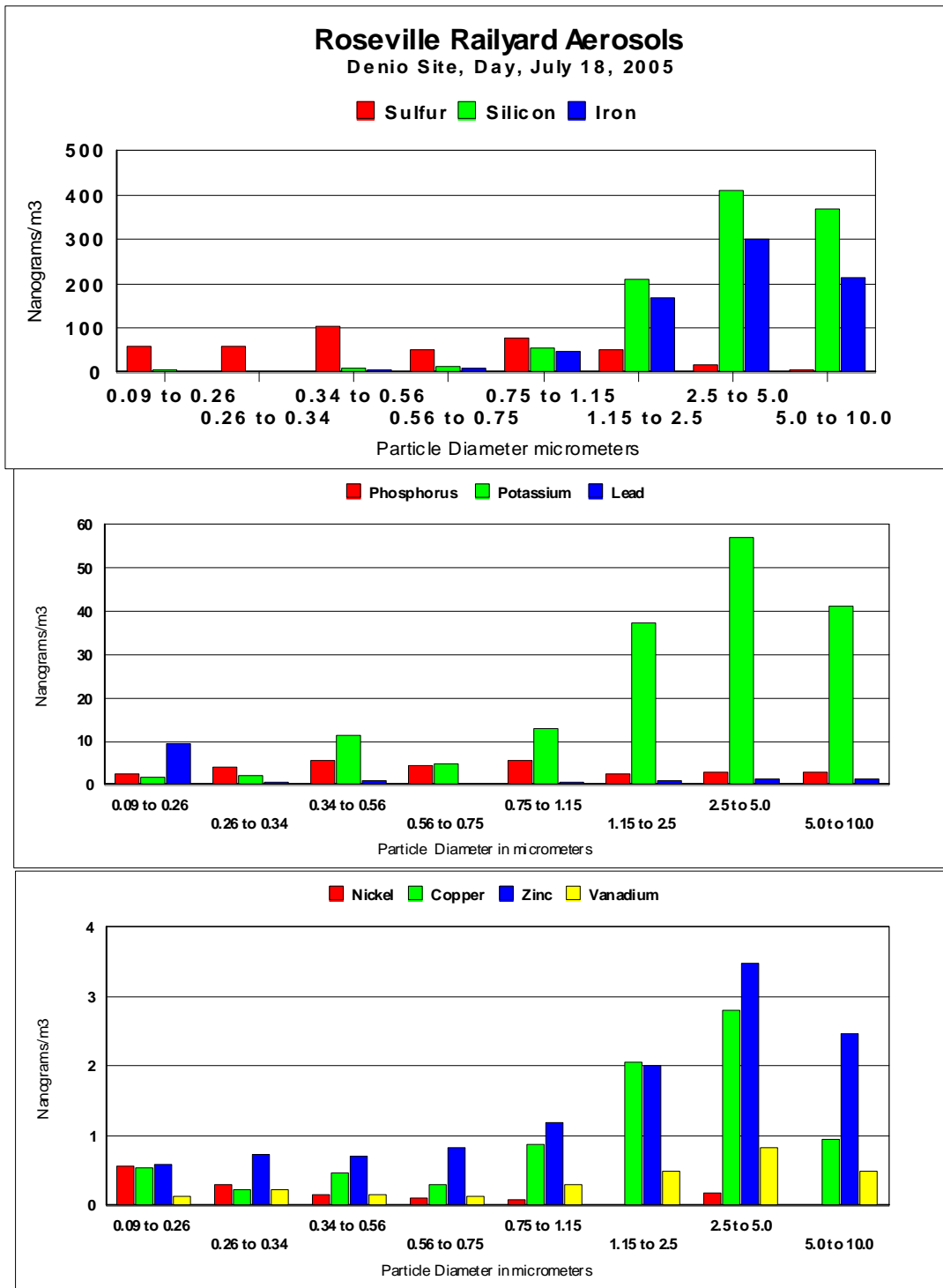


Figure 41 Size Distribution of elements on July 18, 2006, during day time winds from the southwest roughly parallel to the rail yard.

One of the most unexpected finding was that much of the same behavior occurred during daylight hours, when winds typically blew to the Denio site roughly parallel with to rail yard tracks and at a higher wind velocities.

4. Component D Organic Sample Collection and Analysis, Denio Site

The Roseville Railyard is a large source of diesel emissions. Most of the analysis done thus far in RRAMP have focused on monitoring gasses (NO, NO_x) and particulate matter, (Black Carbon (EC) mass, PM_{2.5} mass), enhanced by mass and elemental composition as a function of particle size from the DRUM samplers. However, these alone may not accurately assess the toxicity of the diesel emission from locomotives since the emissions of chemicals from locomotives have not been well characterized. If locomotives are assumed to have the same emission profiles as diesel trucks, then it would appear that they may have an impact. However, there are reasons to believe that the emission profiles from the locomotives may be different than the data from trucks.

The present mass measurements show that the size of the aerosols emitted by locomotives in RRAMP are different than diesel trucks, (Figure 9), so the amount of the emissions that are respirable and the toxic chemicals contained therein may also be different. Thus any accurate assessment of the rail yard will need to determine the toxicity, by measuring the PAH concentrations, of the locomotive emissions at the site. For this reason, we added sample collection suitable for organic analysis towards the end of the summer, 2005 campaign, in the hopes of eventually being able to conduct organic analysis of the aerosols downwind of the Roseville Railyard. The samples were collected and placed in freezers until funds could be obtained to do the analysis. This section of the Final Report contains the results of these analyses.

1. Methods

We collected particulate matter from August to October, 2005 at the Denio downwind site using an 8-stage DRUM sampler and a Lundgren impactor (see table 1, repeated below). The Lundgren impactor has a high flow rate (~130 L/min) that collects considerable mass, but the size cut points are rather coarse (50% cut points of 17µm, 5µm, 2µm and 0.5µm for the four stages) for diesel exhaust. However, the large amount of mass collected gives a high degree of sensitivity. A quartz filter was then used to collect aerosols with a diameter of less than 0.5µm. The Lundgren impactor was deployed for 2 – 10 days intervals to collect a single set of samples (4 stages, 1 filter and 2 blanks).

The other sampler utilized will be the 8-stage DRUM sampler with aluminum substrates, which is identical to the sampler used for elemental and mass analyses. Using identical samplers will ensure accurate comparisons between the elemental and organic results. This sampler has a much lower flow rate (~16 L/min), so less mass will be collected and the sensitivity of the analysis will be lower. However, this sampler has 8 fractions with most of them being smaller than the Lundgren impactor. This understanding in which size fractions the PAHs reside is particularly important since it will determine how much of the total PAH load is present in the respirable aerosol fraction. Since the flow rate of this sampler is much lower, it was run for 6 weeks to

collect a set of samples (8 stages, one filter and 3 blanks). For this study, we were able to modify the DRUM sampler to accept an after filter.

We obtained two sets of Lundgren impactor strips and filters, which will give a total of 10 samples (4 size fractions and a filter for each of 10 days of operation). The 8-stage DRUM will give a total of 9 samples during its six-week long operation (8 stages + a filter). Therefore, there will be a total of 19 samples that will be extracted and analyzed for PAHs and *n*-alkanes. In addition, there were approximately 8 blanks to ensure that the sample substrates were clean and that there was little/no contamination from sample handling. After sample collection, the samples were stored in sealed glass jars at -20°C until sample extraction.

2. Sample analysis

Each sample was tested for four classes of compounds, namely PAHs, alkanes, organic acids and sugars. The first two classes of chemicals are non-polar and are often the result of primary emission sources. The organic acids and the sugars/levoglucosan are polar chemicals that require derivatization prior to analysis. The organic acids arise from both combustion processes and from biological materials while the sugars are almost always biological in origin. Levoglucosan is a famous tracer of biomass combustion (“wood smoke”), so it was determined to assess the contribution of wood smoke to the aerosols that were collected. Considering that the sample collection period was in the summer, we did not anticipate significant wood smoke signatures in the samples.

Each of the field samples was enriched with 100 ng of a series of deuterated PAHs and *n*-alkanes to determine the extraction efficiency of the analytical method. The labeled PAHs were: phenanthrene-*d*₁₀, fluoranthene-*d*₁₀, pyrene-*d*₁₀, chrysene-*d*₁₂, and benzo[*k*]fluoranthene-*d*₁₂ (Cambridge Isotope Laboratories Inc. Andover, MA) while the *n*-alkanes were *n*-tetracosane-*d*₅₀ and hexatriacontane-*d*₇₄ (Cambridge Isotope Laboratories Inc.). The samples were also enriched with benzoic-*d*₆ acid and succinic-¹³C₂ acid to represent the organic acids that are in the samples.

Each sample was placed in a 10 ml centrifuge vial and extracted three times with 7 ml of toluene (HPLC grade, Burdick and Jackson, Muskegon, MI) to remove the non-polar fraction and then the samples were then extracted three times with 7ml of methanol (purge-and-trap grade, Fisher Scientific Company, Fair Lawn, NJ). For the first extraction with each solvent, the sample centrifuge tube was wrapped in aluminum foil to protect it from light and then placed on a test tube shaker (Labquake series 1104, Barnstead Thermolyne, Dubuque IW) for 20 hours. After the first solvent wash, the samples were centrifuged at 3000 RPM (IEC Clinical Centrifuge, International Equipment Co., Needham Heights, MA) for 5 minutes to settle any solids. The solution was removed and transferred to another centrifuge tube for concentration by nitrogen evaporation. The second and third washes with each solvent were conducted for 2 hours each, thus the total extraction time was 24 hours for each solvent. After each wash, the sample was centrifuged before the solution was removed. The non-polar (toluene) and

polar (methanol) extracts were stored separately. For each sample, the toluene and methanol fractions were reduced to 2 ml by nitrogen evaporation.

The analysis of PAHs and *n*-alkanes only utilized the toluene fraction since these compounds will only be found in this fraction. One milliliter (50% of the sample extract) was removed and passed through a pasture pipet clean-up column consisting of 1.5 g of silica gel (70-320 mesh, Fisher Scientific Co.) to remove polar chemicals that may interfere with the analysis. The silica gel column was eluted with 7 ml toluene. The extract was concentrated by nitrogen evaporation to 100 μ l and then it was transferred to a GC vial. Pyrene-*d*₁₀ was then added to the sample, giving a concentration of 100pg/ μ l, to serve as an internal standard. The samples were then ready for analysis by gas chromatography- ion trap mass spectrometry (GC-MS).

The analysis of sugars and acids required derivatization by BSTFA (Supelco, Bellefonte, PA), which is a silylation reagent. In this case, 100 μ l of the toluene extract and 100 μ l of the methanol extract, which represent 5% of the total sample mass, were added to a GC vial. The extract was evaporated to dryness by nitrogen evaporation in the GC vial. The samples were re-constituted in 100 μ l of a 50:50 BSTFA:pyridine derivatization solution (pyridine from Aldrich Chemical Co.). The samples were then placed on a drybath heater set to 40°C for 24 hours. After derivatization was complete, the samples were uncapped and pyrene-*d*₁₀ was added as an injection standard. The samples were then ready for analysis by GC-MS.

All samplers were quantified using a Varian 3400 GC coupled to a Saturn 2000 ion trap mass spectrometer (Varian Inc., Walnut Creek, CA). The analytical column was a Varian Factor Four High Temperature Column (30m length, 0.25mm ID, 0.1 μ m film thickness, and 5% phenyl substituted stationary phase). Helium was used as the carrier gas with a linear velocity of 37cm/sec. The oven program for the PAH and *n*-alkane analyses was: initial temperature of 64°C held for 5 minutes, then ramp 5°C/min to 375°C, and hold for 5 minutes. The sugar and acid analysis had a similar program except that it started at 35°C (hold 5 minutes), and then ramped 5°C to 330°C. Sample introduction consisted of 5 μ l injection of the sample extract onto a glass wool-packed injection port liner that was maintained at 5°C or more below the boiling temperature of the sample solvent. The injection port temperature was then increased to 375°C for the PAH and *n*-alkane analyses and 300°C for the sugar and acid analysis. This causes the analytes to volatilize from the injection port and move onto the column before the column temperature is increased. The PAH analysis was the only exception to this procedure since 20 μ l of the sample was injected rather than 5 μ l to achieve greater sensitivity.

The analysis of the sugars, acids and *n*-alkanes utilized a simple electron ionization (EI) mass spectrometer program with a scan range of 50 to 650 mass units. All instrumental conditions were Varian default settings except for the target ion count, which was reduced from 20,000 to 10,000. The ion trap temperature was set at 220°C for all analyses. The PAH analysis program was different in that it used MS-MS techniques to improve sensitivity and selectivity. In this case, the molecular ion of each PAH was isolated and then further fragmented by collision-induced disassociation where resonant

excitation was used to impart energy to the ions. The resonant excitation energy was optimized for each PAH to produce the maximum abundance of secondary ions. Identification and quantification was conducted using the product ions, which typically consisted of the loss of H₂ from the molecular ion.

Quantification was conducted by a six-point calibration curve for each class of chemicals. If a field sample had a concentration that exceeded the calibration curve, then the sample was diluted 10-fold and re-analyzed to bring the response within the calibration curve. For the *n*-alkanes, we only had authentic standards of C₁₆, C₂₄, C₃₀, and C₃₆ *n*-alkanes. The other alkanes between C₂₀ and C₃₅ are tentatively identified by their mass spectra and their retention time sequence. Quantification assumed the same relative response as the nearest authentic standard, which may create a minor bias in calibration. In the case of the acids and sugars, the calibration curve was derivatized alongside the samples to keep the derivatization time and conditions identical to the field samples. Pyrene-*d*₁₀ was used as the injection standard for all analyses. The other labeled compounds added to the sample before extraction were used to determine the extraction efficiency of the analytical method. The data are not corrected for extraction efficiencies of the analytes. All final concentration data are rounded to two significant digits of accuracy.

The results provide size-resolved PAH and alkane data from downwind of the Roseville Railyard. The important aspect of this research is determine the PAH concentrations in the aerosol size fractions that can penetrate into the deep lung, and thus represent the greatest exposure hazard. This is particularly important for the rail yard since the emissions from locomotive engines have not been well characterized in terms of the size of the particulate matter emitted, thus we need to determine the size distribution of the aerosols and the associated PAHs to assess the potential health effects.

3. Results for Organic Constituents

Recoveries of isotopically labeled compounds from samples

One of the best measures of the efficacy of an analytical method is the recovery of isotopically labeled surrogate compounds to the samples. Since the isotopically labeled compounds have a different mass from the “native” analytes, they do not interfere with the analytes in the samples. However, the isotopically labeled analytes have the same chemical properties and behavior as the native analytes. Therefore a good recovery of the labeled surrogate compounds from the samples gives a high degree of confidence that the native analytes were also effectively extracted.

A series of 9 labeled surrogate compounds were added to all samples and blanks. The recoveries of these labeled compounds were generally good to acceptable (Table 6). Phenanthrene had the lowest recovery of any of the PAHs at 54.6%, but this was expected since phenanthrene is a semi-volatile PAH and could easily evaporate from the samples during processing. The recoveries of all of the heavier PAHs and the two *n*-alkanes were good. Only two organic acids were utilized in this. Benzoic acid showed 118.5% recovery, which suggests that the spiking solution may have been inaccurately

measured. Succinic acid (AKA butanedioic acid) showed a poor recovery partly due to the low response of the instrument to this compound. In the future, long chain alkanolic acids (e.g. octadecanoic acid) should be added to the surrogate solution mixture since they were the most abundant organic acids detected and their chemistry is significantly different from the benzoic and succinic acid surrogates that were utilized.

Table 6. Average recovery (%) of isotopically labeled compounds to all the samples and blanks ($n = 27$)

Compound	Recovery (%)
<u><i>n</i>-alkanes</u>	
<i>n</i> -tetracosane- d_{50} (C ₂₄)	71.0
<i>n</i> -hexatriacontane- d_{74} (C ₃₆)	73.0
<u>PAHs</u>	
phenanthrene- d_{10}	54.6
chrysene- d_{12}	76.9
benzo[<i>k</i>]fluoranthene- d_{12}	74.1
benzo[<i>g,h,i</i>]perylene- d_{12}	86.9
<u>acids</u>	
benzoic- d_6 acid	118.5
succinic- $^{13}\text{C}_2$ acid	50.5

Based on the recovery data of the labeled surrogates from all the sample matrices (aluminum foil and quartz filters), it appears that the analytical method was effective for the heavier PAHs, *n*-alkanes and some of the organic acids. The data reported herein has not been corrected using the above recovery data, so we would anticipate that there is approximately a $\pm 30\%$ error for most of the chemicals.

a. Polycyclic aromatic hydrocarbons (PAHs)

The results from the PAH analysis clearly showed high concentrations of PAHs in the particulate matter (Table 7) with the majority of the PAH mass being collected in the ultra-fine stage (0.26 to 0.09 μm) and the afterfilter (Figure 43). The presence of PAHs in the ultra-fine size fraction corresponds well to previous observations of PAHs in diesel emissions (Zielinska et al, 2004; Gertler et al, 2002). The presence of a strong marker for fresh diesel emissions was expected.

Note that the Lundgren sampler was only operated at night when the air is coming from the rail yard, thus it has higher concentrations. For this reason, the 8 DRUM results are scaled by a factor 2.57 to account for PAHs only at night (from the NO ratios of Figure 2.a, x 2.0) and the ratio of EC, 1.4 (Table 3, x 1.29) to allow better comparison to the Lundgren data. This amounts essentially to an assumption that all PAHs come from the rail yard on night winds.

Table 7. Concentrations (pg/m³) of particulate PAHs observed at the Roseville Rail Yard in the summer of 2005.

Compound	8-stage DRUM (8/5 - 9/27)	8-stage DRUM (scaled x 2.6) (8/5 - 9/27)	Early Lundgren (9/27 - 10/7)	Late Lundgren (10/7 - 10/17)
Phenanthrene	21	55	110	100
Anthracene	<MQL	<MQL	20	20
1-methylphenanthrene	<MQL	<MQL	32	28
Fluoranthene	57	147	160	160
Pyrene	74	190	310	300
Benz[a]anthracene	^a	^a	^a	^a
Chrysene+ triphenylene	24	62	130	130
Benzo	68	175	350	330
[b+k]fluoranthene				
Benzo[e]pyrene	90	231	360	350
Benzo{a}pyrene	68	175	270	280
Perylene	<MQL	<MQL	35	36
Indo[1,2,3-cd]pyrene	84	216	240	230
Dibenz[a,h]anthracene	100	257	270	270
Benzo[g,h,i]perylene	230	591	650	650
Coronene	175	450	380	370

^a Unable to quantify compound due to analytical problem, namely excessive enrichment of chrysene-*d*₁₂ that saturated the ion trap mass spectrometer.

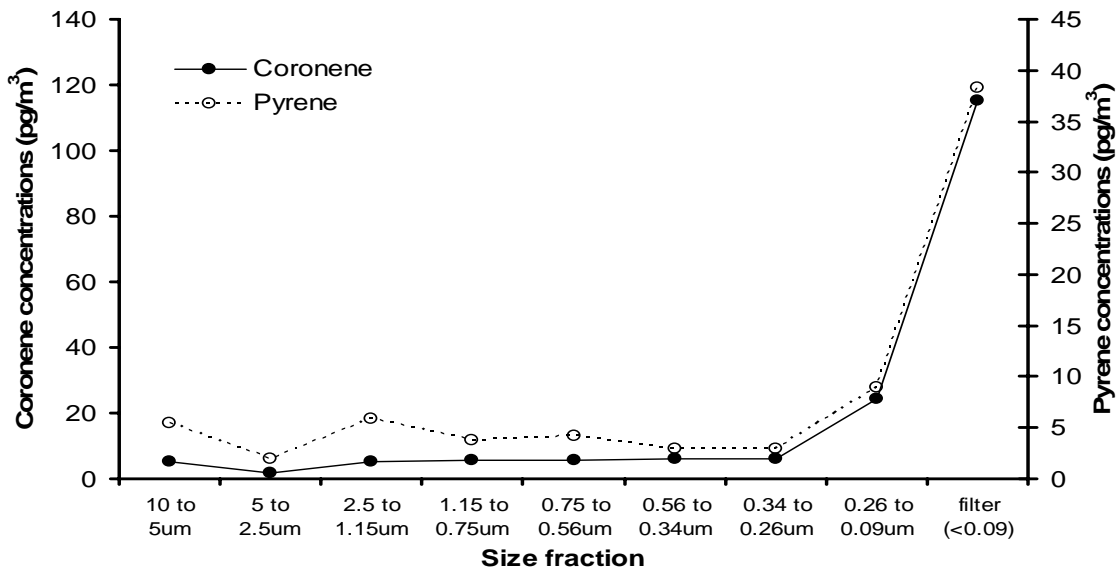


Figure 42. Coronene and pyrene concentrations (pg/m³) in the different size fractions of the 8-stage DRUM sampler and the afterfilter.

The presence of the PAHs in the ultra-fine stage indicates that the diesel source was close to the sampler since the particulates had not coagulated into larger particles, which also suggests that the source of the particulates was the rail yard.

The PAH results from the Lundgren sampler also support these observations. This sampler was only operated during the nighttime hours when the local meteorology brings a weak down-slope breeze across the rail yard and to the sampling site. Therefore, the higher concentrations observed by this sampler were expected and support the assertion that they are coming from the site. The air concentrations were approximately 4 times higher than the 8-stage DRUM, which appears to be the result of the 8-stage DRUM samples being “diluted” by the daytime sampling that lacked any rail yard influence (Figure 3 a, x 2) and the increasing mass in the fall periods (x 1.28). The combination of these factors give a multiplicative factor of 2.57, which is presented in the tables. Inversions become more common in fall and winter, raising the very fine mass from a value of $2.25 \mu\text{g}/\text{m}^3$ in summer (DRUM sages 7 + 8, 0.34 to $0.09 \mu\text{m}$) to $6.6 \mu\text{g}/\text{m}^3$ measured in February, 2006, using identical equipment. Thus, the Lundgren samplers were collecting in periods that would tend to have higher masses at the Denio site. In summary, the mass differences in organic matter from the summer 8 DRUM samplers and the fall night-only Lundgren samplers are consistent.

The PAHs from the locomotive diesel engines showed a very different trend in terms of the PAH profile compared to diesel engines used in trucks and other on-road applications. The PAH profile from the locomotives had considerably more of the heavy PAHs with molecular weights greater than 252 compared to the on-road diesel trucks and the NIST standard reference materials (Figure 43). This trend was observed with all three samples collected, namely the 8-stage DRUM and both of the Lundgren samples.

The higher proportion of the high molecular weight PAHs of locomotive emission may affect the overall toxicity of these emission compared to smaller diesel engines since the larger PAHs classes include some of the more toxic PAHs such as benzo{a}pyrene. Therefore, the standard cancer assessment based on diesel truck particulate mass may be biased on the low side. While it appears that the locomotive emissions have a higher proportion of heavier PAHs, it is unclear from these data whether the PAHs are arising from the large-bore engine technology, the locomotive fuel, which is different from the diesel fuel used in trucks, or the lubricating oils.

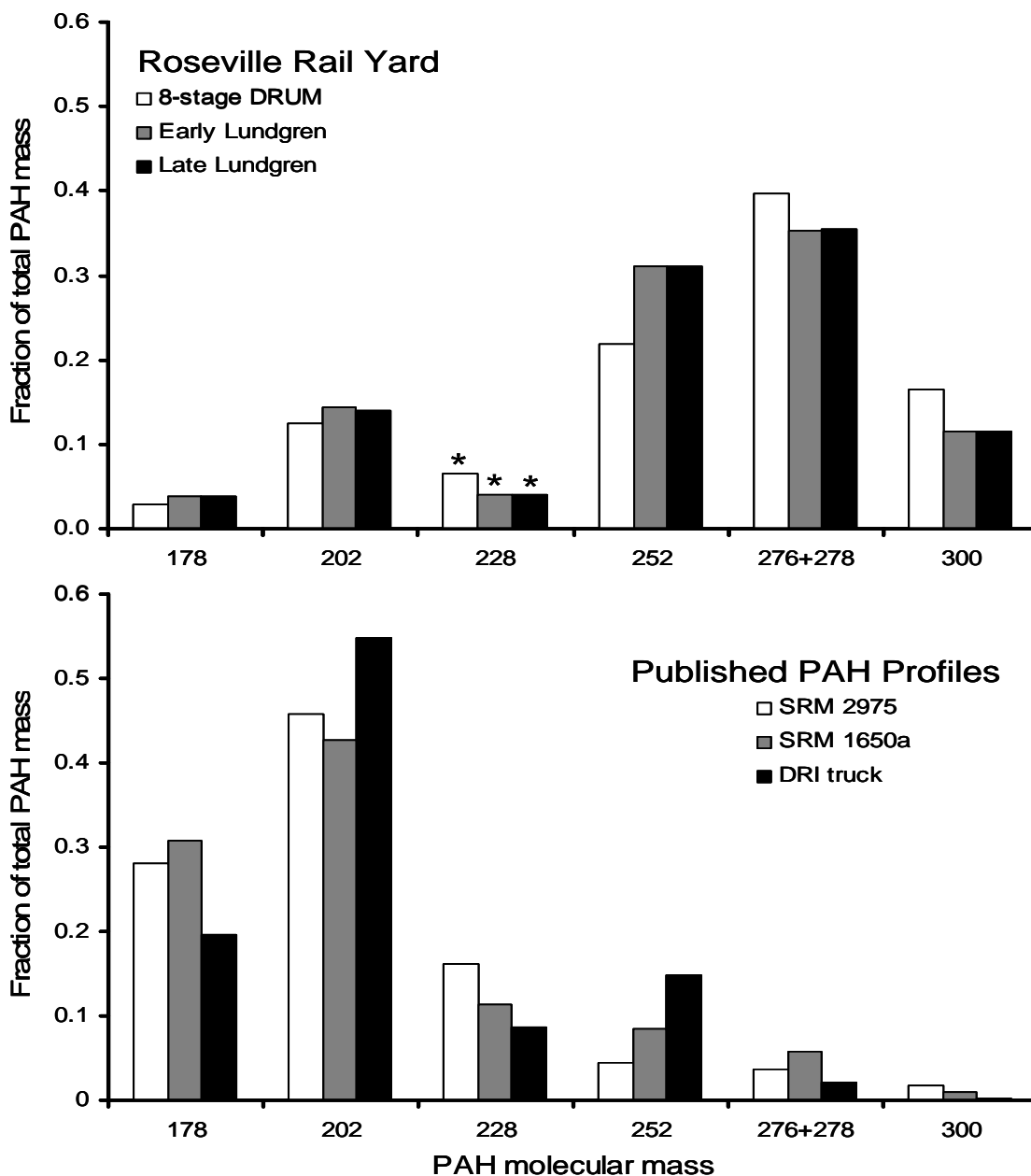


Figure 43. Profiles of PAHs as a function of molecular mass from the Roseville rail yard and the literature.

The molecular mass of benzo{a}pyrene is 252. Note that the molecular profile of the 8 DRUM (summer) and the Lundgren sampler (fall) are essentially identical. The “228” values in the Roseville samples are an underestimate since we could not quantify benz{a}anthracene due to an analytical problem.

One possible explanation for different PAH profiles is that the lighter PAHs could “blow-off” of the sample during the long sample collection periods. We do not believe this to be a significant effect since the “early” and “late” Lundgren samples had almost the identical profiles, yet the “early” samples were in the sampler for a week and a half

longer than the “late” samples. If blow-off was significant, then we would expect the samples exposed to the air stream for a longer period of time to have lower proportions of the lighter (178 and 202 amu) PAHs. This was not observed. Furthermore, the 8-stage DRUM sampler collected material for 6 weeks, and its profile is likewise very similar to the Lundgren samples that were only 1.5 weeks in duration and only operated at night. Therefore, the PAH profile does not appear to be the result of “blow-off” during sample collection.

b. Alkanes:

The second class of chemicals investigated was the alkanes and related hydrocarbons. Unlike the PAHs, there were appreciable alkanes in the field blanks, but the concentration of alkanes were generally low enough not to interfere with the quantification of the alkanes (Table 8).

Table 8. Concentrations (ng/m³) of particulate *n*-alkanes observed at the Roseville Rail Yard in the summer of 2005.

Compound	8-stage DRUM (8/5 to 9/27)	8-stage DRUM (8/5 to 9/27) (scaled x 2.6)	Early Lundgren (9/27 to 10/7)	Late Lundgren (10/7 to 10/17)
C ₂₀ <i>n</i> -alkane	0.25	0.64	1.1	1.0
C ₂₁ <i>n</i> -alkane	0.50	1.29	2.1	1.7
C ₂₂ <i>n</i> -alkane	0.42	1.08	3.6	2.8
C ₂₃ <i>n</i> -alkane	0.94	2.42	5.2	4.0
C ₂₄ <i>n</i> -alkane	1.3	3.34	2.8	1.5
C ₂₅ <i>n</i> -alkane	2.5	6.43	7.5	5.8
C ₂₆ <i>n</i> -alkane	2.8	7.11	7.6	5.7
C ₂₇ <i>n</i> -alkane	4.4	11.3	10	7.5
C ₂₈ <i>n</i> -alkane	4.5	11.6	9.4	4.2
C ₂₉ <i>n</i> -alkane	9.4	24.2	17	11
C ₃₀ <i>n</i> -alkane	5.7	14.7	11	3.8
C ₃₁ <i>n</i> -alkane	8.6	22.1	13	5.9
C ₃₂ <i>n</i> -alkane	4.2	10.6	7.0	0.5
C ₃₃ <i>n</i> -alkane	4.2	10.8	6.4	1.3
C ₃₄ <i>n</i> -alkane	1.4	3.6	2.7	< MQL
C ₃₅ <i>n</i> -alkane	0.76	1.95	1.9	< MQL
C ₃₆ <i>n</i> -alkane	0.94	2.42	1.3	< MQL
Total identified alkanes	53	140	110	55
Undifferentiated hydrocarbon	210	540	530	450

Note that the Lundgren sampler was only operated at night when the air is coming from the rail yard. The “undifferentiated hydrocarbon envelope” represents the

integration of m/z 57 (C_4H_9) between the C_{20} and C_{39} n -alkanes where the mass calibration was based on the n -alkane standards.

Both the 8-stage DRUM and the Lundgren samples showed that the C_{29} n -alkane was the most abundant chemical observed with concentrations in 9 to 17 ng/m^3 . Unlike the PAH data, the concentrations of alkanes were different between the early and the late Lundgren samples with the early sample having concentration that were almost twice as high as the late sample. The 8-stage and early Lundgren samples had no clear pattern of odd-even carbon number species. This would suggest a petroleum source of the hydrocarbons. However, the late Lundgren sample had a clear preference for odd-number hydrocarbons, particularly for the heavier alkanes. This pattern would suggest a biological source for the hydrocarbon rather than a petroleum source. The lower alkane concentrations and the odd-length chain bias suggests that there was a background biogenic source of hydrocarbons on which the rail yard emissions are superimposed.

In addition to the specific n -alkanes that were identified and quantified, there was a large “envelope” of undifferentiated hydrocarbons that approximately eluted between C_{23} and C_{39} n -alkanes (Figure 44). This undifferentiated hydrocarbon envelope was integrated by selecting only m/z ion 57, which corresponds to C_4H_9 fragment between the C_{20} and C_{39} n -alkanes where the mass calibration was based on the n -alkane standards. As a double-check, ion 85 (C_6H_{15}), which is another common ion from saturated alkane chains, was also selected and integrated. The results agreed between the two methods within 10%, thus giving a reasonable degree of confidence in the identification of the “envelope” as mostly alkanes. It should also be noted that this extract was the toluene extract from the samples, thus non-polar constituents would be removed from the aerosols but not the more polar chemicals. This further contributes to the confidence in the identification. The estimated mass of the undifferentiated alkane envelope was 210 ng/m^3 for the 8-stage DRUM sampler while it was 530 and 450 ng/m^3 in the early and late Lundgren sampler. The identified n -alkanes represented anywhere between 12 and 25% of the undifferentiated hydrocarbon envelope. The undifferentiated alkane envelope showed interesting trends as a function of particle size (Figure 45). The highest concentrations were found on the afterfilter followed by the 2.5 to 1.15 and the 1.15 to 0.75 μm size fraction. This differs from the PAH results since the PAHs lacked the relatively high concentrations in the accumulation mode. The presence of the alkanes in the accumulation mode in the absence of PAHs suggest that there is a separate source of these undifferentiated hydrocarbons in addition to diesel combustion emissions.

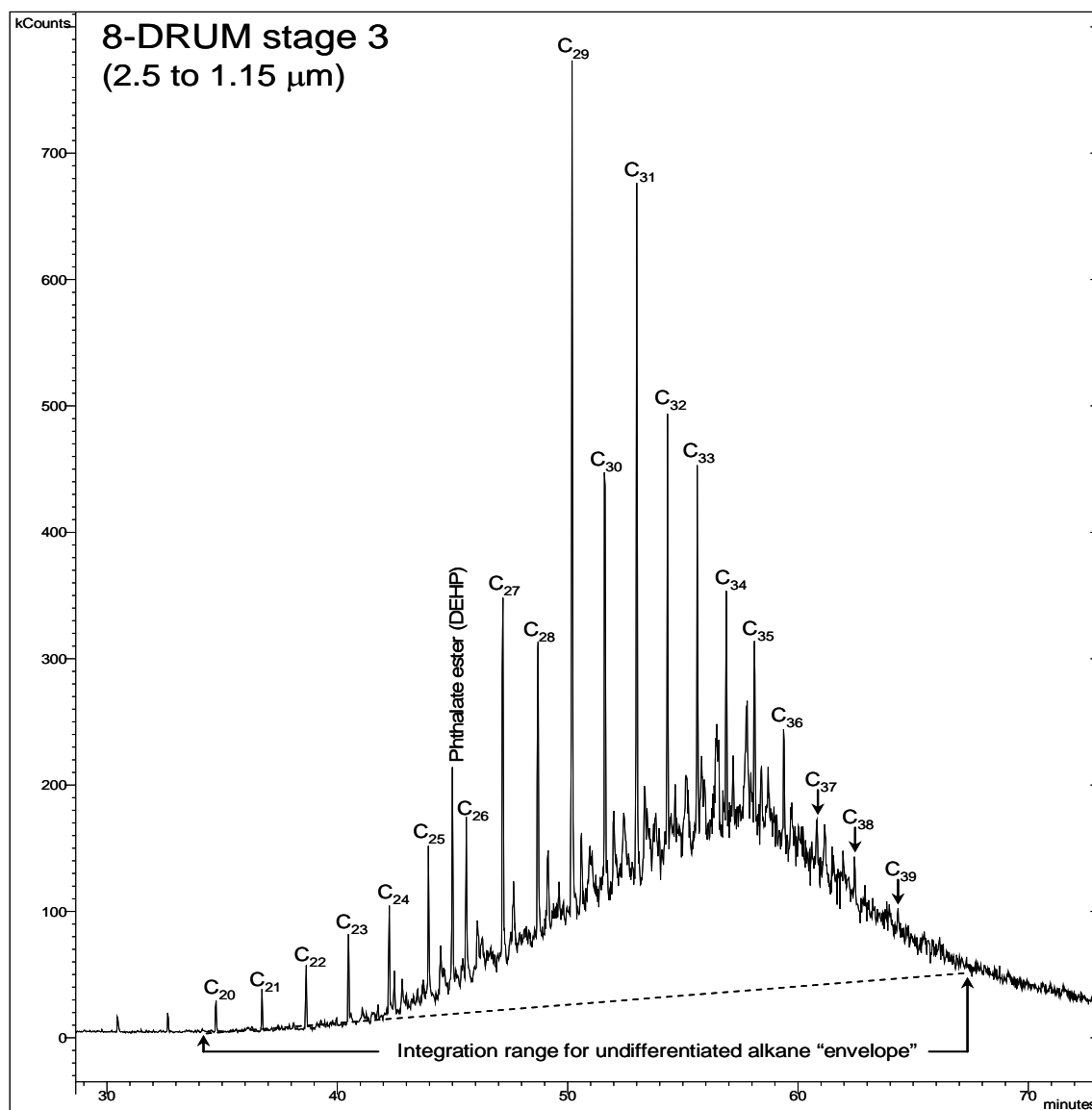


Figure 44. A selected ion chromatogram of m/z 57 showing the undifferentiated hydrocarbon "envelope". The n -alkanes are labeled by their carbon number.

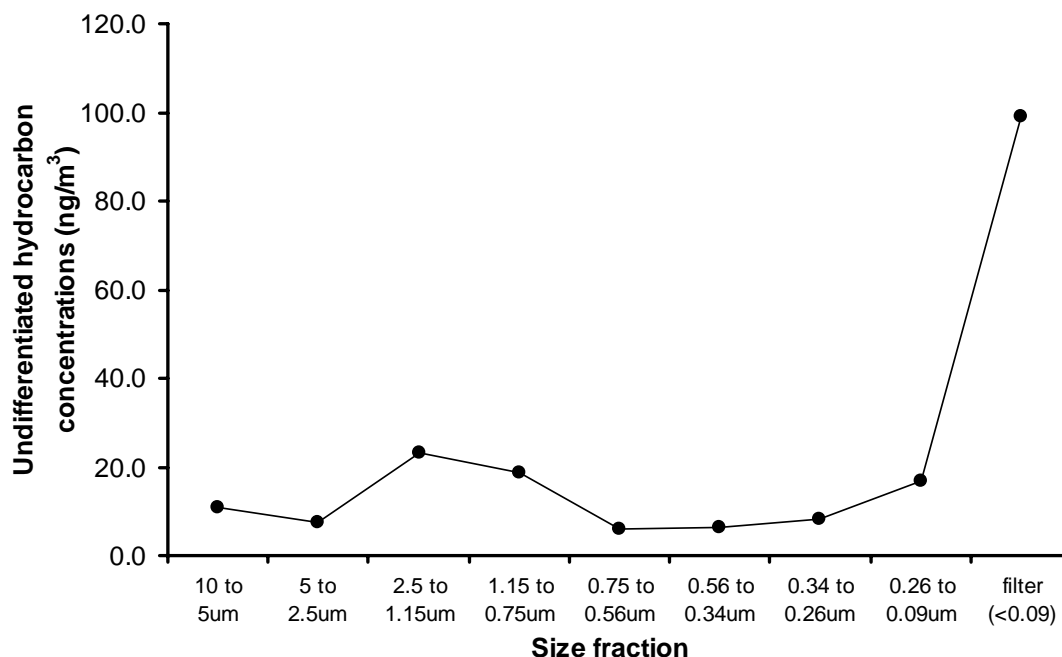


Figure 45 Concentrations of undifferentiated hydrocarbons in different size fractions of the 8-stage DRUM sampler.

Another interesting trend in the alkane results is the fraction of each alkane that was collected on the after filter differs with the size of the alkane (Figure 46). Quartz filters are famous for condensing organic vapors from the gas phase, so it is probable that alkanes in the gas phase were condensing on the filter. The results clearly show that increasing the carbon number of the alkane results in less of the alkane being collected on the after filter and more of the chemical being trapped on the aerosols that were impacted on the drums. The larger and heavier alkanes are simply not present in the gas phase of the atmosphere. Therefore, it appears that the lighter alkanes are passing through the impactor stages as a gas and then condensing on the filter. The implication of these results is that the *n*-alkanes may be volatilizing from the site in the gas phase as well as some particulate re-suspension.

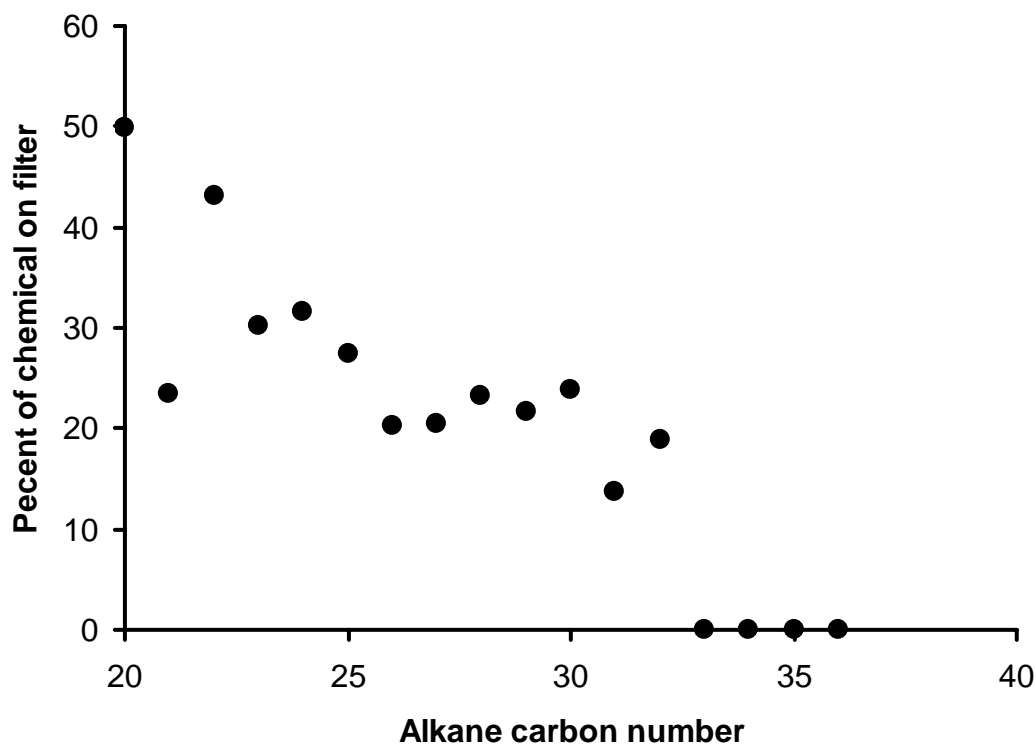


Figure 46. The fraction of *n*-alkanes collected on the after filter of the 8-stage DRUM. The C₃₃ to C₃₆ alkanes were not detected on the filter.

c. Organic acids

The particulate-associated organic acids were dominated by the long-chain alkanolic acids (Table 9) and hexadecanoic and octadecanoic acids in particular. The high abundance of these two acids strongly suggests a biological source for this particulate matter. This biological source can be either suspended bio-aerosols (pollen, microbes, spores, etc.) or biomass combustions (e.g. wood smoke). Another potential source would be cooking oil that may have been used at the nearby farmer's market. However, the presence of these acids combined with the effective absence of adjacent odd-number chain-length acids implies a non-petroleum source of this organic matter that is not associated with the rail yard.

Table 9. Concentrations (ng/m³) of particulate organic acids observed at the Roseville Rail Yard in the summer of 2005. Note that the Lundgren sampler was only operated at night when the air is coming from the rail yard.

Compound	8-stage DRUM (8/5 to 9/27)	8-stage DRUM (8/5 to 9/27) (scaled x 2.6)	Early Lundgren (9/27 to 10/7)	Late Lundgren (10/7 to 10/17)
Decanoic acid	< MQL	< MQL	< MQL	< MQL
Undecanoic acid	2.2	5.7	< MQL	< MQL
Dodecanoic acid	0.09	0.23	< MQL	< MQL
Tridecanoic acid	0.63	1.62	< MQL	< MQL
Tetradecanoic acid	0.43	1.11	< MQL	< MQL
Pentadecanoic acid	0.72	1.85	< MQL	< MQL
Hexadecanoic acid	4.6	11.8	7.7	8.4
Heptadecanoic acid	0.30	0.66	0.51	0.46
Octadecanoic acid	4.6	10.1	7.6	7.7
Nonadecanoic acid	0.05	0.13	0.08	< MQL
9-octadecenoic acid; (oleic acid)	0.70	1.80	0.79	< MQL
Butanedioic acid	1.6	4.1	5.1	5.5
Pentanedioic acid	0.65	1.67	1.4	1.5
Hexanedioic acid	1.3	3.34	0.41	0.41
Heptanedioic acid	0.23	0.59	0.74	0.77
Octanedioic acid	0.53	1.36	3.8	4.8
Nonanedioic acid	0.98	2.52	3.0	3.3
Decanedioic acid	0.05	0.13	0.61	0.63
2,3-hydroxybutanedioic acid	0.61	1.57	3.3	3.4
2-methyl-2-butenedioic acid	< MQL	< MQL	0.21	< MQL
<i>Cis</i> -pinonic acid	< MQL	< MQL	< MQL	< MQL
Pinic acid	0.10	0.26	4.0	3.6
<i>Trans</i> -norpinic acid	< MQL	< MQL	< MQL	< MQL
Sum of acids	20	51	40	42

The scaling factor for night-time only emissions for RRAMP sources is not necessarily true for these acids. Thus, the agreement (or lack thereof) between the scaled data and the night only Lundgren data is just another tool to identify sources. However, there are a number of cases for which the scaling makes the DRUM 24 hour data agree better with the nighttime only Lundgren data, hinting at a mixture of biogenic and anthropogenic sources. 0

The concentrations of the predominant organic acids as a function of aerosol size further supports the identification of these chemicals as having a biological source (Figure 47). Octadecanoic acid was only found in the larger size fractions greater than 0.75µm and the afterfilter. Additionally, there was appreciable mass in the largest size

fraction between 5 and 10 μm , which is typically the domain of suspended dust. Therefore, these largest particles simply contain biological materials as part of the ambient dust. The hexadecanoic and octadecanoic acids were effectively absent from the fine particulate sizes, except for the afterfilter, thus implying that combustion probably was not a significant source of these acids.

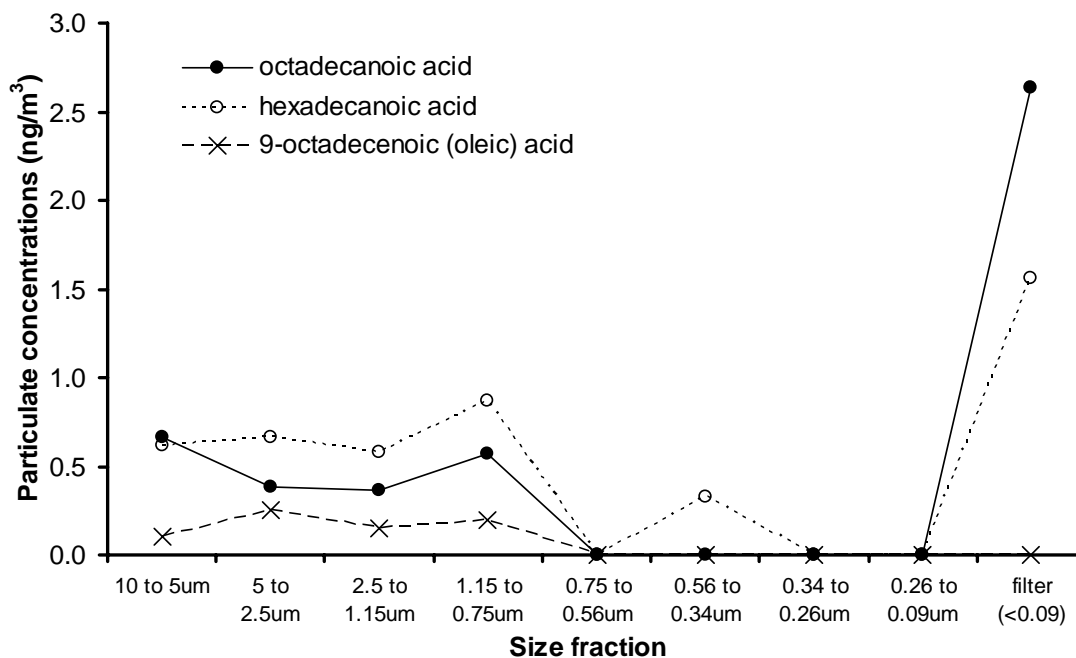


Figure 47. Concentration of octadecanoic, hexadecanoic and 9-octadecenoic (oleic) acid as a function of particle size.

c. Sugars and other polyols

The last group of chemicals investigated were the sugars and other polyhydroxylated compounds (Table 10). The sugars are clearly of biological origin and therefore do not come from the rail yard. However, the sugars, including levoglucosan, can add a considerable amount of organic matter in the particulate phase. Therefore, the sugars need to be accounted for if simple EC/OC measurements are conducted in the future to assess the emissions of organics from the rail yard.

Table 10. Concentrations (ng/m³) of particulate sugars observed at the Roseville Rail Yard in the summer of 2005.

Compound	8-stage DRUM (8/5 to 9/27)	Early Lundgren (9/27 to 10/7)	Late Lundgren (10/7 to 10/17)
Methyl-B-L-arabinopyranoside	< MQL	< MQL	< MQL
D-arabitol	1.5	3.2	2.9
Levoglucozan	2.2	9.7	12
Fructose	2.6	3.2	3.4
Glucose	3.7	5.2	4.8
Mannitol	2.0	3.3	3.2
Inositol	0.32	0.50	0.52
Sucrose	7.3	5.2	5.7
2-methylthreitol	0.60	0.60	0.73
2-methylerythritol	1.9	1.8	2.2

Seven of the eight sugars for which we had standards were detected in the 8-stage DRUM sampler. Sucrose was the most abundant sugar (7.3 ng/m³) followed by glucose (3.7 ng/m³). The high concentrations of refined table sugar (sucrose) implies that the some of the aerosols were generated from cooking at the “farmer’s market” nearby. The mass of sucrose was greater than either of the most abundant organic acids and comparable to the single most abundant *n*-alkane, which emphasizes the importance of a thorough organic chemical assessment including species that were not anticipated to be important emissions from the rail depot. While the presence of sucrose suggests a source of the aerosols, the notable absence of levoglucozan effectively eliminates biomass burning as an appreciable source of the aerosol. These samples were collected in the late summer when home heating by fireplaces is non-existent and agricultural burning had not yet commenced, so these results, which are very low relative to other published values, make intuitive sense. It also suggests that the high concentrations of the hexadecanoic and octadecanoic acids are the result of primary biogenic origin rather than biomass combustion.

The size distribution for the sugars showed the highest mass loading in the largest size fraction (Figure 48). This size distribution suggests that the sugars are present in larger aerosols that may have been mechanically generated. Once again, this indicates that they had been formed at the “farmer’s market” and the associated cooking activities at that site. The high concentration of the sugars may also be indicative of soil microbes since many of the sugars are used in metabolic processes. Thus, the profile of the sugars could also indicate that the re-suspended dust from a biological origin. There is a livestock auction building very close to the Denio’s site that would be a potential candidate for this type of biologically-rich dust.

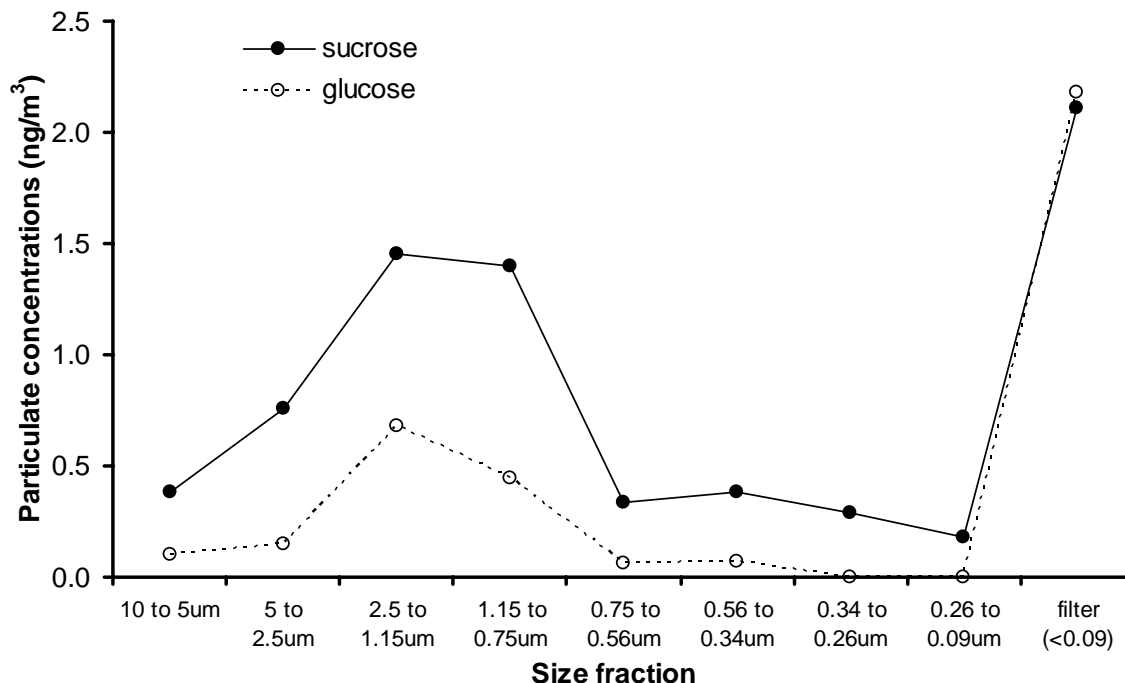


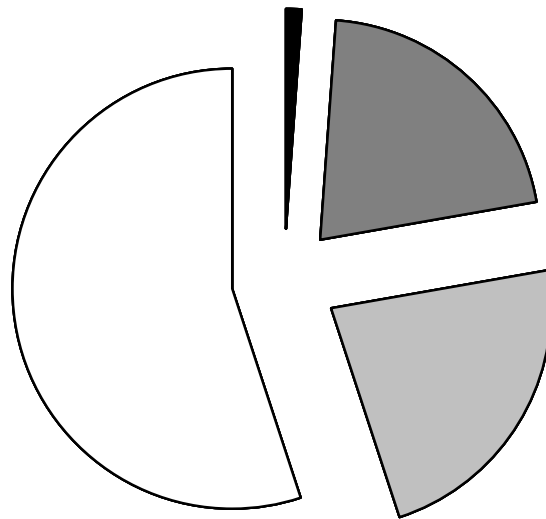
Figure 48. Sucrose and glucose concentrations (ng/m^3) as a function of aerosol size.

The last two chemicals quantified were the 2-methyltetrols which have been recently shown to be a major contributor to biogenic secondary aerosols. These compounds are believed to originate from the atmospheric oxidation of isoprene and other volatile biogenic gases.

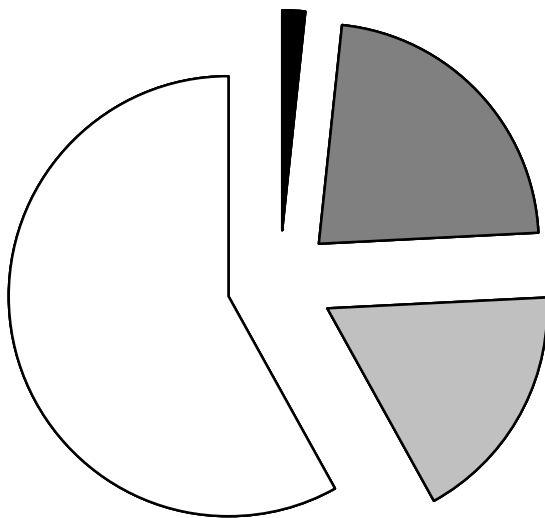
Aerosol Composition Profiles

The relative fraction of the different identified organic constituents (Figure 49) shows that the identified alkanes represent the greatest proportion of the identified mass while sugars represented 18 to 25% of the identified mass and organic acids were 21 to 31% of the mass. The PAHs, which are considered one of the more toxic components of the aerosols, were 1.1 to 2.0% of the identified organic matter. These chemical profiles show that a considerable fraction of the organic matter probably originated from sites other than the Roseville rail yard. In particular, the sugars and the long-chain alkanolic acids are likely biological and/or cooking in origin. Therefore, it is important to conduct chemical speciation at the site since simple EC/OC analysis may over-estimate the contribution of organic matter from the rail yard since it cannot speciate the different sources of the organic matter.

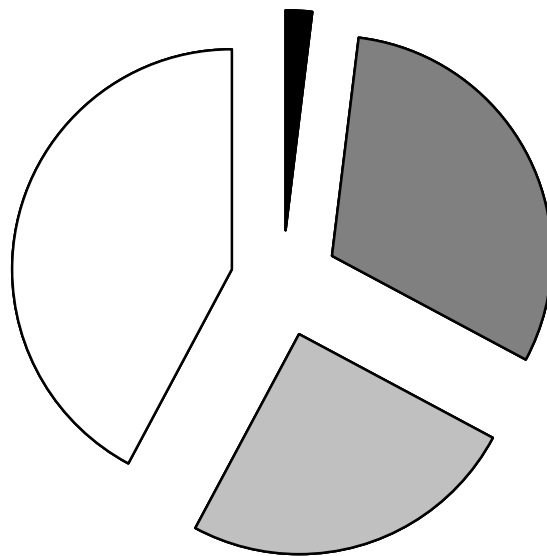
■ PAHs □ Sugars and polyols
 ■ Organic acids □ Identified alkanes



8-stage DRUM



Early Lundgren



Late Lundgren

Figure 49 Fraction of the identified organic mass belonging to the four different classes of chemicals identified.

The next aerosol composition calculation attempts to reconstruct the total aerosol mass, as measured by beta-gauge, from the known elemental and organic constituents (Figure 50). For this calculation, the elements of Al, Si, Ca, Ti, Mn, and Fe are assumed to be in their oxide states that are common of the crustal materials. This roughly doubles the weight of each of these elements. Sulfur is assumed to be in the sulfate form, which results in the sulfur contribution to aerosol mass to be 4.125 times sulfur. (Malm et al, 1994) The elements (and assumed elemental oxides) are summed for each size fraction of the 8-stage DRUM sampler.

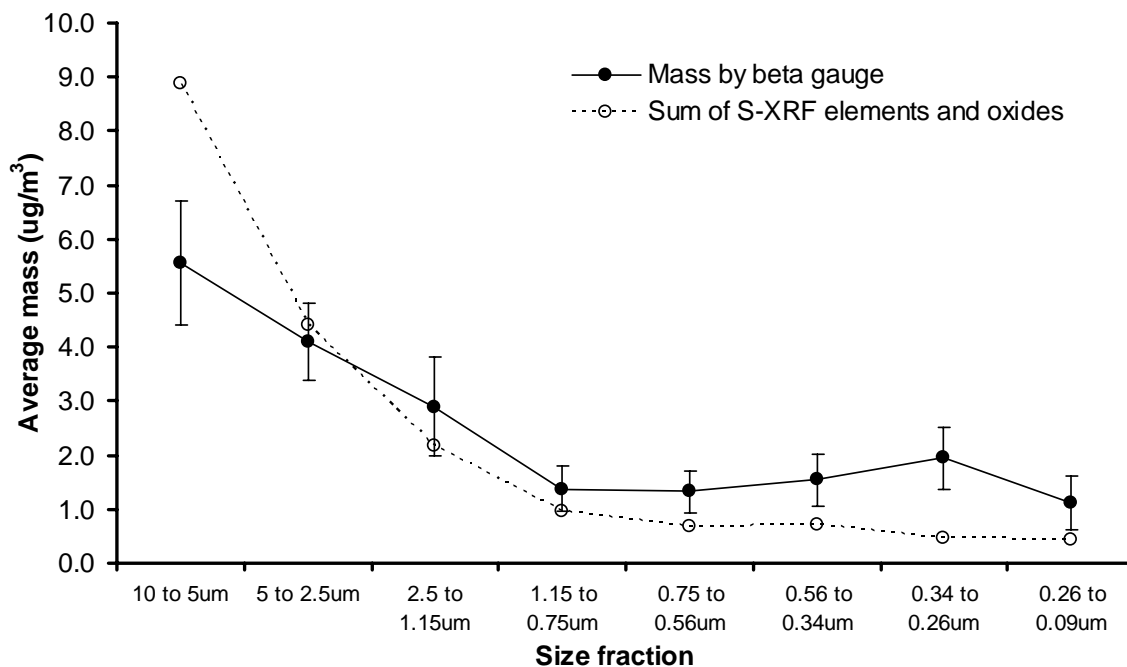


Figure 50. Mass of aerosols as determined by beta gauge and by the sum of the elements and oxides as determined by S-XRF.

The results (Figure 49) showed that the elemental mass was the largest fraction of the aerosol mass in the coarse stages and then the importance of elemental mass declines with the smaller size fractions. In the largest size fraction, the estimated elemental contribution to total aerosol mass exceeded the beta-gauge measured mass, but this is probably the result of the addition of many separate elemental measurements to determine the S-XRF elements and oxides. In all cases, the contribution of organic chemicals to the total mass measured by beta-gauge was relatively minor. Stage 4 (1.8%) and stage 8 (1.6%) had the greatest contributions, mostly due to the “undifferentiated alkane envelope” (Figure 51). The remaining mass was attributed as “unknown”. Although it was not measured, we would expect elemental carbon to make up a considerable fraction of the unknown mass since the samples were a dark black color that is typical of elemental carbon. Also, the fraction of the unknown mass was larger in the finer size fractions that would be combustion processes and diesel.

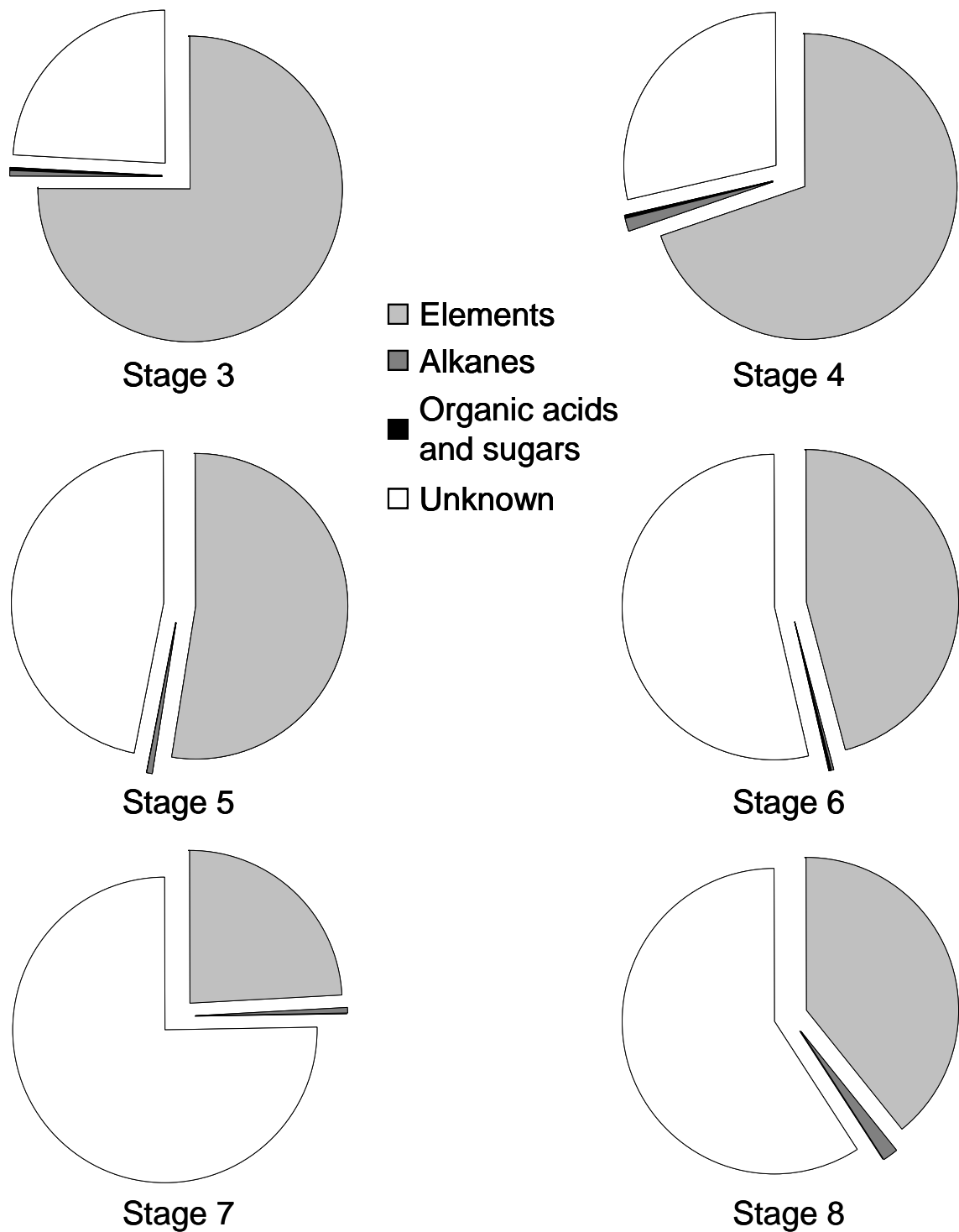


Figure 51. Composition of aerosol mass as determined by beta-gauge.

1. Comparisons to diesel truck data

The relative distribution of PAHs into heavier and more toxic modes, as shown in Figure 43 (repeated below), is not by itself adequate to determine impacts from Roseville rail yard aerosols.

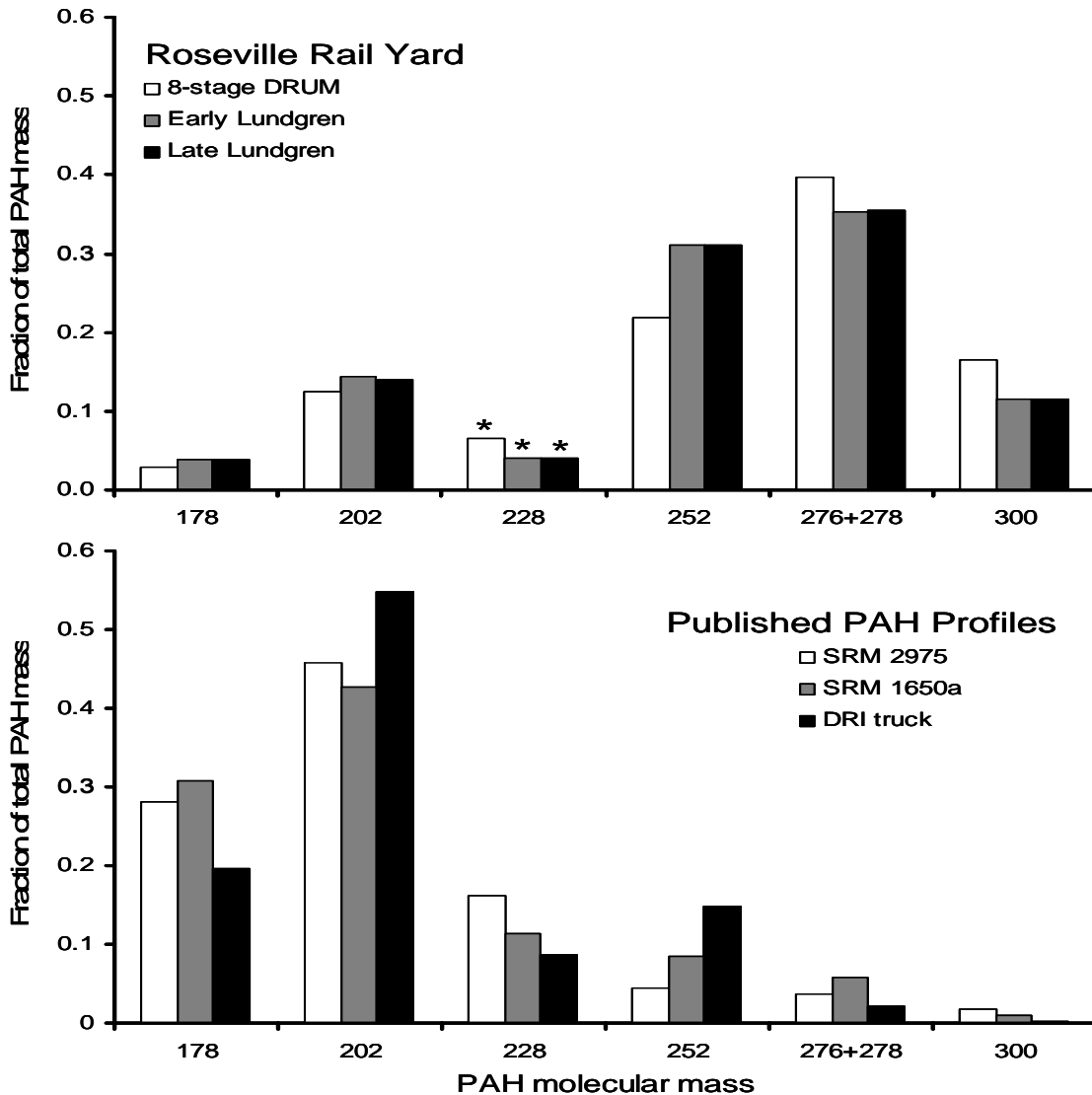


Figure 43. Profiles of PAHs as a function of molecular mass from the Roseville rail yard and the literature.

It is also necessary to determine the mass of PAHs in the aerosols, and/or the ratio as a fraction of total aerosol mass, fine mass, and/or elemental carbon, to allow estimates of aerosols impacts. The most direct way is to form the ratio of PAHs to the major diesel aerosol component, elemental carbon. This is not available from the NIST diesel SRM 1650a and SRM 2975, but these data are available from the Desert Research Institute Report to the National Renewable Energy Laboratory, 2004. (Zielinska et al, 2004). An

additional source is from the work of Gertler et al (2004) in a report to the Health Effects Institute and publications (Gertler et al, 2002, Gertler et al, 2004). For the Roseville data, elemental carbon was measured at the Denio and Pool sites through October, 2005.

In addition, during the summer, very fine mass was also measured at the Denio and Pool sites, allowing a comparison to size resolved data in Zielinska et al 2004. These data can be further sorted by total material at the Denio site, and the difference between the Pool and Denio sites. These estimates are necessary because no upwind-downwind organic measurements were taken. Combining the data on Table 1 for elemental carbon (EC) and Table 8 for benzo{a}pyrene, we can form ratios that can be compared to literature values, rail yard data to trucks.

These calculations have been done in Table 11.

There are three columns of results, the first being for very fine/ultra fine mass, and the second and third for elemental carbon (EC).

Using only mass data to form the ratio, we suffer from the uncertainty as to how one accounts for the $< 0.09 \mu\text{m}$ components not measured by the DELTA 8 DRUM. The first mass values in Table 11 assume that there is negligible mass below $0.09 \mu\text{m}$ diameter, which is unrealistic and gives a high ratio, 12.7

The next two measures use estimates of the missing sub- $0.09 \mu\text{m}$ estimated from the difference of the RRAMP $\text{PM}_{2.5}$ and the measured DRUM masses, and an estimate using the ratio observed for diesel trucks in Zielinska et al 2004. Using only the mass data, we obtain a mean RRAMP/truck ratio 7.5 ± 4.0 .

However, in the final analysis, we drop the unrealistic highest ratio, 12.7, and arrive at a mean mass ratio of 4.8 ± 2.7 .

Considerably more data exist that allow us to form a ratio to elemental carbon (EC) the largest single component of diesel exhaust by mass. These data were compared with literature emission rates of benzo{a}pyrene derived from both laboratory studies (Zielinska et al, 2004) and on-roadway tunnel studies (Gertler et al, 2002). Ratios were derived elemental carbon (EC), for the DELTA 8 DRUM in summer, and two Lungdren impactors in fall. Finally, we used both total EC at the Denio site and the EC difference, Denio to Pool site. This generated 15 different ratios based on the method used.

Table 11 Comparison of RRAMP Benzo{a}pyrene results to literature values for diesel trucks, in a highway tunnel (Gertler et al, 2002) and in the laboratory (Zielinska et al, 2004). The most precise values for the rail yard/truck ratios are in bold type.

RRAMP – Denio site	Period	Ratio – vf/uf mass laboratory	Ratio - EC/DRI laboratory	Ratio – EC/highway tunnel
8 DRUM – very fine mass	7/21 – 8/17	12.7		
8 DRUM – vf mass corr. by PM _{2.5} diff.	7/21 – 8/17	3.0		
8 DRUM – vf mass corr. by DRI ratio	7/21 – 8/17	6.8		
Mass average - corrected		4.8 ± 2.7		
8 DRUM – all EC	8/5 – 9/27		5.15	3.7
8 DRUM – corr. by EC diff.	8/5 – 9/27		9.02	6.7
Lundgren 5 drum – all EC	9/27 – 10/7		6.18	4.5
Lundgren 5 drum – corr. by EC diff.	9/27 – 10/7		13.9	10.1
Lundgren 5 drum – all EC	10/7 – 10/17		6.41	4.7
Lundgren 5 drum – corr. by EC diff.	10/7 – 10/17		14.4	10.5
Average values (all)	7/21 – 10/17	7.5 ± 4.0	9.2 ± 3.7	6.7 ± 2.7
Average values (Denio EC only)	7/21 – 10/17		5.9 ± 0.6	4.3 ± 4.0
Grand weighted average (EC + mass, Denio only)	7/21 – 10/17		5.5 ± 0.7	

A raw average of the 15 values gives a ratio of the RRAMP benzo{a}pyrene to diesel trucks of 7.7 ± 3.5 . However, we conclude that the Denio – Pool difference in EC is not a good match to the Denio-only PAHs. Removing these data, and weighting the averages by errors, we derive 5.5 ± 0.7 . This means that there was about 5.5 times more benzo{a}pyrene from the RRAMP aerosols than from diesel truck aerosols, per unit very fine/ultra fine mass and per unit elemental carbon.

Combining this with the PAH ratio data above, we find that the factor of 5.5 is made up equally from the shift in mass of the PAHs to heavier masses in RRAMP and an increase in the gross emission rate of PAHs.

While we used EC to scale from summer to fall conditions we could easily have used mass if we had had it. This is important since inversions become more common in fall and winter, raising the very fine mass from a value of $2.25 \mu\text{g}/\text{m}^3$ in summer (DRUM sages 7 + 8, 0.34 to $0.09 \mu\text{m}$) to $6.6 \mu\text{g}/\text{m}^3$ measured in February, 2006, using identical equipment. Thus, the Lundgren samplers were collecting in periods that would tend to have higher masses at the Denio site, and the factor may be greater than the 1.25 used from the EC data. This would improve the 8 DRUM to Lundgren agreement.

Component E

Aerosol sampling, winter, 2006, and comparison to heavily traveled secondary streets

Aerosol concentrations in the Sacramento region typically maximize in winter months when stagnation and inversions are common. For this reason, even though the upwind-downwind Pool site to Denio Site relationship of summer was degraded, it was decided to obtain at least 2 weeks of winter data to complete the 6 month period and gain an annual perspective. In addition, in order to aid in comparison of the rail yard data to other local pollution sources, the same protocol was applied to the Arden Middle School site, 25 m downwind of heavily traveled (65,000 v/day) Watt Avenue, a road that typically has about 1.5% truck traffic. This work is not part of the grant but a contribution from Breathe California of Sacramento-Emigrant Trails Health Effects Task Force and the UC Davis DELTA Group. Two DELTA 8 DRUM samplers with ultra-fine after filters were placed at Arden Middle School, Jan. 27. On February 10, they were both moved to the Denio site downwind of the Roseville Railyard. As shown below (Figure 52), the weather during each two week period was roughly comparable, with Arden having slightly better ventilation.

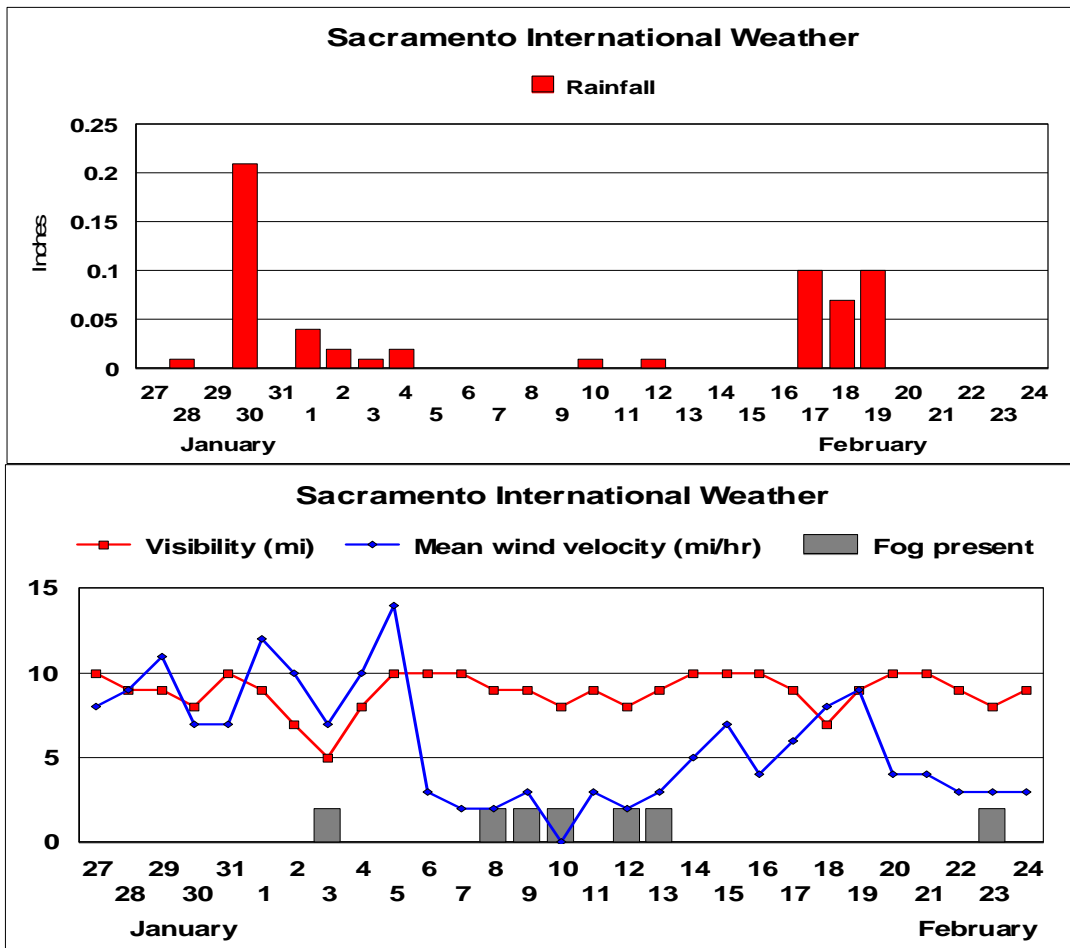


Figure 52 Meteorology during the winter sampling, 2006

The Arden outdoor site was on the roof of the teacher ready room, about 25 m from the edge of the nearest traffic lane and above a small (6 car) parking lot. It was at the same elevation but about at ½ the distance to Watt Avenue that we used in 2003 and 2005. The roof (painted white) was filthy with black soot.

Below (Figure 53) we show the actual particles photographed in natural light (hence the bluish tinge to the clean Mylar). There is an obvious soil like component at the Denio site absent at the Arden site, but other than that, the traces seen roughly comparable.

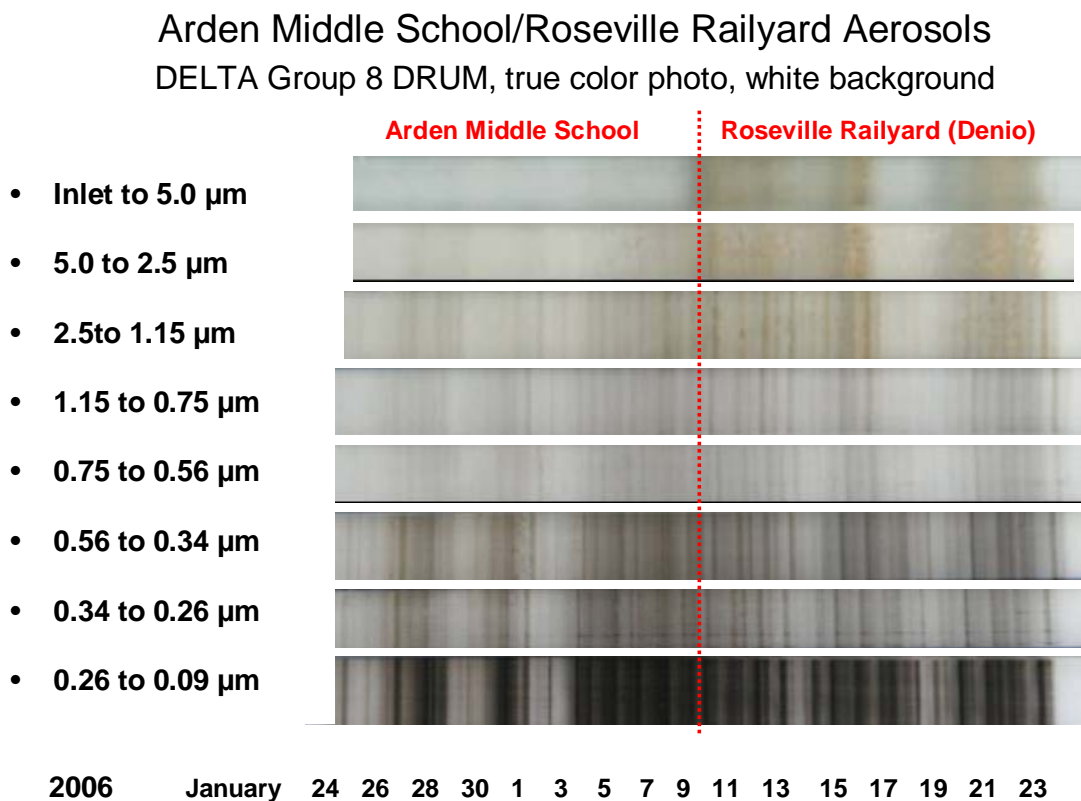


Figure 53 Photograph of winter drum strips, Watt Ave at Florin versus Denio site

Based on the compositional information, the finest 2 stages (< 0.34 µm) are dominated by automobile and diesel exhaust, while there is clearly additional smoke impact on the 0.56 to 0.34 µm stage.

Mass measurements were made by soft beta ray transmission by the DELTA Group, and these are shown below (Figure 54).

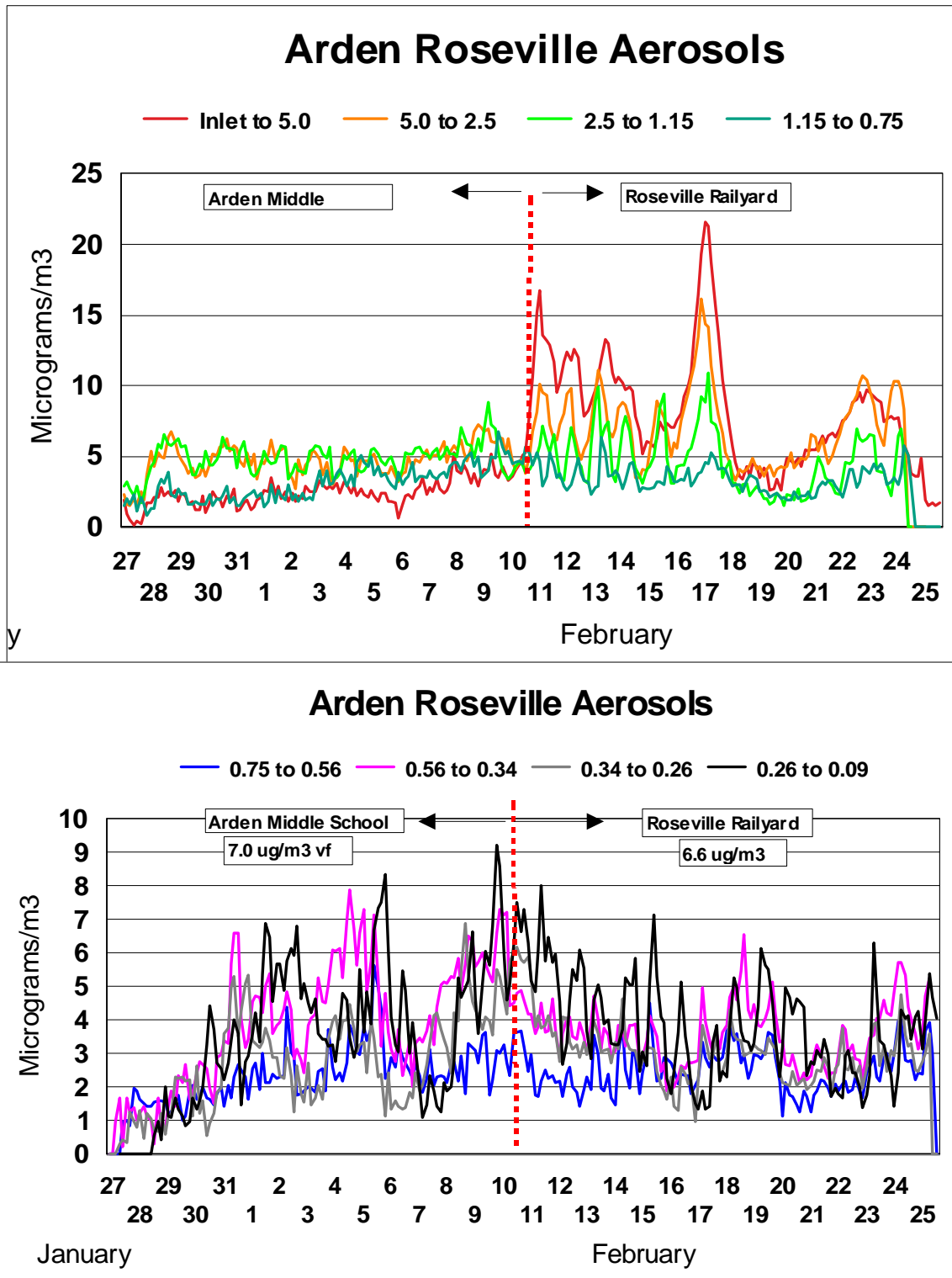


Figure 54 Coarse and fine mass at Watt and Arden versus the Denio site, winter, 2006

Qualitative comparison to winter, 2004 study

Arden Middle School Very Fine Aerosols

DELTA 8 DRUM, $0.26 > D_p > 0.09 \mu\text{m}$

January 16 – February 4, 2004



January 24 – February 10, Arden roof:
February 10 - 24 – Denio site – Roseville rail yard



Figure 55 Photographs of winter DRUM strips, Watt/Arden, 2004, vs Watt/Arden and Denio, 2006

Compositional analyses were made of the winter samples. First, chlorine in coarse modes is plotted, generally an indicator of sea salt and strong marine winds (Figure 56).

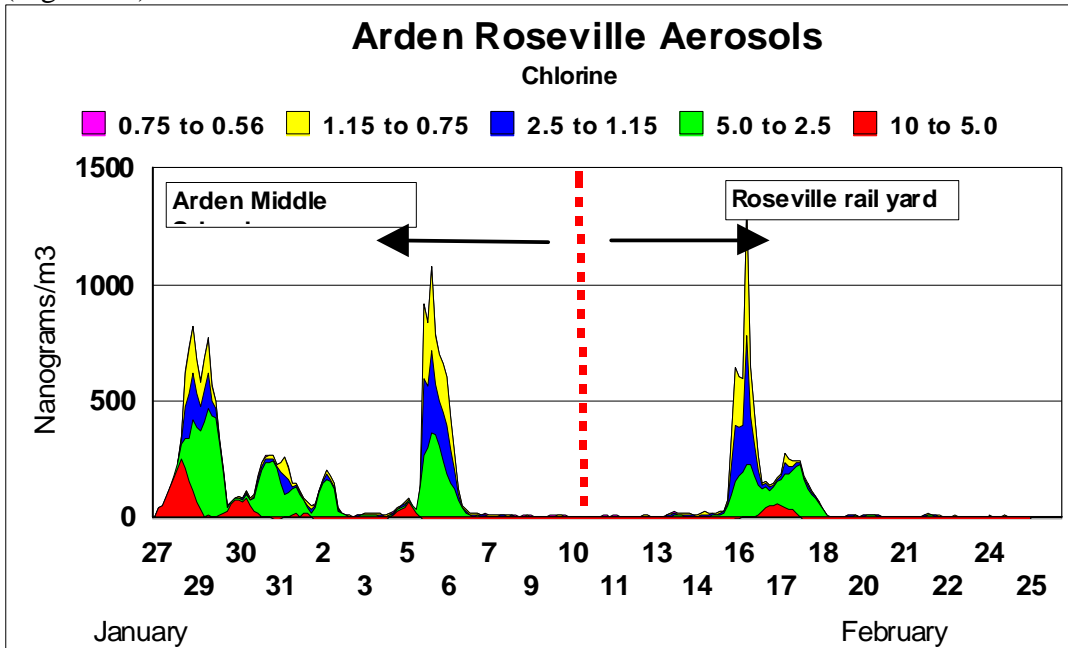


Figure 56 Chlorine aerosols (sea salt) at Watt/Arden and Denio, winter, 2006

The second element is iron, a tracer of soil. This can be matched to the coarse mass fraction seen only at the Denio site in mass (Figure 57).

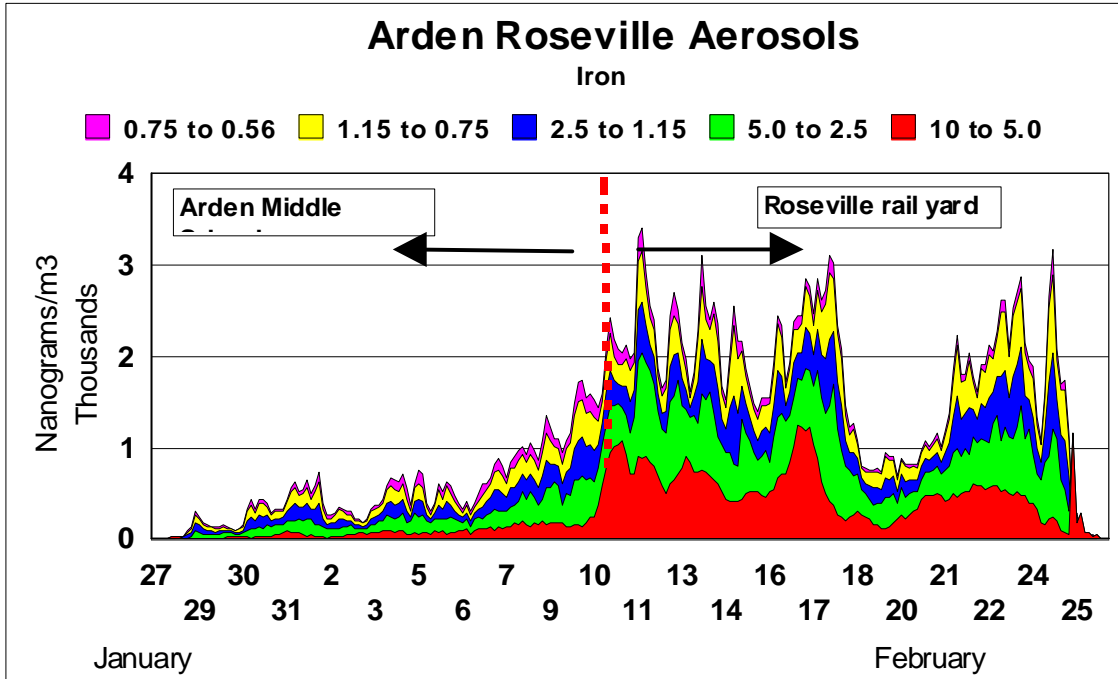


Figure 57 Iron aerosols (soil) at Watt/Arden vs Denio, winter, 2006

Finally, we plot sulfur (Figure 58). The peaks from January 29 through February 6 are associated with Bay Area sources as shown by both the chlorine and the vanadium (Figure 59), generally a tracer of heavy fuel oil. Note that the sulfur at the Denio site shows the characteristic diurnal maxima and minima pattern only weakly present at Arden Middle School.

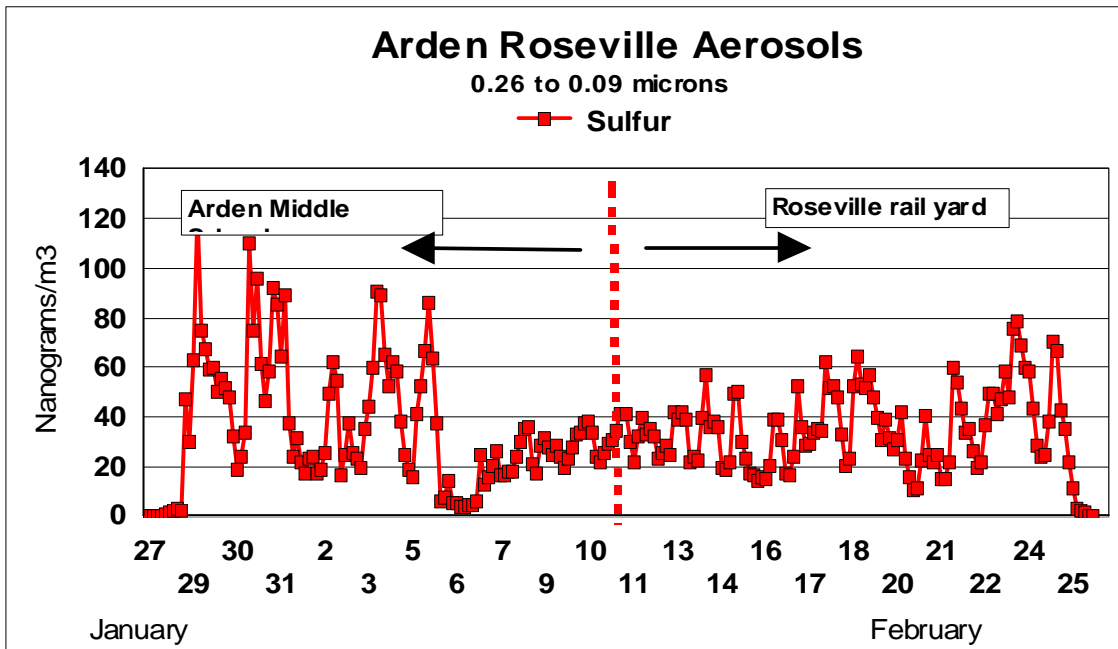


Figure 58 Iron aerosols (soil) at Watt/Arden vs Denio, winter, 2006

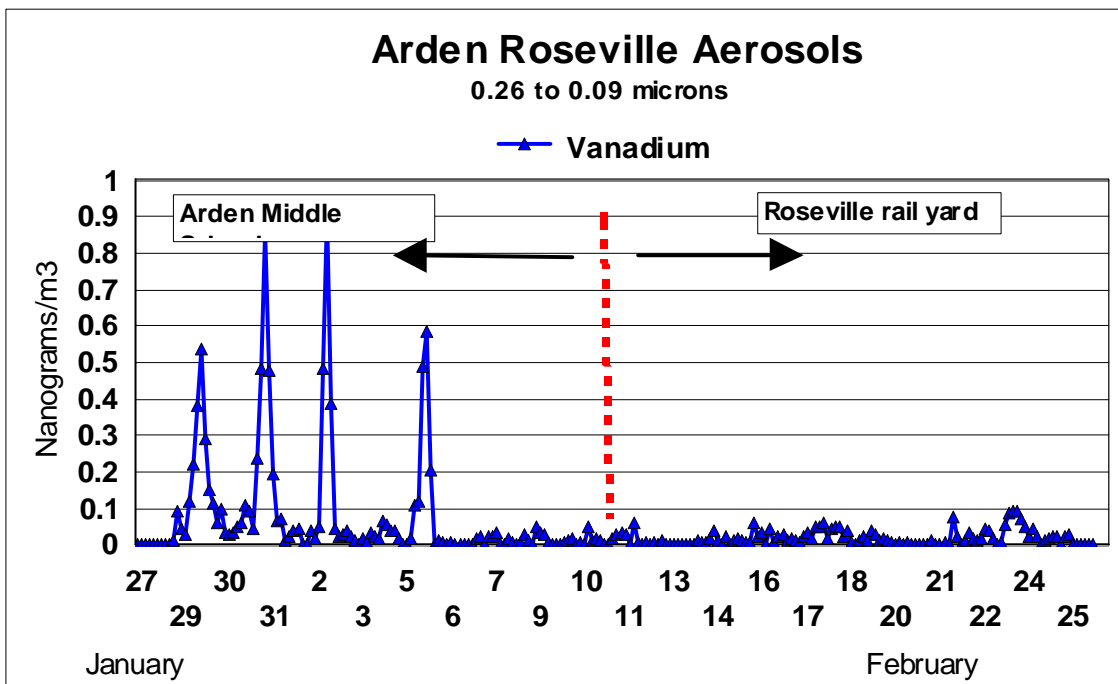


Figure 59 Vanadium aerosols (heavy fuel oil) at Watt/Arden vs Denio, winter, 2006

Potassium in the coarser modes is a component of soil. Compare this (Figure 60) plot to iron.

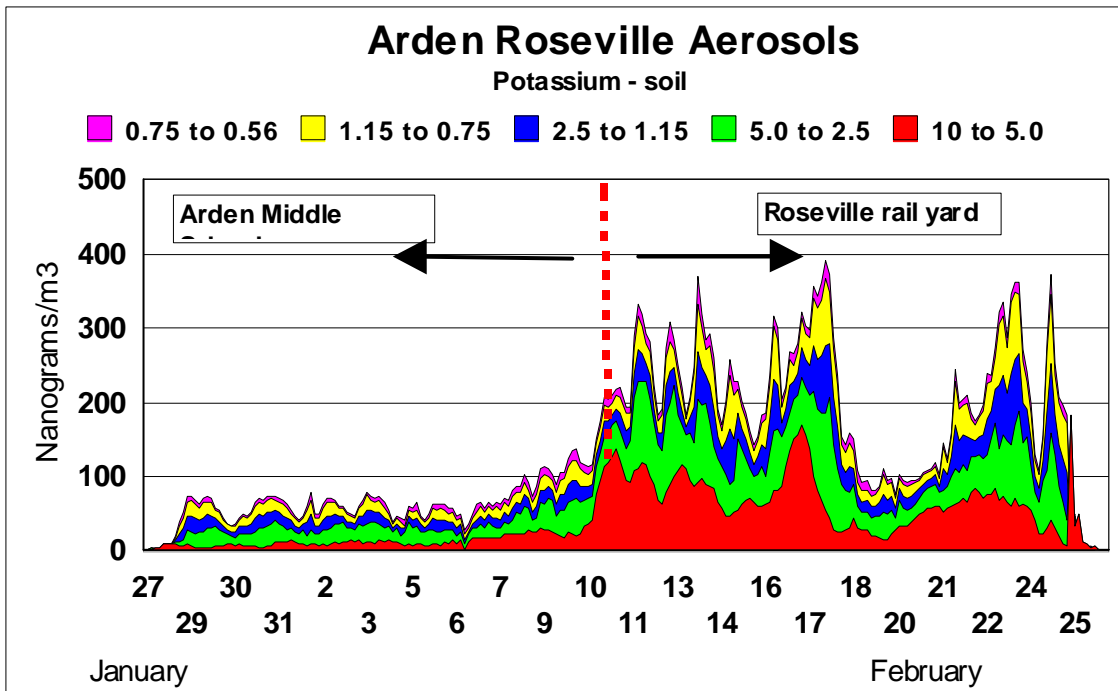


Figure 60 Coarse potassium aerosols (soil) at Watt/Arden vs Denio, winter, 2006

Potassium in the finer modes has both a biomass combustion component (0.35 to 0.75 μm) and an internal engine combustion component ($< 0.34 \mu\text{m}$) (Figure 61).

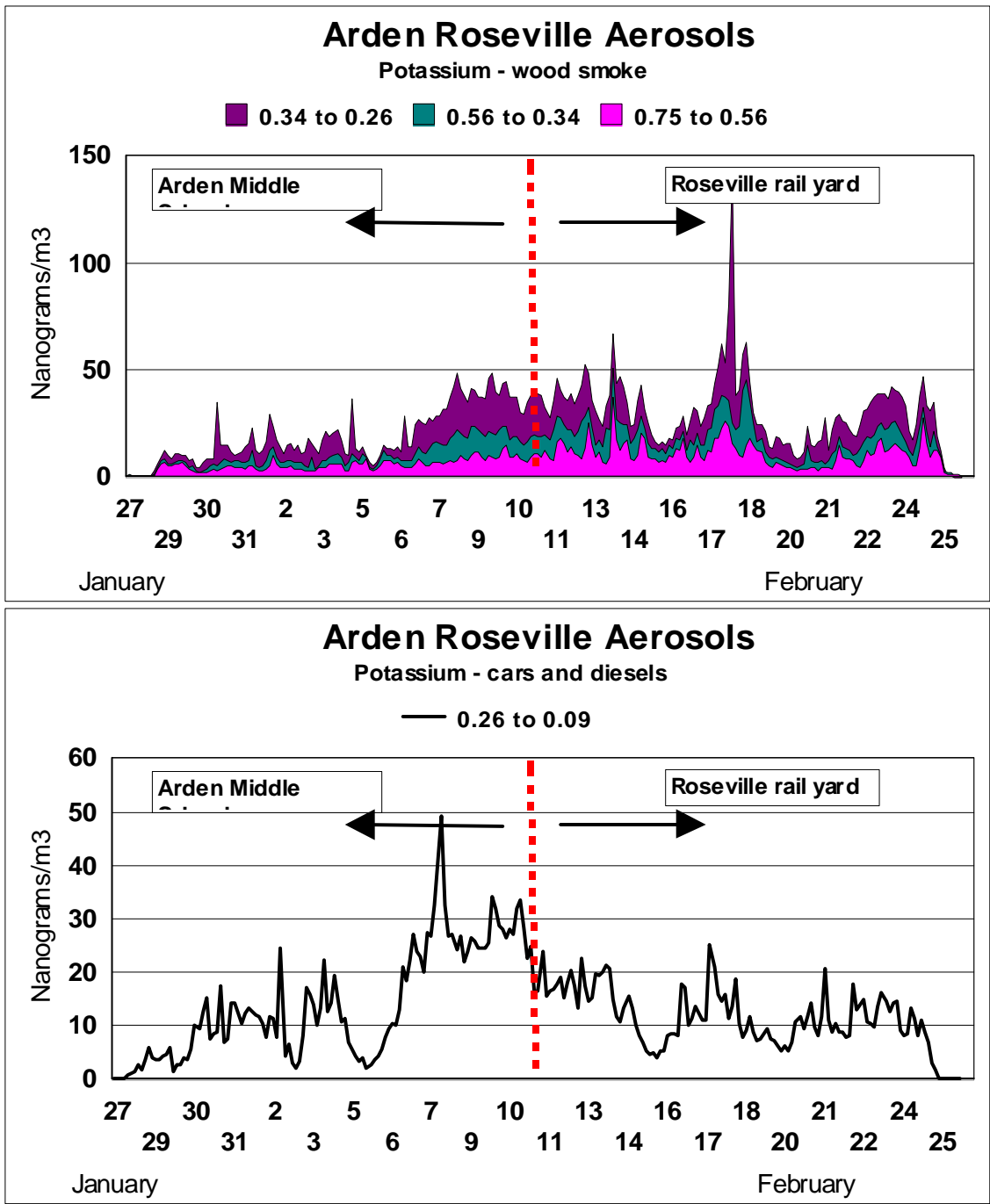


Figure 61 a, b Accumulation mode potassium aerosols (wood smoke) and very fine potassium aerosols (vehicular) at Watt/Arden vs Denio, winter 2006

Examining the very fine zinc signature (Figure 62), we can add the phosphorus component from the zinc thiophosphate stabilizer in lubricating oils. Ignoring the period of high Bay Area transport, we can see that the Zn/P ratio is smaller at the rail yard than at Watt Ave, most likely a reflection of the differences between the spark emission dominated Watt Ave. and the diesel dominated Roseville Railyard.

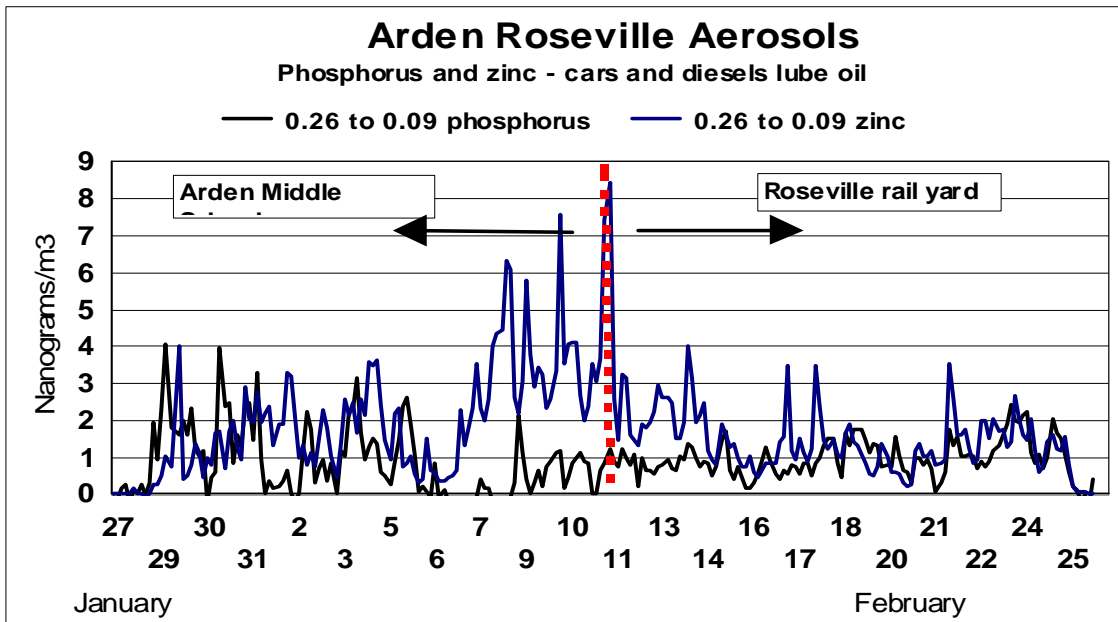


Figure 62 Very fine mode phosphorus and zinc aerosols (vehicular) at Watt/Arden vs Denio, winter 2006

Finally, for completeness sake, we include some typically anthropogenic metals (Figure 63). The high nickel levels from the Bay Area are the match to the vanadium values, above, as both are in heavy oils. The high copper levels at Arden at the moment lack any rationale.

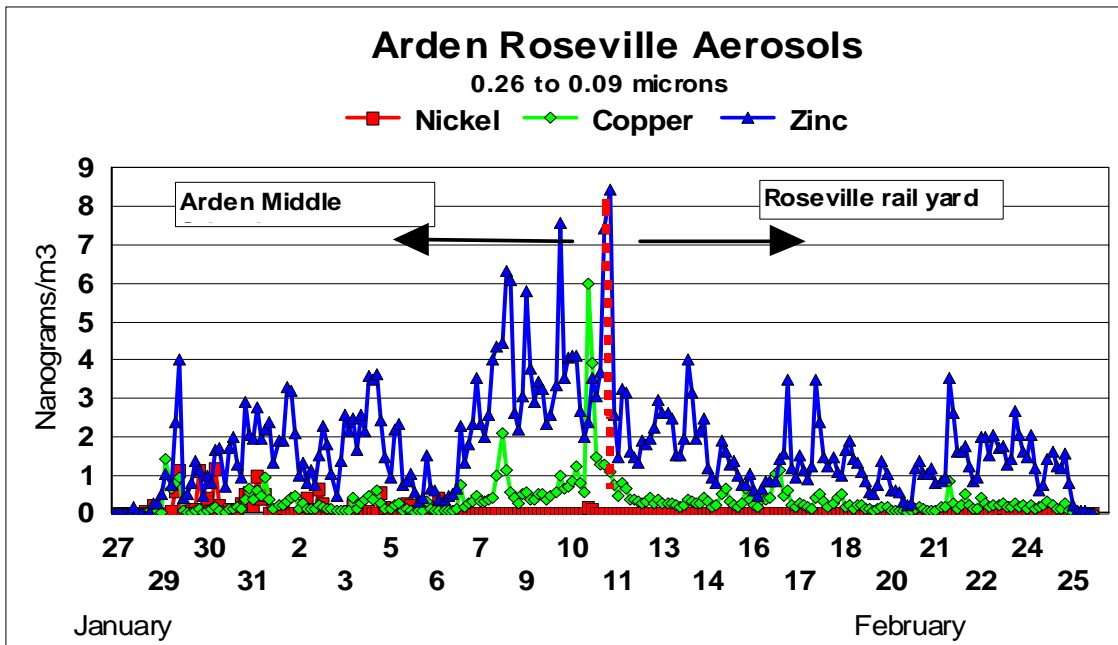


Figure 63 Very fine mode Ni, Cu, and Zn zinc aerosols at Watt/Arden vs Denio 2006

The implications of the winter data, although limited in time and with no Denio-Pool comparison, are still useful for an overall evaluation of the impact of the Roseville Railyard on local aerosols.

From the RRAMP data of Table 3, we see that the average $PM_{2.5}$ at the Denio site was $13.15 \mu\text{g}/\text{m}^3$, and the Pool site $10.2 \mu\text{g}/\text{m}^3$, July through October. The DRUM data from summer show a Denio – Pool enhancement of $1.35 \pm 0.27 \mu\text{g}/\text{m}^3$ during the same period when BC is $1.2 \mu\text{g}/\text{m}^3$ and the Denio – Pool $PM_{2.5}$ mass was $4.7 \mu\text{g}/\text{m}^3$. Thus, we can conclude that essentially all of the very fine-ultra fine mass difference in summer is BC.

No discernable trend is seen in $PM_{2.5}$ at the Denio site as we move into fall, despite a rise in BC from $1.2 \mu\text{g}/\text{m}^3$ to $1.8 \mu\text{g}/\text{m}^3$ in that period, for an average of $1.5 \mu\text{g}/\text{m}^3$. Using the Denio – Pool subtraction, we conclude that circa $\frac{1}{2}$ of the $2.95 \mu\text{g}/\text{m}^3$ of the $PM_{2.5}$ mass is in the form of BC, summer through fall, and almost entirely in the very fine-ultra fine mass fraction.

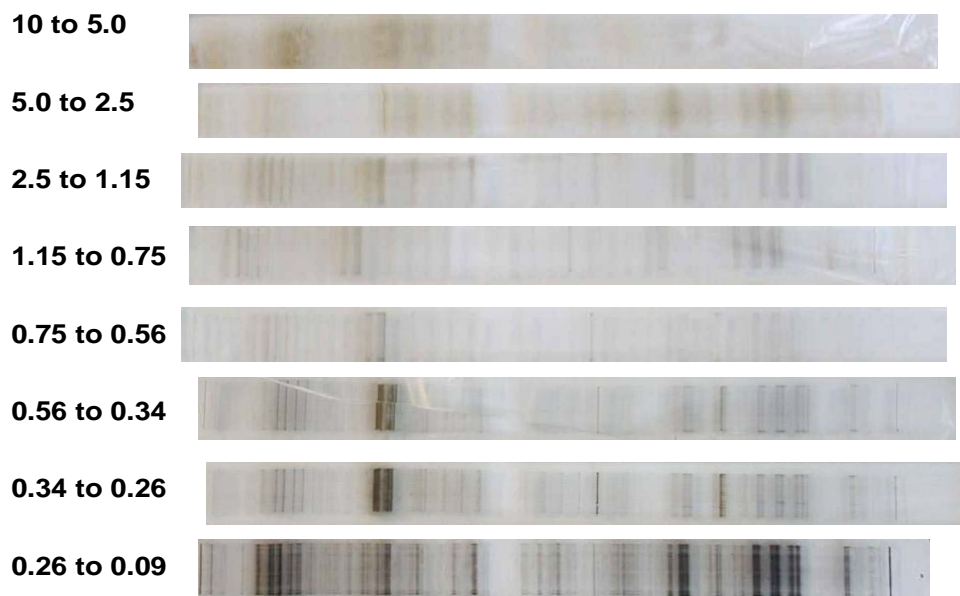
A linear progression of the BC data until winter would give an estimate of $2.7 \mu\text{g}/\text{m}^3$. The very fine ($< 0.25 \mu\text{m}$) aerosol from the 8 DRUM data showed a mass of $2.25 \mu\text{g}/\text{m}^3$ in summer and $6.6 \mu\text{g}/\text{m}^3$ in winter, a factor of 2.9, somewhat greater than the factor 2.25 estimated for BC in the same period. Thus, we can estimate that the annual average BC enhancement for the Denio site is about $2 \mu\text{g}/\text{m}^3$, and $4.4 \mu\text{g}/\text{m}^3$ of very fine-ultra fine mass.

Component F

Collection of aerosols at the Pool and Denio sites, summer, 2006, and at the Pool, Denio, and Church Street sites, summer, 2007.

One of the primary goals of the RRAMP and Breathe California's HETF programs was to track the progress of UPRR's mitigation efforts. Our capabilities can track changes, such as sulfur emissions, that are unavailable from standard RRAMP measurements. Thus, samples were taken with 8 DRUM samplers, with 3 hr resolution, over a period of 6 weeks at the Pool and Denio site, summer 2006, and at the Pool, Denio, and Church Street sites, summer 2007. The Church Street site was added since it is possible that the Denio site might not be available in summer 2008, and without a comparison, some of the usefulness of the early Denio-only data would be lost. These samples will be analyzed for mass, photographed, then archived for potential future analysis.

APB 13th and T Street Aug 22 – Oct 2, 2007



Roseville rail yard Pool site Aug 22 – Oct 2, 2007

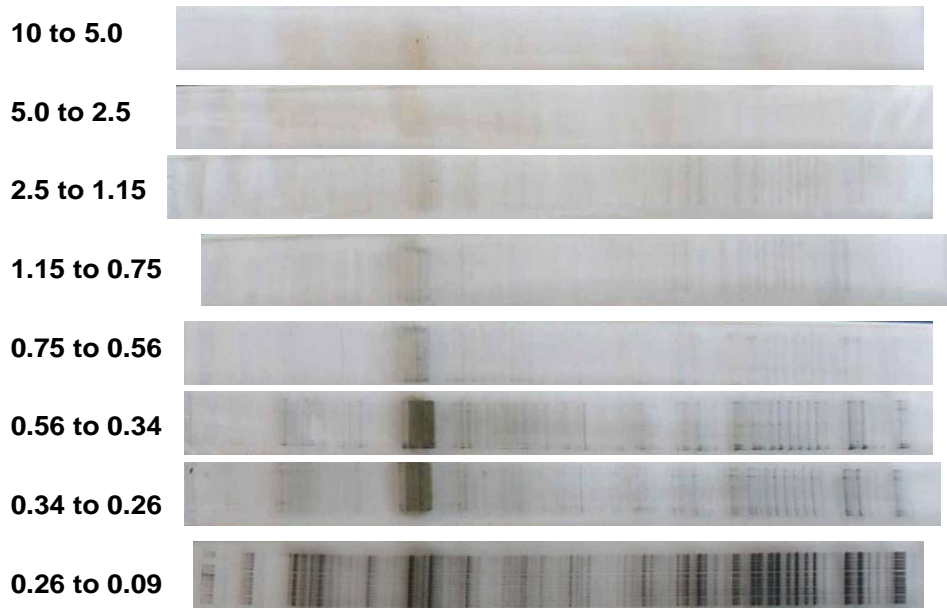
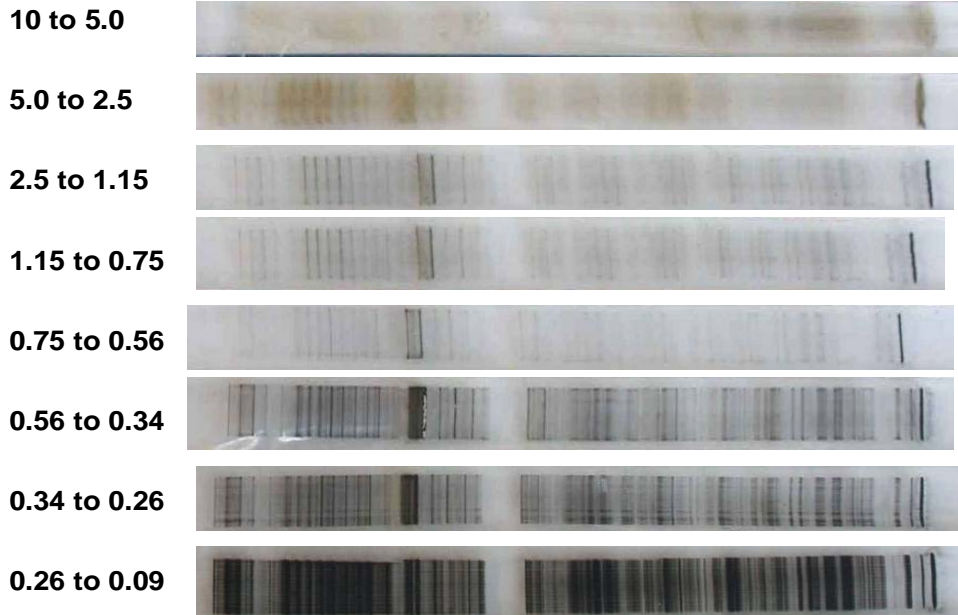


Figure 64 Comparison of downtown and the Roseville Pool site

Roseville rail yard Denio site Aug 22 – Oct.4, 2007



Roseville rail yard Church Street Aug 22 – Oct. 4 2007

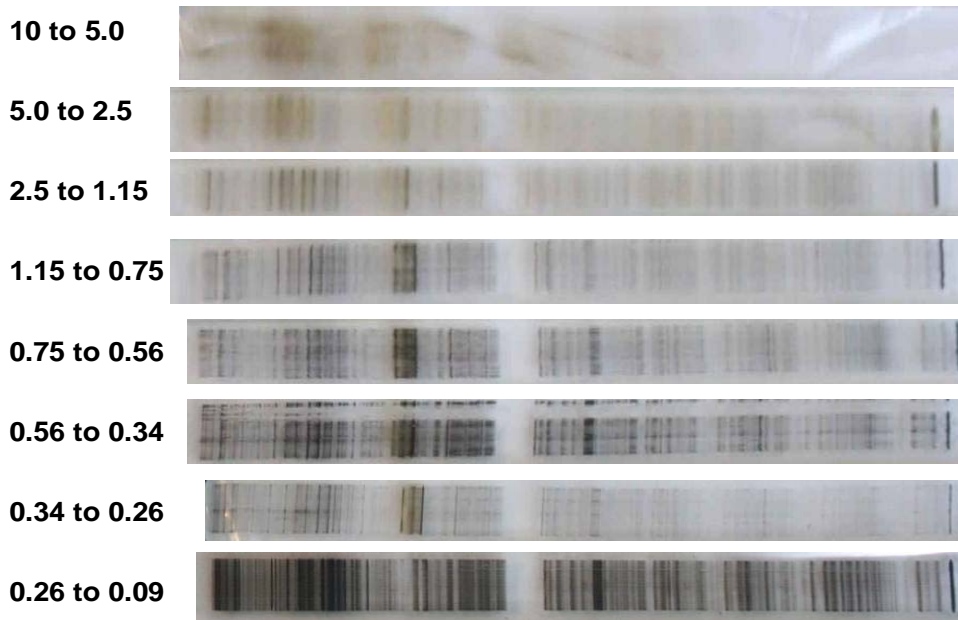


Figure 65 Comparison of the Denio and Church Street sites

From these comparisons, it can be seen that the Roseville Pool site, generally upwind of the rail yard, is very similar to downtown Sacramento at the ARB 13th and T Street sites. The brown fine mass in early September is the Plumas County “Moonlight” fire, while the whiter band is an artifact introduced to aid in timing. It is also clear that the Denio site is darker (soot?) in the very fine modes than the Church Street site.

Component G

Mitigation options proposed by the HETF for the Roseville Railyard

These studies identify the Roseville Railyard as a source of aerosols with potential for health impacts. It is thus essential that efforts are made to reduce these impacts. This process has already been started with a Memorandum of Understanding (MOU) between the UPRR, Placer County APCD, and other local, state, and federal air pollution agencies. The MOU outlines actions being taken by UPRR, with validation by the RRAMP program. However, the results of these studies have raised other concerns not addressed in the original MOU, such as the presence of metal-rich soil aerosols blowing from the site, and the potential for more serious health impacts because of the nature of the rail yard diesel emissions.

In parallel with other ongoing mitigation efforts, such as those centered on Watt Avenue, we propose a four phase program:

1. Mitigation of the diesel sources,
2. Mitigation options within the rail yard itself, including contaminate soils,
3. Mitigation from the rail yard fence to downwind receptors such as houses, schools, and playgrounds; and
4. Mitigation at the receptors, generally focusing on indoor air quality.

1. Mitigation of the diesel sources

These mitigations are largely included in the original MOU and updated periodically to ascertain progress. They include a variety of options, such as newer, cleaner engines, changes in fuel, modifications of yard operations to reduce engine idling, future tests with a hood system to capture and treat exhaust, and other actions. The final RRAMP report will document these actions.

In addition to specifications in the MOU, we recommend:

- installation of the highest level Verified Diesel Emission Control Systems (VDECS) commercially available for the model year, duty cycle and body configuration of the locomotive; with the system upgraded as higher levels of VDECS become available;
- accelerated replacement of line haul locomotives operating in California;
- retrofit or rebuild of line haul locomotives with lower emitting technology;
- use of alternative fuels, truck engines, and hybrid engines in switcher locomotives;
- retrofit of non-locomotive rail yard diesel rail yard equipment;
- emissions testing for switcher locomotives and/or incentives to replace oil-burning locomotives;
- since this report highlights the role of used lubricating oil in toxic emissions, we recommend immediate replacement of used lubricating oil prior to any engine repair or testing operations in the rail yard; and
- research of the modification of lubricating oil formulations to reduce toxic emissions.

2. Mitigation options within the rail yard itself

No matter how much mitigation is made in the sources, there will still be diesel effluent. In addition, there appear to be anomalously high emissions of fine metals from the yard, likely a result of high temperature working of metals. .

Further, analysis of coarse and fine particles downwind of the railyard show elevated levels of lead and other heavy metals that are not common in the surrounding urban environment in the concentrations measured. A strong possibility exists that these concentrations result from dust generating activities within the railyard on soils contaminated over the decades by the dumping of paint wastes, shop wastes, and steam locomotive boiler slag.

Emissions of fugitive dust within the railyard should be minimized, especially from portions of the yard that contain contaminated surface soils. Fugitive dust control measures include the paving of areas traversed by mobile equipment and the stabilization of inactive disturbed soils to reduce dust from operational activities and windblown soil entrainment. Soil stabilization should be performed using dust palliatives and soil berms constructed to prevent further vehicle disturbance, as well as by reintroducing vegetation on bare soil areas.

The use of vegetation barriers within the rail yard, generally aligned in parallel with the tracks, and at the boundary fences, can have strong effects in several ways. First, it will reduce the wind velocities across contaminated soil. Second, barriers such as evergreen trees have been shown to reduce aerosols in the size mode of diesel emissions by attachment to the needles and leaves. Third, by hampering lateral transport of the wind and creating eddies behind vegetation at high winds, pollutants are lofted vertically, reducing near rail yard concentrations. These mitigations have secondary benefits in improved scenery, reduced sounds, and carbon sequestration.

Below we show an example of recent data from a HETF/UC Davis study of vegetation funded by Sacramento Metropolitan AQMD. In it we show the removal of very fine (D_p , 0.26 μm) particles passing at low speed through redwood vegetation in the UC Davis Mechanical Engineering wind tunnel. These results are in substantial agreement with theoretical analyses based on the enhanced removal by diffusion for very fine particles if a surface is available. We have also confirmed that the particles, once impacted, do not re-emit under strong winds or shaking.

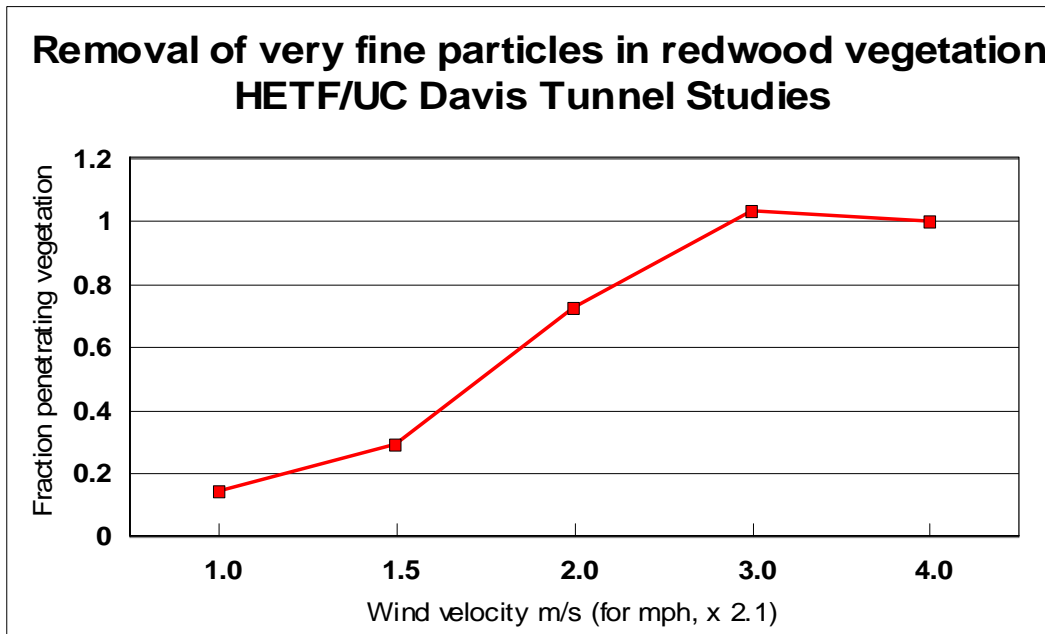


Figure 66 Preliminary data on removal rate of very fine ($0.26 > D_p > 0.09 \mu\text{m}$) on redwood branches in the UC Davis mechanical Engineering wind tunnel

The barriers should grow to be essentially complete (vegetation touching) in a few years up to a height of roughly the mixing zone on the roadway, which is typically about 3 m (16 feet) high. This can also be accomplished with bushes in front of the trees, and recent studies (Baldauf et al, US EPA) have shown 30% removal of ultra fine particles even with sound walls. Excellent examples of effective barriers can be seen on I-5 south of the Business 80 (W-X) freeway, and south of I-80 just west of Fairfield on the new Paradise valley development.

3. Mitigation from the rail yard fence to downwind receptors, houses, schools, playgrounds, etc.

Clearly, the best possible mitigation beyond the rail yard fence is distance. The rail yard as a source certainly is of the same order as the 50,000 vehicle/day threshold in the law that requires schools to be sited at least 500 ft away from the source.

Distance can be made yet more effective by the same sort of barriers mentioned in Mitigation 2, especially through use of evergreen vegetative barriers. Modification of street tree planting types could aid in this process, with redwoods, deodar, live oak, and oleander already tested and shown effective.

4. Mitigation at the receptors, generally focusing on indoor air quality

There is a growing appreciation that indoor air quality is a major factor in total person-dose-days exposure to airborne contaminants. There is a growing literature on methods to clean indoor air.

The special case of the rail yard, however, offers special options. Since the most toxic materials are in the very fine and ultra fine size modes, these particles have an ability to travel short distances to a surface. Our studies in indoor filtration with simple passive electrostatic filters at Arden Middle School showed surprisingly high effectiveness for a filter that can be used to replace existing furnace filters. In this study, very fine aerosols at the school location averaged $7 \mu\text{g}/\text{m}^3$ in a winter study, 2006 (see Figure 53). Current theory estimates that about $\frac{3}{4}$ of fine particles ($D_p < 2.5 \mu\text{m}$) should penetrate an average building, yielding an expected indoor concentration of a little over $5 \mu\text{g}/\text{m}^3$. Installation of a simple passive electrostatic non-HEPA filter on a recalcitrating indoor gas fired heating unit resulted in measured very fine particulate mass of $1.8 \mu\text{g}/\text{m}^3$.

This result is being evaluated in the SMAQMD study, but this is in accord with theory that states filters become more effective as particle sizes decrease below $0.1 \mu\text{m}$. This, as with the vegetation, the very fine modes of the Roseville Railyard diesel exhaust, and the fact that almost all of the most potent carcinogens with molecular masses of 252 (benzo[a]pyrene) or higher lie in particle sizes below $0.09 \mu\text{m}$ (Figure 42), also allows enhanced and more effective options for mitigation.

Efforts should be made to evaluate the presence of rail yard aerosols inside homes, and support should be given to aid the residences to reduce the concentrations.

References:

- Baldauf, R. Personal communication (2007)
- Bench, G., P.G. Grant, D. Ueda, S.S. Cliff, K.D. Perry, and T. A. Cahill. The use of STIM and PESA to respectively measure profiles of aerosol mass and hydrogen content across Mylar rotating drum impactor samples. 2001 *Aerosol Science and Technology* 36:642-651.
- Cahill, Thomas A. and Paul Wakabayashi. Compositional analysis of size-segregated aerosol samples. Chapter in the ACS book *Measurement Challenges in Atmospheric Chemistry*. Leonard Newman, Editor. Chapter 7, Pp. 211-228 (1993).
- Cahill, T.A., P. Wakabayashi, T. James. Chemical State of Sulfate at Shenandoah National Park During Summer 1991 *Nuclear Instruments and Methods in Physics Research B: Beam Interactions with Materials and Atoms*, 109/110 542-547, (1996)
- Cahill, Thomas A., Kent Wilkinson, and Russ Schnell. Composition analyses of size-resolved aerosol samples taken from aircraft downwind of Kuwait, Spring, 1991. *Journal of Geophysical Research*. Vol. 97, No. D13, Paper no. 92JD01373, Pp. 14513-14520, September 20 (1992).
- Cahill, T.A., C. Goodart, J.W. Nelson, R.A. Eldred, J.S. Nasstrom, and P.J. Feeney. Design and evaluation of the drum impactor. *Proceedings of International Symposium on Particulate and Multi-phase Processes*. Teoman Ariman and T. Nejat Veziroglu, Editors. Hemisphere Publishing Corporation, Washington, D.C. 2:319-325. (1985).
- Cahill, T. A. Comments on surface coatings for Lundgren-type impactors. *Aerosol Measurement*. Dale A. Lundgren, Editor. University Presses of Florida, Pp. 131-134 (1979).
- Draxler, R.R. and Rolph, G.D., 2003. HYSPLIT (HYbrid Single-Particle Lagrangian Integrated Trajectory) Model access via NOAA ARL READY Website (<http://www.arl.noaa.gov/ready/hysplit4.html>). NOAA Air Resources Laboratory, Silver Spring, MD.
- Raabe, Otto G., David A. Braaten, Richard L. Axelbaum, Stephen V. Teague, and Thomas A. Cahill. Calibration Studies of the DRUM Impactor. *Journal of Aerosol Science*. 19.2:183-195 (1988).
- Rolph, G.D., 2003. Real-time Environmental Applications and Display sYstem (READY) Website (<http://www.arl.noaa.gov/ready/hysplit4.html>). NOAA Air Resources Laboratory, Silver Spring, MD.
- Wesolowski, J.J., W. John, W. Devor, T.A. Cahill, P.J. Feeney, G. Wolfe, R. Flocchini. Collection surfaces of cascade impactors. In *X-ray fluorescence analysis of environmental samples*. Dzubay, T., Editor. Ann Arbor Science, Pp. 121-130 (1978).
- Zielinska, B., Cahill, T.A , Steve Cliff, Michael Jimenez-Cruz, and Kevin Perry, Elemental analysis of diesel particles from MOUDI samplers, Final Report to Doug Lawson, the National Renewable Energy Laboratory, Golden, CO (2004)

Acknowledgments:

The authors wish to acknowledge the continual support, encouragement, and expert scientific guidance of the Health Effects Task Force of Breathe California of Sacramento-Emigrant Trails, its Chair, Jan Sharpless, and its Consultant, Betty Turner.

The staff of the Placer County APCD were exemplary in their support of our field analyses and their provision of meteorology and data from RRAMP.

The authors also gratefully acknowledge the NOAA Air Resources Laboratory (ARL) for the provision of the HYSPLIT transport and dispersion model and/or READY website (<http://www.arl.noaa.gov/ready.html>) used in this publication.

This report has benefited greatly from the comments and suggestions of the RRAMP Technical Advisory Committee, but the opinions expressed herein are solely those of the authors.

Appendix QA:

The DRUM cuts are sharp and fully predictable by standard aerodynamic principles, and mis-sizing by bounce-off is reduced to less than 1 part in 5,000 by mass by a light grease coating (Wesolowski et al, 1979, Cahill 1979, Cahill et al, 1985).

A side by side comparison study of DRUM and other samplers was done on October 2 – 14, 2005, at Davis as part of the Quality Assurance component of the new EPA Particulate Matter Research Center grant to UC Davis which will be using DELTA Group DRUM samplers and analysis, 2005-2010.

However, an error in the modification in old DRUM #4, (1987) the Pool site sampler, resulted in an internal leak in that could not be detected during field sampling at RRAMP using standard vacuum and flow audit devices. It was discovered after analyses of the co-located sampling for quality assurance purposes at the Denio site and confirmed by disassembly of the unit. This invalidated all size modes from the Pool sampler except the finest, $0.26 > D_p > 0.09 \mu\text{m}$, which as a critical orifice has separate quality assurance checks. The side by side comparison yielded an average of $0.72 \mu\text{g}/\text{m}^3$ for the Denio sampler, $0.68 \mu\text{g}/\text{m}^3$ for the Pool site.

Comparison between data on DRUM samplers to standard PM is difficult due to:

1. Sharper size cut profiles, DRUM vs filters, especially important near the PM_{10} and $\text{PM}_{2.5}$ cut points,
2. Differences in the way impactors handle aerosols, since air is not drawn through the deposit, preserving chemical information sometimes lost in filters (i.e., sulfuric acid, Cahill et al, 1996)
3. Lack of ultra fine data below $0.09 \mu\text{m}$. This latter problem is especially important near strong combustion sources.
4. Time registration. DRUM samplers have errors in timing inherent to continuous sampling. The finite width of the impaction slot introduces an irreducible averaging over $1 \frac{1}{2}$ to 3 hr, the stretching of the Mylar onto the analysis frame adds typically 6 ± 3 hr of uncertainty. The relative time uncertainty is very small, 10 min/day, so that alignment of DRUM data with high precision gas and particulate data (such as NO) is an essential next step in data reduction.
5. Propagation of error problems. To match a single 24 hr $\text{PM}_{2.5}$ RRAMP filter, one has to sum 96 individual $1 \frac{1}{2}$ hr mass measurements or 48 3 hr elemental values from the DRUM samplers.
6. Dilution of the mass signal. The aerosols are spread over 8 size modes, resulting in almost a reduction of 10 in the amount of mass available to analyze on each stage.

2. Analysis

The UC Davis DELTA Group performs analyses by 7 different non-destructive methods, also described in publications and the 135 page DRUM Quality Assurance

Document, latest version 1/2005 (DQAP ver. 1/05), posted on the DELTA web site <http://delta.ucdavis.edu>.

c. Mass

Analysis was completed for mass values every 1 ½ hours in 8 size modes for the entire period. Each strip was analyzed at least 2 times, and the standard deviation of the data are included in the data file. An example of the precision repeated measurements of DRUM strip is shown below.

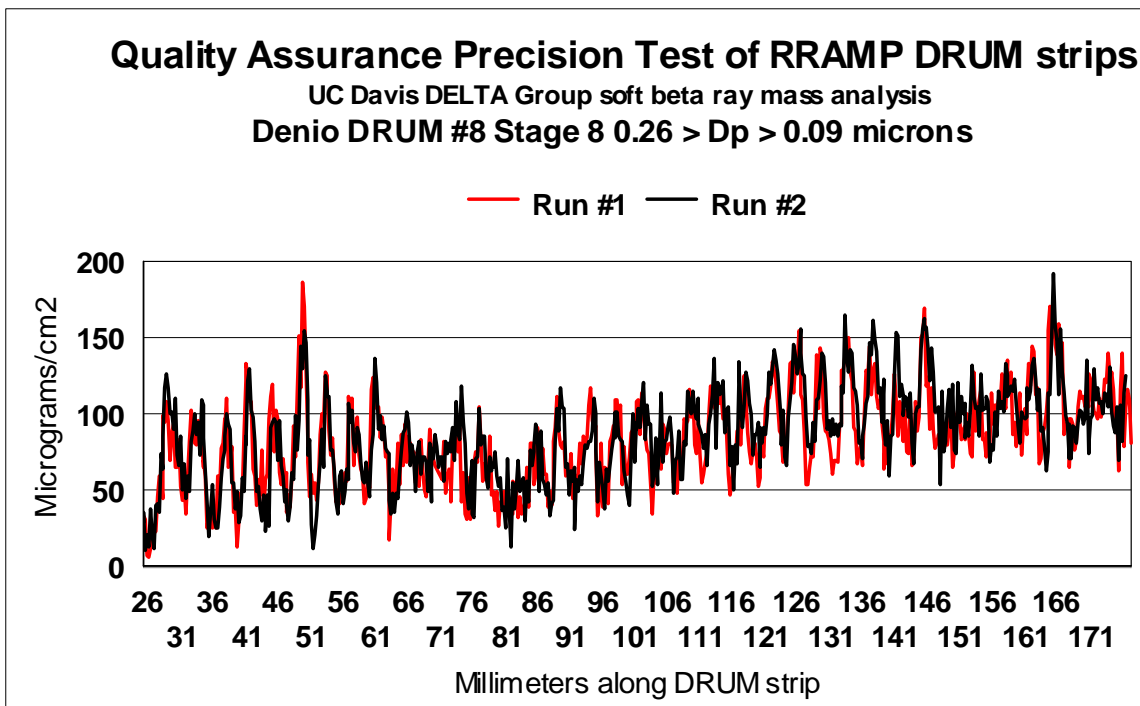


Figure 1 Precision test for mass

Note that since the strip was remounted, the test also validates relative time precision. Any measurements where the analysis differs by more than $\pm 10\%$ are independently re-run until agreement is achieved.

As mentioned above, comparisons with 24 hr filters are difficult. There have been 2 recent comparisons completed and one in progress (the US EPA PMRC Center tests at Davis) in rural conditions where the lack of ultra fine particulate mass should not be a major effect. The first was with IMPROVE and the National Park Service at Yosemite NP, 2002. (Final Report, 2004) Despite having to average 144 soft beta mass measurement (data taken every hour in 6 size modes), there is good overall agreement ($r^2 = 0.74$, slope = 1.14). However, the worst agreement occurred on 4 successive days with the arrival of fresh forest fire smoke from massive fires in Oregon.

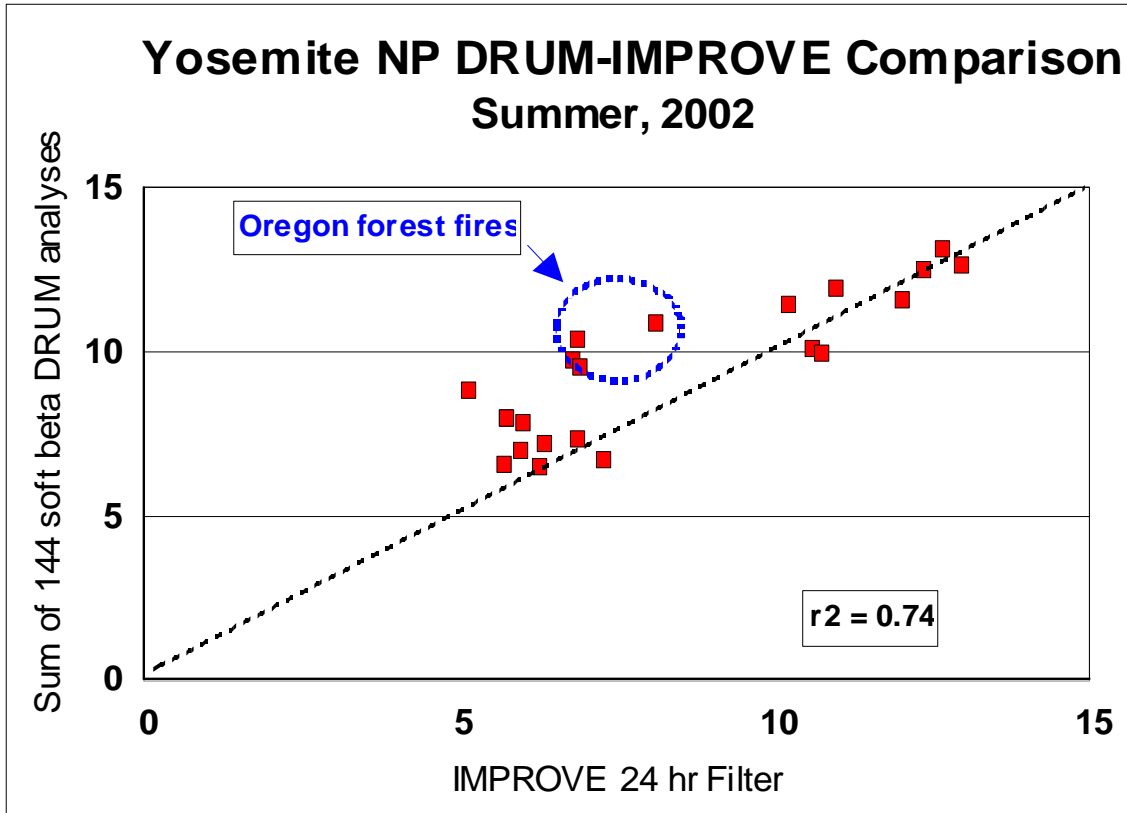


Figure 2 DRUM mass versus filters at Yosemite NP

The second test involved a comparison of DRUM mass at Davis to the district PM_{2.5} data at Woodland, roughly 10 miles away.

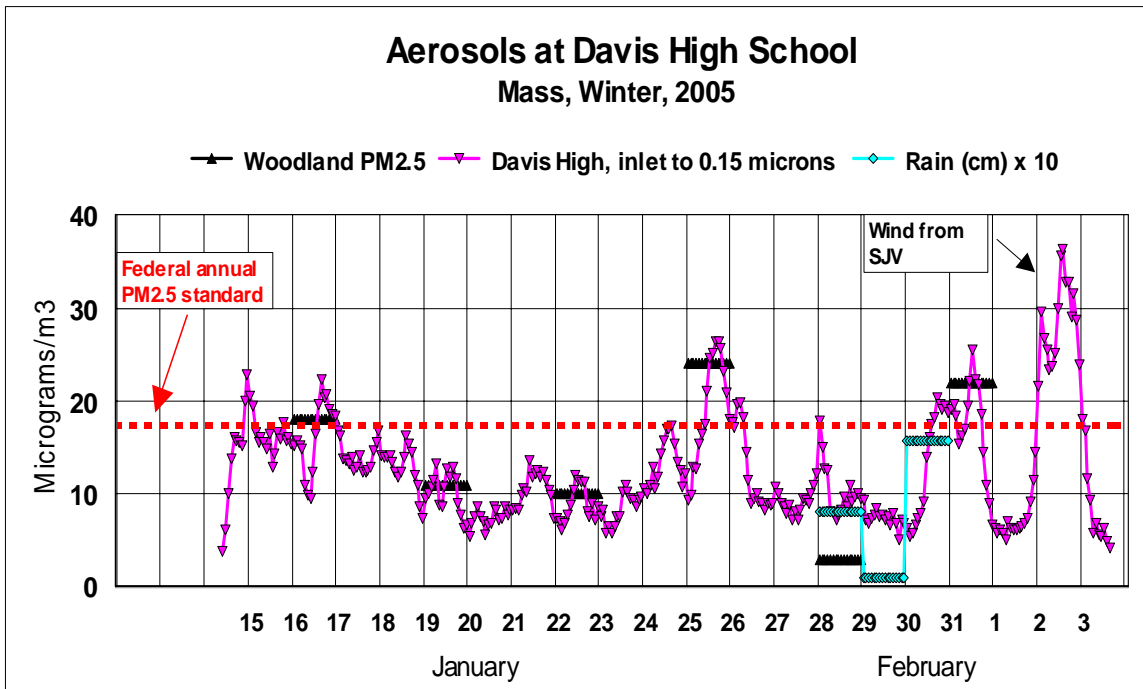


Figure 3 DRUM versus district filter sampler, Yolo County

In summary, DRUM mass data are vital for elucidating temporal and size behavior of aerosols while suffering some loss of accuracy and precision when compared to standard filter methods.

c. Compositional Analysis of Elements

The samples collected by the DRUM sampler are designed to allow highly sensitive elemental analysis by the new DELTA Group designed aerosol analysis system of the x-ray micro beam of the Advanced Light Source, Lawrence Berkeley NL (Bench et al, 2002). The method, synchrotron-induced x-ray fluorescence (S-XRF) has been used by the DELTA Group since 1992, (Cahill et al, 1992) but in its present form since 1999.

Table 2 S-XRF comparison, all blind tests since 1999

Study and date	Methods	Average ratio, Al to Fe	Std. dev.	Average ratio, Cu to Pb	Std. dev.
BRAVO, 1999	PIXE vs S-XRF	0.99	0.04		
BRAVO, 1999	CNL XRF vs S-XRF			1.24	0.14
FACES, 2001	ARB XRF vs S-XRF	0.93	0.21	1.02	0.08
FACES, 2001	ARB RAAS vs S-XRF	(0.98)	0.27	(0.74)	0.23
ARB LTAD 2005	DRI XRF vs S-XRF	1.037	0.085	0.907	0.009
All prior studies	Average	0.984	0.15	0.977	0.115

The S-XRF system has been tested in blind inter-comparisons since 1999, and all of these are shown above. Typically 32 elements are recorded for each analysis, all of which can be traced back to NIST primary (SRM # 1832, SRM # 1833) or secondary (Micromatter thin film) standards. Over 250,000 S-XRF analyses have been done by the DELTA Group since completion of the system in 1999.

The sensitivity of S-XRF is typically about 10 x better than standard XRF since the polarized x-rays eliminate over 90% of the x-ray background and the beam intensity is almost unlimited. This allows the standard analysis duration of 30 seconds to achieve a sensitivity for a DRUM sampler of about 0.01 ng/m³ for elements between titanium and bromine, and roughly 0.03 ng/m³ for most other elements reported. Below we show the MDLs for the RRAMP program, Stage 8 (0.26 to 0.09 µm diameter) of the 8 DRUM impactor.

S-XRF analysis of RRAMP			
Elements	MDLs (ng/m ³)	Elements	MDLs (ng/m ³)
Sodium	2.0	Cobalt	0.02
Magnesium	0.14	Nickel	0.02
Aluminum	0.09	Copper	0.03
Silicon	0.15	Zinc	0.05
Phosphorus	0.20	Gallium	0.001
Sulfur	0.20	Arsenic	0.001
Chlorine	0.02	Selenium	0.002
Potassium	0.02	Bromine	0.005
Calcium	0.05	Rubidium	0.01
Titanium	0.015	Strontium	0.02
Vanadium	0.003	Yttrium	0.15
Chromium	0.003	Zirconium	0.15
Manganese	0.005	Molybdenum	0.25
Iron	0.05	Lead	0.15

Minimum detected limits for organic analyses are a much more complex problem for organics than for elements due to the need for complex particle analysis protocols and presence of interferences. However, with the use of isotopically labeled organic compounds introduced at the very beginning of the analytical process, robust values have been achieved for RRAMP.

Minimum detectable limits (pg/m³) of particulate PAHs observed at the Roseville Rail Yard in the Summer of 2005. The MDL is for a single stage (or filter) since the chemical needs to be detected on only one stage to be detected for the whole sampling period.

Compound	8-stage DRUM Sampler	Lundgren Sampler
Phenanthrene	2.8	1.4
Anthracene	7.9	3.9
1-methylphenanthrene	0.61	0.30
Fluoranthene	1.3	0.65
Pyrene	1.5	0.72
Benz[<i>a</i>]anthracene	^a	^a
Chrysene + triphenylene	8.9	4.4
Benzo [<i>b+k</i>]fluoranthene	3.5	1.7
Benzo[<i>e</i>]pyrene	0.69	0.34
Benzo[<i>a</i>]pyrene	0.71	0.35
Perylene	4.4	2.2
Indo[1,2,3- <i>cd</i>]pyrene	4.0	1.9
Dibenz[<i>a,h</i>]anthracene	2.7	1.3
Benzo[<i>g,h,i</i>]perylene	3.2	1.6
Coronene	5.5	2.7

^a Compound not reported due to an interference.

Appendix B Delta Group DRUM Publications

History: The Air Quality Group (AQG, 1971 – 1997) and the Detection and Evaluation in Long-range Transport of Aerosols (DELTA Group, 1997 – present) have always preferred on fundamental and scientific grounds to perform experiments with continuous sampling of size and compositionally resolved aerosols. The samplers used have varied in time (typical time resolutions have and can be varied at will):

1. Lundgren sampler 1972-1974 , thereafter 5 stages, slots, 4 hr resolution, 160 L/min
2. Multiday sampler 1973 – 1981 3 stages, slots, 24 hr resolution 35 L/min
3. DRUM samplers
 - a. Jetted 8 DRUM 1985 – 1995 8 stages, jets, 3 hr resolution, 1.0 L/min
 - b. DELTA 8 DRUM 1996 – 8 stages, slots, 3 hr resolution 10.0 L/min
 - c. DELTA 8 DRUM, 2001 – 8 stages, slots, 3 hr resolution 16.7 L/min
 - d. DELTA 3 DRUM, 2001 – 3 stages, slots, 3 hr resolution 22.5 L/min
 - e. 8 DRUM upgrade, 2005 – 8 stages, slots, 3 hr resolution 16.7 L/min

The publications below are roughly separated by instrument in inverse chronological order. The numbers are the identifiers in the Master AQG/DELTA master publication list

Publications from DRUM samplers (slotted, 3 and 8 stage, types b through e)

- 04-4 Cahill, T. A., Cliff, S.S., Shackelford, J.F., Meier, M., Dunlap, M., Perry, K.D., Bench, G., and Leifer, R. Very fine aerosols from the World Trace Center collapse piles: Anaerobic incineration? ACS Symposium Series 919, 152-163 (2005)
- 04-3 Seinfeld, J.H., Carmichael, G.R., Arimoto, R, Conant, W. C., Brechtel, F. J., Bates, T. S., Cahill, T. A., Clarke, A.D., Flatau, B.J., Huebert, B.J., Kim, J., Markowicz, K.M., Masonis, S.J., Quinn, P.K., Russell, L.M., Russell, P.B., Shimizu, A., Shinzuka, Y., Song, C.H., Tang, Y., Uno, I., Vogelmann, A.M., Weber, R.J., Woo, J-H., Zhang, Y. ACE-Asia: Regional Climatic and Atmospheric Chemical Effects of Asian Dust and Pollution, *Bulletin American Meteorological Society* 85 (3): 367+ MARCH 2004
- 04-2 Han, J.S, K.J. Moon, J.Y. Ahn, Y.D. Hong, Y.J Kim, S. Y. Rhu, Steven S. Cliff, and Thomas A. Cahill, Characteristics of Ion Components and Trace Elements of Fine Particles at Gosan, Korea in Spring Time from 2001 to 2002, *Environmental Monitoring and Assessment* 00: 1-21, 2003

- 04-1 Thomas A. Cahill, Steven S. Cliff, Michael Jimenez-Cruz, James F. Shackelford, Michael Dunlap, Michael Meier, Peter B. Kelly, Sarah Riddle, Jodye Selco, Graham Bench, Patrick Grant, Dawn Ueda, Kevin D. Perry, and Robert Leifer, Analysis of Aerosols from the World Trade Center Collapse Site, New York, October 2 to October 30, 2001. *Aerosol Science and Technology* 38; 165–183 (2004)
- 03-1 Cahill, C.F. Asian Aerosol Transport to Alaska during ACE-Asia. *J. Geophys. Res.* 108 (D23), 8664 (2003)
- 03-4 Reuter, John E., Cahill, Thomas A., Cliff, Steven S., Goldman, Charles R., Heyvaert, Alan C., Jassby, Alan D., Lindstrom, Susan, and Rizzo, Davis M., An Integrated Watershed Approach to Studying Ecosystem health at Lake Tahoe, CA-NV, in *Managing for Healthy Ecosystems* Rapport et al, ed., CRC Press, New York, 1283-1298 (2003)
- 01-1 V. Shutthanandan, S. Thevuthasan, R. Disselkamp, A. Stroud, A. Cavanaugh, E.M. Adams, D.R. Baer, L. Barrie, S.S. Cliff, T.A. Cahill. Development of PIXE, PESA and transmission ion microscopy capability to measure aerosols by size and time. 2001 *Nuclear Instruments and Methods in Physics Research B: Beam Interactions with Materials and Atoms*.
- 01-4 Graham Bench, P.G. Grant, D. Ueda, S.S. Cliff, K.D. Perry, and T. A. Cahill. The use of STIM and PESA to respectively measure profiles of aerosol mass and hydrogen content across Mylar rotating drum impactor samples. 2001 *Aerosol Science and Technology* 36:642-651.
- 00-1 Miller, Alan E. and Thomas A. Cahill. Size and compositional analyses of biologically active aerosols from a CO₂ and diode laser plume. 2000 *International Journal of PIXE*. Vol. 9, Nos. 3 & 4.
- 99-3 Perry, Kevin D., Thomas A. Cahill, Russell C. Schnell, and Joyce M. Harris. Long-range transport of anthropogenic aerosols to the NOAA Baseline Station at Mauna Loa Observatory, Hawaii. 1999 *Journal of Geophysical Research Atmospheres*. Vol. 104, No. D15, Pages 18,521-18,533.
- 98-2 Pryor, S.C., R. J. Barthelmie, L. L. S. Geernaert, T. Ellerman, and K. Perry. Aerosols in the Western Baltic: Results from ASEPS '97. *Submitted to the 5th International Aerosol Conference, Edinburgh, 12-18th September, 1998*.
- 97-1 Cahill, Thomas A., and Kevin D. Perry. Asian Transport of Aerosols to Mauna Loa Observatory, Spring. 1994 *Climate Monitoring and Diagnostics Laboratory, No. 23, Summary Report 1994-1995, U.S. Department of Commerce National Oceanic and Atmospheric Administration Environmental Research Laboratories/CMDL 94-95, pp 114-116*.

Publications from DRUM samplers (jetted 8 drum, type a)

- 97-8 Perry, Kevin, Cahill, T.A., Eldred, R. A., Dutcher, D.D, Gill, T.E. Long-range transport of North African dust to the eastern United States. 1996 *Journal of Geophysical Research-Atmospheres*, 102, D10, 11,225-11,238.
- 97-10 Cahill, Catherine F., D.D Dutcher, P.H. Wakabayashi, M. Geever, and S.G. Jennings. 1997 The size-resolved chemical composition of natural and anthropogenic aerosols at Mace Head, Ireland. *Proceedings of a Specialty*

- Conference sponsored by Air & Waste Management Association and the American Geophysical Union. *Visual Air Quality: Aerosol and Global Radiation Balance*, Vol. I, pp. 487-497.
- 97-11 Perry, Kevin D., T.A. Cahill, R.C. Schnell, J.M. Harris. 1997 Long-range transport of anthropogenic aerosols to the NOAA Baseline Station at Mauna Loa Observatory, Hawaii. Proceedings of a Specialty Conference sponsored by Air & Waste Management Association and the American Geophysical Union. *Visual Air Quality: Aerosol and Global Radiation Balance*, Vol. I, pp. 130-139.
- 97-16 Cahill, Thomas A., K.D. Perry, Dutcher, D.D, R.A. Eldred, D.E. Day. 1997 Size/compositional profiles of aerosols at Great Smoky Mountains National Park during SEAVS. Proceedings of a Specialty Conference sponsored by Air & Waste Management Association and the American Geophysical Union. *Visual Air Quality: Aerosol and Global Radiation Balance*, Vol. II, pp. 1049-1056.
- 96-6 T.A. Cahill, P. Wakabayashi, T. James. Chemical State of Sulfate at Shenandoah National Park During Summer 1991 *Nuclear Instruments and Methods in Physics Research B: Beam Interactions with Materials and Atoms*, 109/110 (1996) 542-547.
- 95-4 Cahill, Thomas A. Compositional Analysis of Atmospheric Aerosols. 1995 *Particle-Induced X-Ray Emission Spectrometry*, Edited by Sven A. E. Johansson, John L. Campbell, and Klas G. Malmqvist. *Chemical Analysis Series*, Vol. 133, pp. 237-311. John Wiley & Sons, Inc.
- 94-5 Reid, Jeffrey S., Thomas A. Cahill, and Micheal R. Dunlap. Geometric/aerodynamic equivalent diameter ratios of ash aggregate aerosols collected in burning Kuwaiti well fields. 1994 *Atmospheric Environment*, Vol.28, No. 13, pp. 2227-2234.
- 93-1 Cahill, Thomas A. and Paul Wakabayashi. Compositional analysis of size-segregated aerosol samples. Chapter in the ACS book *Measurement Challenges in Atmospheric Chemistry*. Leonard Newman, Editor. Chapter 7, Pp. 211-228 (1993).
- 90-1 Hering, Susanne V., Bruce R. Appel, W. Cheng, F. Salaymeh, Steven H. Cadle, Patricia A. Mulawa, Thomas A. Cahill, Robert A. Eldred, Marcelle Surovik, Dennis Fitz, James E. Howes, Kenneth T. Knapp, Leonard Stockburger, Barbara J. Turpin, James J. Huntzicker, Xin-Qui Zhang, and Peter H. McMurry. Comparison of sampling methods for carbonaceous aerosols in ambient air. *Aerosol Science and Technology*. 12:200-213 (1990).
- 90-2 Cahill, Thomas A., Marcelle Surovik, and Ian Wittmeyer. Visibility and aerosols during the 1986 carbonaceous species methods comparison study. *Aerosol Science and Technology*. 12:149-160 (1990).
- 90-5 Cahill, Thomas A. Analysis of air pollutants by PIXE: The second decade. *Nuclear Instruments and Methods in Physics Research*, North-Holland. B49:345-350 (1990).
- 88-1 Raabe, Otto G., David A. Braaten, Richard L. Axelbaum, Stephen V. Teague, and Thomas A. Cahill. Calibration Studies of the DRUM Impactor. *Journal of Aerosol Science*. 19.2:183-195 (1988).

- 88-2 Cahill, Thomas A. Investigation of particulate matter by size and composition during WATOX, January 1986. *Global Biogeochemical Cycles*. 2:1:47-55, Paper No. 8J0052, March (1988).
- 88-4 Cahill, Thomas A., Marcelle Surovik, Robert A. Eldred, Patrick J. Feeney, and Nehzat Motallebi. Visibility and particulate size at the 1986 "Carbon Shoot-out" and 1987 "WHITEX" programs. *Proceedings of the Air Pollution Control Association 81st Annual Meeting*. Dallas, TX, June 19-24. Paper No. 88-54.2:1-20 (1988).
- 88-7 Annegarn, H.J., T.A. Cahill, JPF Sellschop, and A. Zucchiatti. Time sequence particulate sampling and nuclear analysis. Adriatico Research Conference on Aerosols. Trieste, Italy, July 22-25, 1986. *Physica Scripta*. 37:282-290 (1988).
- 87-4 Annegarn, H., Zucchiatti, A., Sellschop, J., Booth-Jones, P. PIXE characterization of airborne dust in the mining environment. Fourth International PIXE Conference, Tallahassee, FL, June 9-13, 1986. *Nuclear Instruments and Methods in Physics Research*. B22:289-295 (1987).
- 87-7 Cahill, Thomas A., Patrick J. Feeney, and Robert A. Eldred. Size-time composition profile of aerosols using the drum sampler. Fourth International PIXE Conference. Tallahassee, FL, June 9-13, 1986. *Nuclear Instruments and Methods in Physics Research*. B22:344-348 (1987).
- 87-9 Feeney, P.J., T.A. Cahill, H.J. Annegarn, R. Dixon, and P. Beveridge. Solar-powered aerosol samplers for use with PIXE analysis. Fourth International PIXE Conference. Tallahassee, FL, June 9-13, 1986. *Nuclear Instruments and Methods in Physics Research*. B22:349-352 (1987).
- 87-13 Eldred, Robert A., Thomas A. Cahill, Patrick J. Feeney, and William C. Malm. Regional patterns in particulate matter from the National Park Service network, June 1982 to May 1986. In *Transactions TR-10; Visibility Protection: Research and Policy Aspects*. P. Bhardwaja, Editor. Pittsburgh, PA: APCA, Pp. 386-396 (1987).
- 87-14 Cahill, Thomas A., Patrick J. Feeney, Robert A. Eldred, and William C. Malm. Size/time/composition data at Grand Canyon National Park and the role of ultrafine sulfur particles. In *Transactions TR-10; Visibility Protection: Research and Policy Aspects*. P. Bhardwaja, Editor. Pittsburgh, PA: APCA, Pp. 657-667 (1987).
- 86-1 Braaten, D.A. and T.A. Cahill. Size and composition of Asian dust transported to Hawaii. *Atmospheric Environment* (Great Britain). 20:1105-1109 (1986).
- 86-7 Cahill, T.A. Physical methods in air pollution research: The second decade. *Physics in Environmental and Biomedical Research*. S. Onori and E. Tabet, Editors. World Scientific Pub. Co., Pp. 55-61 (1986).
- 85-3 Cahill, T.A., C. Goodart, J.W. Nelson, R.A. Eldred, J.S. Nasstrom, and P.J. Feeney. Design and evaluation of the drum impactor. *Proceedings of International Symposium on Particulate and Multi-phase Processes*. Teoman Ariman and T. Nejat Veziroglu, Editors. Hemisphere Publishing Corporation, Washington, D.C. 2:319-325. (1985).

Publications from the Multiday 2 drum sampler (plus afterfilter)

- 90-11 Motallebi, Nehzat, Thomas A. Cahill, and Robert G. Flocchini. Influence of particulate size on statistical studies of visibility at California regions. *Atmosfera*. Pp. 111-126 (1990).
- 90-12 Motallebi, Nehzat, Robert G. Flocchini, Leonard O. Myrup, and Thomas A. Cahill. A principal component analysis of visibility and air pollution in six California cities. *Atmosfera*. Pp. 127-141 (1990).
- 82-3 Cahill, T.A. and D.A. Braaten. Size characteristics of Asian dust sampled at Mauna Loa Observatory. *Geophysical Monitoring for Climatic Change*. J. Harris and B. Bodhaine, Editors. Summary Report No. 11 (1982).
- 81-1 Flocchini, R.G., T.A. Cahill, Marc L. Pitchford, R.A. Eldred, P.J. Feeney, and L.L. Ashbaugh. Characterization of particles in the arid West. *Atmospheric Environment*. 15:2017-2030 (1981).
- 81-3 Cahill, Thomas A. Innovative aerosol sampling devices based upon PIXE capabilities. *Nuclear Instruments and Methods*. 181:473-480 (1981).
- 81-4 Cahill, Thomas A. Ion beam analysis of environmental samples. Symposium on Recent Developments in Biological and Chemical Research with Short Lived Radioisotopes. American Chemical Society Meeting. Honolulu, Hawaii, 1979. *Short-Lived Radionuclides in Chemistry and Biology*. John W. Root and Kenneth A. Krahn, Editors. No. 27:511-522. Advances in Chemistry Series, No. 197 (1981).
- 81-6 Leifer, R., L. Hinchliffe, I. Fisenne, H. Franklin, E. Knutson, M. Olden, W. Sedlacek, E. Mroz, T. Cahill. Measurements of the stratospheric plume from the Mount St. Helens eruption: Radioactivity and chemical composition. *Science*. 214:904-907 (1981).
- 81-7 Cahill, T.A., B.H. Kusko, L.L. Ashbaugh, J.B. Barone, R.A. Eldred, and E.G. Walther. Regional and local determinations of particulate matter and visibility in the southwestern United States during June and July, 1979. Symposium on Plumes and Visibility. Grand Canyon, AZ, 1980. *Atmospheric Environment*. 15:2011-2016 (1981).
- 81-8 Pitchford, A., Pitchford, M., Malm, W., Flocchini, R., Cahill, T., Walther, E. Regional analysis of factors affecting visual air quality. Symposium on Plumes and Visibility. Grand Canyon, AZ, 1980. *Atmospheric Environment*. 15:2043-2054 (1981).
- 81-9 Macias, E.S., J.O. Zwicker, J.R. Ouimette, S.V. Hering, S.K. Friedlander, T.A. Cahill, G.A. Kuhlmeier, and L.W. Richards. Regional haze in the southwestern US, II: Source Composition. Symposium on Plumes and Visibility. Grand Canyon, AZ, 1980. *Atmospheric Environment*. 15:1971-1986 (1981).
- 81-10 Flocchini, R., Cahill, T., Ashbaugh, L., Eldred, R., Feeney, P., Shadoan, D. Regional scale synoptic air monitoring for visibility evaluation based on PIXE analyses. *Nuclear Instruments and Methods*. 181:407-410 (1981).
- 81-11 Flocchini, Robert G., Thomas A. Cahill, Lowell L. Ashbaugh, Robert A. Eldred, and Marc Pitchford. Seasonal behavior of particulate matter at three rural Utah sites. *Atmospheric Environment*. 15:315-320 (1981).

- 81-12 Pitchford, Marc, Robert G. Flocchini, Ronald G. Draftz, Thomas A. Cahill, Lowell L. Ashbaugh, and Robert A. Eldred. Silicon in submicron particles in the Southwest. *Atmospheric Environment*. 15:321-333 (1981).
- 81-13 Cahill, T.A. Size-chemical profiles of environmental samples by PIXE. *Proceedings of the American Nuclear Society Meeting*. San Francisco, CA. IEEE Series: Terrestrial and Extraterrestrial Radiation II. Pp. 71-73 (1981).
- 81-15 Barone, J.B., L.L. Ashbaugh, B.H. Kusko, and T.A. Cahill. The effect of Owens Dry Lake on air quality in the Owens Valley with implications for the Mono Lake area. *Atmospheric Aerosol: Source/Air Quality Relationships*. P. Radke, Editor. No. 18:327-346. ACS Symposium Series, No. 167 (1981).
- 81-16 Cahill, Thomas A., Lowell L. Ashbaugh, and Bruce Kusko. Size-elemental profiles of fine particulate matter at Mauna Loa and Hilo, Hawaii. *Geophysical Monitoring for Climatic Change*. J.J. DeLuisi, Editor. Summary Report No. 9, December, P. 103 (1981).
- 80-3 Cahill, T.A., J. Barone, R.A. Eldred, R.G. Flocchini, D.J. Shadoan, and T.M. Dietz. Influence of sulfur size distribution on optical extinction. *Environmental and Climatic Impact of Coal Utilization*. J.J. Singh and A. Deepak, Editors. Academic Press, Pp. 213-244 (1980).
- 80-4 Cahill, T.A. Proton microprobes and particle-induced x-ray analytical systems. *Annual Reviews Nuclear and Particle Science*. 30:211-252 (1980).
- 79-2 Cahill, Thomas A. Comments on surface coatings for lundgren-type impactors. *Aerosol Measurement*. Dale A. Lundgren, Editor. University Presses of Florida, Pp. 131-134 (1979).
- 78-2 Eldred, Robert A., Thomas A. Cahill, and Robert G. Flocchini. Bromine loss from automotive particulates at California sites. *Proceedings of the 71st Annual Meeting of the Air Pollution Control Association*. June 25-30. Paper No. 78-69.6:2-15 (1978).
- 78-3 Wesolowski, J.J., W. John, W. Devor, T.A. Cahill, P.J. Feeney, G. Wolfe, R. Flocchini. Collection surfaces of cascade impactors. In *X-ray fluorescence analysis of environmental samples*. Dzubay, T., Editor. Ann Arbor Science, Pp. 121-130 (1978).
- 78-8 Flocchini, Robert G., Thomas A. Cahill, Robert A. Eldred, Lowell L. Ashbaugh, and John B. Barone. Sulfur size distribution by season and site in California. *Proceedings of the 71st Annual Meeting of the Air Pollution Control Association*. Houston, TX, June 25-30. Paper No. 78-39.6:3-15 (1978).
- 77-4 Cahill, Thomas A. X-ray analysis of environmental pollutants. *Environmental Pollutants*. T.Y. Toribara et al., Editors. Plenum Press, Pp. 457-463 (1977).
- 76-3 Flocchini, Robert G., Thomas A. Cahill, Danny J. Shadoan, Sandra J. Lange, Robert A. Eldred, Patrick J. Feeney, Gordon W. Wolfe, Dean C. Simmeroth, and Jack K. Suder. Monitoring California's aerosols by size and elemental composition. *Environmental Science and Technology*. 10:76-82 (1976).
- 76-4 Cahill, T.A., R.G. Flocchini, R.A. Eldred, P.J. Feeney, S. Lange, D. Shadoan, and G. Wolfe. Monitoring of smog aerosols with elemental analysis by accelerator beams. *Proceedings of the 17th Materials Research Symposium*. Gaithersburg, MD, October 7-11, 1974. National Bureau of Standards Special Publication, 422:1119-1136 (1976).

Publications from Lundgren 4 drum sampler (plus afterfilter)

- 80-5 Cahill, T.A. and L.L. Ashbaugh. Size/composition profiles of resuspended fly ash. *Environmental and Climatic Impact of Coal Utilization*. J.J. Singh and A. Deepak, Editors. Academic Press, Pp. 569-573 (1980).
- 78-5 Cahill, Thomas A. Results of highway particulate investigations in California. *Proceedings Federal Highway Administration Symposium on Environmental Impacts of Highway Transportation*. Charlottesville, VA. (1978).
- 75-2 Feeney, P.J., T.A. Cahill, R.G. Flocchini, R.A. Eldred, D.J. Shadoan, and T. Dunn. Effect of roadbed configuration on traffic derived aerosols. *Journal of the Air Pollution Control Association*. 25:1145-1147 (1975).
- 75-3 Ensor, D.S, T.A. Cahill, and L.E. Sparks. Elemental analysis of fly ash from combustion of a low sulfur coal. *Proceedings of the 68th Annual Meeting-Air Pollution Control Association*. Boston, MA. Paper No. 75-33.7:1-18 (1975).
- 75-5 Cahill, Thomas A. Ion-excited x-ray analysis of environmental samples. Chapter 1 of *New uses for ion accelerators*. James Ziegler, Editor. Plenum Press, Pp. 1-72 (1975).
- 74-4 Azevedo, J., R.G. Flocchini, T.A. Cahill, and P.R. Stout. Elemental composition of particulates near a beef cattle feedlot. *Journal of Environmental Quality*. 3:171-174 (1974).
- 74-5 Cahill, T.A., R.G. Flocchini, R.A. Eldred, P.J. Feeney, S. Lange, D. Shadoan, and G. Wolfe. Use of ion beams for monitoring California's aerosols. *Proceedings of the 2nd Annual NSF-RANN Trace Contaminants Conference*. Asilomar, Pacific Grove, CA. Paper No. LBL-3217:133-134 (1974).